RICE UNIVERSITY

Characterization and Rheology of Water-in-Oil Emulsion from Deepwater Fields

By

MOHAMMED S. ALWADANI

A THESIS SUBMITTED
IN PARTIAL FULFILLMENT OF THE
REQUIREMENTS FOR THE DEGREE

Master of Science

APPROVED, THESIS COMMITTEE:

_____
George J. Hirasaki, A. J. Hartsook Professor
Chemical Engineering

_____
Clarence A. Miller, Louis Calder Professor
Chemical Engineering

_____
Walter G. Chapman, William W. Akers
Professor Chemical Engineering

HOUSTON, TEXAS

JULY 2009

ABSTRACT

Characterization and Rheology of Water-in-Oil Emulsion from Deepwater Fields

by

MOHAMMED S. ALWADANI

Seafloor pipeline transport of viscous crude oil may be problematic because of high oil viscosity. This problem is compounded when water cut increases and stable emulsions form that have apparent viscosities significantly exceeding the oil itself. Reducing such high viscosity requires better understanding of emulsion properties. This study focuses on the characterization of water-in-oil emulsions by nuclear magnetic resonance (NMR) and their rheological behavior with and without demulsifiers present. Experimental data from NMR experiments show that the emulsion is very stable and needs demulsifier that can enhance the coalescence between droplets and hence aid separation. With presence of an optimal nonionic demulsifier, emulsion viscosity can be reduced by as much as one order of magnitude and reaches the oil viscosity at high temperatures. The selection of optimal coalescer depends on operation conditions. Increasing the temperature requires more hydrophilic coalescer to separate water from oil. Knowledge of emulsion behavior at different conditions helps in selecting the optimum parameters in either the early design phase or the oilfield operation.

Acknowledgements

I would like to express my gratitude to all those who gave me the possibility to complete this thesis. I am deeply indebted to my co-advisors Dr. George Hirasaki and Dr. Clarence Miller whose help, inspiring suggestions and encouragement helped me in all the time of my research. My thanks and appreciation goes also to Dr. Walter Chapman for serving on my thesis committee.

It is difficult to overstate my gratitude to Saudi Aramco's management for their trust in me and providing me with this opportunity to acquire the knowledge and expertise in order to contribute to Saudi Aramco’s long-term vision.

My former colleagues supported me in my research work. I wish to extend my warmest thanks to all of them. I am especially grateful to Tianmin Jaing for training me on how to operate NMR tool and analyze the data and assisting in explaining any difficulty I faced. My thanks go also to all people in my group for their direct and indirect assistance and helpful discussion during my work.

Finally, I owe my loving thanks to my wife and my children. Without their love, encouragement and understanding it would have been impossible for me to finish this work. My deepest gratitude goes also to my parents, brothers and sisters for their indefatigable love and support throughout my life. To all of them I dedicate this thesis.

Table of Contents

List of Figures

List of Tables

CHAPTER 1

INTRODUCTION

1.1 Importance of Deepwater Fields

A lot of experts believe that most of the easily developed oil and gas resources have been already found. Henceforth, the best source of new energy resources may be located in the deepwater oil fields such as these in Gulf of Mexico and other frontier areas. Future development of these resources will be both more challenging and more costly. With declining production from near-shore, shallow waters, energy companies have focused their attention on oil and gas resources in water depths of 1,000 feet and beyond [1]. Production from such depths, or greater, is usually named as deepwater production.

According to the recent forecast report issued by U.S. Dept. of the Interior, Minerals Management Service (MMS) [2], Gulf of Mexico (GOM) oil production is forecast to increase significantly over the next several years. The anticipated production will possibly be reaching 1.8 million barrels of oil per day.

In addition to the environmental considerations in deep water productions, there are many technical challenges which remain to be solved. Deepwater operations are a very complex, risky and costly environment and often require significant amounts of time between initial exploration and first production. However, there was a shift toward deeper water over time, and the number of deepwater discoveries continues at a steady rate [2].

In addition to the significant number of deepwater discoveries, the flow rates of deepwater wells and the field sizes of deepwater discoveries are often quite large. These factors are critical to the economic success of deepwater development. Figures 1.1&1.2 illustrate the estimated sizes and locations of proved deepwater fields and show the importance of the deepwater production from Gulf of Mexico to the Nation's energy supply [2].

Therefore, it is very important for deepwater crude oil producers to search for any opportunity that can contribute to save the cost of processing this oil. A special focus on finding solutions and providing the needed creativity and innovative technologies will allow economic developments in this field. This study is an attempt to reduce significant cost associated with transporting the crude oil over considerable distances through undersea pipelines from wellhead to platform.

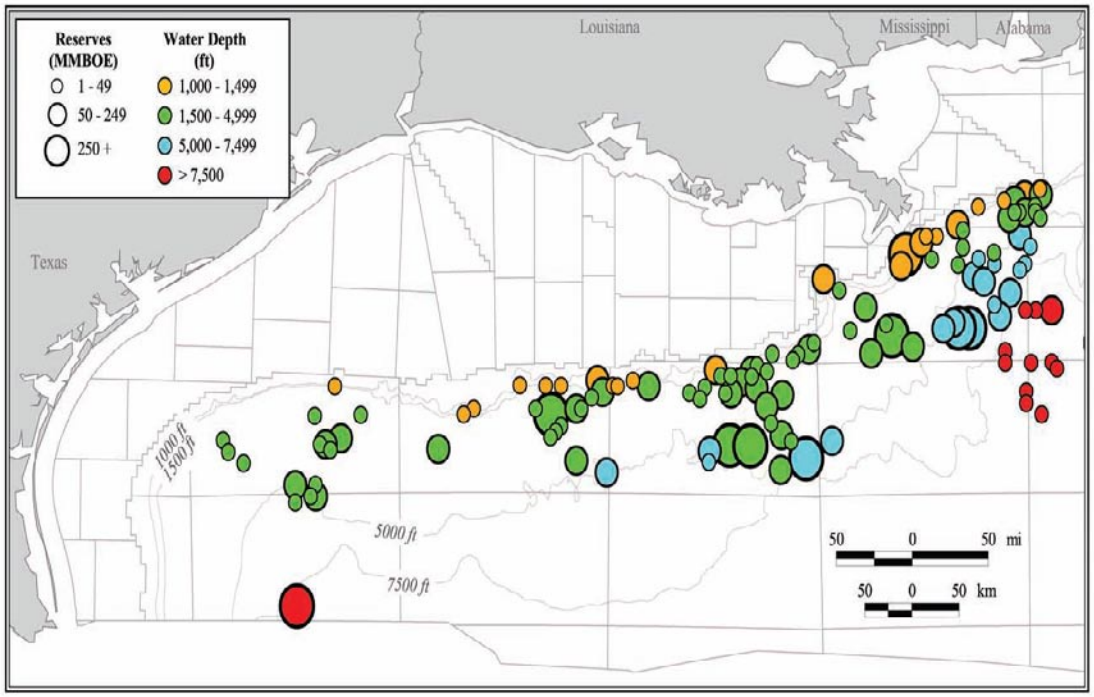

Figure 1.1 Estimated volumes of proved deepwater fields in the Gulf of Mexico [2].

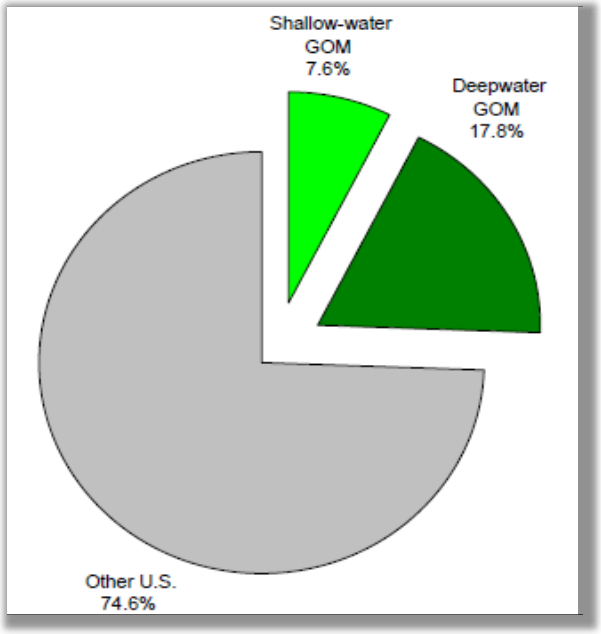

Figure 1.2 Estimated U.S. oil productions in 2007[2].

1.2 Problem Statement

Presence of emulsions is very common in the petroleum industry. They form naturally during the crude oil production and their presence may have a strong impact on the crude oil production and facilities. In general, those emulsions form from flowing through valves, chokes or pumps and are stable due to presence of natural surfactants existing in the crude oil phase. It is known that the viscosity of water-in-oil (W/O) emulsions can be strongly increased by increasing its water volume fraction and by decreasing the temperature. Effective separation of crude oil and water is essential to ensure the quality of separated phases at lowest cost.

The problem of emulsion presence is even worse in the case of deepwater oil fields production since such fields are expected to operate at a full range of water cuts (0 to 90%) over the duration of the field life. Water breakthrough is often expected to occur early in the field life, due to water injection for pressure maintenance in reservoirs. Viscous crude oils tend to emulsify readily, creating problems that are related to the increased emulsion viscosity, anticipated especially at higher water cuts in case of high inversion point. In addition to that, the temperature of crude oil varies widely along the flow from the reservoir to production platform. So the crude oil has to flow for several hundred meters through pipelines at the subsea condition where the temperature could be as low as 4 ^{o}C. Such low temperature values at subsea result in even more viscous fluids which have apparent viscosities significantly exceeding the oil viscosity itself.

Reducing such a high viscosity requires better understanding of emulsion properties. Separation topsides can also be an issue; emulsions can be very stable depending on the properties of the oil and may not easily break under gravity. Therefore, the use of chemicals that work as demulsifiers is commonly employed. Injecting the chemical subsea, either at the manifold or at the tree, can obtain great benefits as it will reduce pressure drop in pipelines and/or enhance the emulsion separation and handling.

Hence, it is important for the industry to find an efficient way of testing and evaluating these chemicals in the lab before applying them in the field. An efficient testing method will lead to an optimization and potential reduction of the quantity of the chemical needed for this purpose, resulting in monetary and most important, environmental benefits. So far, mainly bottle testing has been employed to conduct such measurements. The use of nuclear magnetic resonance (NMR) method will help in characterizing an emulsion and evaluating chemicals' effectiveness to break/invert it. This study focuses on characterizing of water-in-oil emulsions, that formed in deepwater production, by nuclear magnetic resonance (NMR) and studying their rheological behavior at different operation temperatures with and without demulsifiers present.

1.3 Objectives

The main objective of the project is to study and characterize emulsion stability for deepwater oil fields and evaluate chemicals' effectiveness to break/invert such emulsions in order to reduce their viscosity. This study will, specifically, focus on the viscosity of the emulsions created at different temperatures and their tendency to separate with and without the injection of commercial de-emulsifiers. In addition to the bottle testing, the identification of the separation is conducted with the use of NMR technique that can obtain quick information on phase distribution of the emulsion under study. Furthermore, the use of viscosity measurement is also applied to determine the rheological behavior at different operating conditions. Transporting emulsion as water-in oil type, oil continuous, increase the viscosity and, therefore, could have cost impact associated with high pumping requirements. Inverting this type of emulsion into oil-in-water will decrease the viscosity as the continuous phase will change to water and consequently help reducing the cost of pumping. This study could help in identifying whether it is more cost effective for crude oils of moderate viscosity to add a demulsifier to produce coalescence and hence separate/invert emulsion without depending on only conventional bottle testing or sampling.

In this thesis, Chapter 2 presents an overview of the theoretical background and summarizes the basic knowledge on emulsions. These include the emulsion properties, stability, rheology and the demulsification mechanisms used to destabilize emulsion.

Chapter 3 illustrates the use of low-field nuclear magnetic resonance, NMR, and MRI techniques and how they can be effectively utilized to estimate and characterize the emulsion properties.

After that, Chapter 4 is devoted to explain the experimental procedures and the materials used in this work. The procedures of executing the NMR experiment and emulsion preparation method are also described.

The results obtained from this work along with detailed discussion are then described in Chapter 5. Finally, Chapter 6 highlights the conclusions obtained from this work and proposes some possible future ideas that can be applied in the extension of this work.

.

CHAPTER 2

THEORETICAL BACKGROUND

2.1. Basic Principles of Emulsions

Emulsions can be found in almost every part of the petroleum production and recovery process and can be encountered at many stages during drilling, producing, transporting and processing of crude oil. Emulsion can be defined as a dispersion of a liquid within another liquid. The stability is conferred by the presence of agents at the interfaces that may delay the spontaneous tendency of the liquids to separate. Such agents are most commonly molecules with polar and non-polar chemical groups in their structure usually referred to as surfactants- or finely divided solids. The dispersed phase is commonly present in an emulsion in the form of spherical drops [3].

Phase separation in emulsions is imposed by thermodynamics because as the oil and water form two continuous phases while they separate, the interfacial area and therefore the free energy of the dispersion are reduced. As a consequence, the characteristics of the emulsion (drop size distribution, mean drop size and other properties) cannot remain unchanged in time. Therefore, the stability of an emulsion refers to the ability of the dispersion to preserve its properties within a given timeframe [3]. Most of the petroleum emulsions that will be encountered in practice contain oil, water and emulsifying agents and exist in

a metastable state that has high potential barrier to prevent coalescence of the particles.

An emulsion can be classified according to different criteria. In the classic type of emulsion, the two immiscible liquids involved are water and oil. As should be clear from the foregoing discussion, either of these two liquids can be defined as the disperse phase. The disperse phase is sometimes referred to as internal phase, and the continuous phase as the external phase. Depending on which one is the disperse phase, emulsions of quite different physical characteristics are usually obtained [4]. The following types of emulsions are now readily distinguished in principle:

- Oil-in-water (O/W) for oil droplets dispersed in water
- Water-in-oil (W/O) for water droplets dispersed in oil
- Oil-in-water-in-oil (O/W/O) and
- Water-in-oil-water (W/O/W).

The last two types are called multiple emulsions and are also present in some cases in which the dispersed droplets themselves contain even more finely dispersed droplets of a separate phase. Thus, there may occur oil-dispersed-in-water-dispersed-in-oil (O/W/O) and water-dispersed-in-oil-dispersed-in-water (W/O/W) multiple emulsions. More complicated multiple emulsions are also possible.

Finally, the emulsion formation process is called emulsification and it can be made by the action of devices such as a turbine blender, an ultrasonicator, or by the flow of the two phases through a membrane, static mixer or porous

medium [3]. Spontaneous emulsification can also occur when the phases are contacted [5] and can also occur, for example, by chemical reactions [6] or by the nucleation of one phase in another due to a reduction in temperature.

2.2. Emulsion Properties

2.2.1. Morphology of Emulsion

The morphology of emulsion means its presence as either W/O, O/W or multiple emulsions. It is the most basic characteristic of an emulsion, and there are usually some qualitative procedures that can be used to distinguish emulsion type. These are based on the observation of a physical phenomenon that depends on the prevailing polarity in the continuous phase [3]. The morphologies of some different type of emulsions are shown in Figure 1.

Contacting a drop of the emulsion with water or oil and observing whether the external phase is miscible or not with it is one of the simple methods that can be used to distinguish between simple and multiple emulsions. However, results from this type of test are sometimes unclear and do not allow to differentiate between them. The electrical conductivity measurements can also be used to determine the type of emulsion. The aqueous phase in an emulsion usually contains electrolytes and in most cases non-polar liquids exhibit very low electrical conductivity. Therefore, the conductivity of emulsion is very high when the aqueous phase is continuous and very low when the oil is the continuous phase [7]. Moreover, the optical microscopy method can also be used to discern

between simple and multiple emulsions because of the difference between the water and oil phase under microscopy observation.

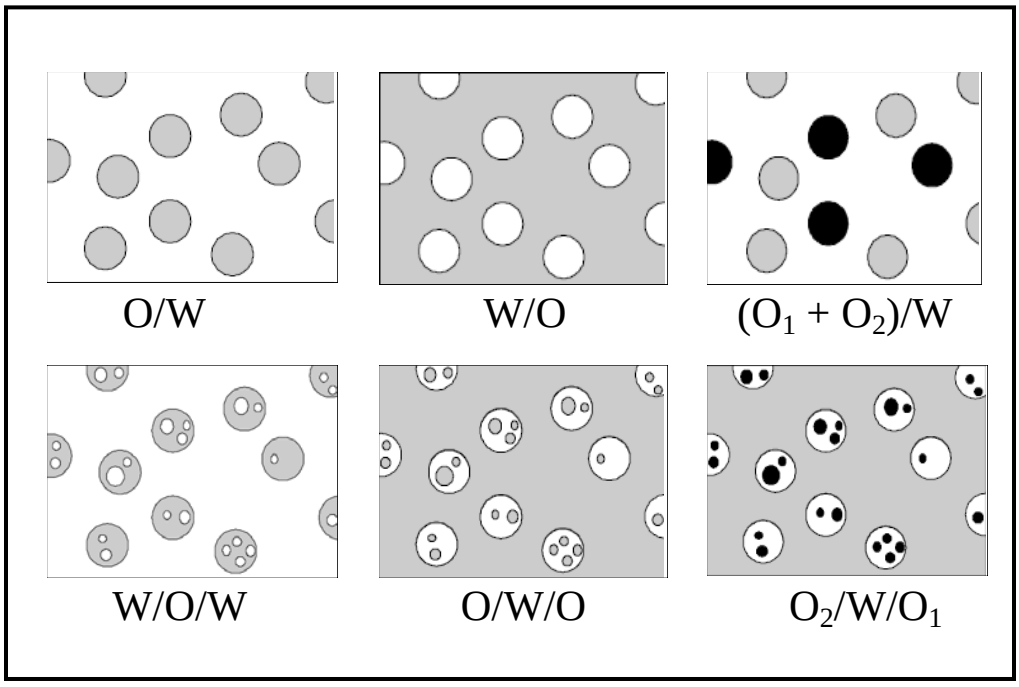

Figure 2.1: Morphologies of different type of emulsions [3].

2.2.2. Phase Inversion

The phenomenon of phase inversion refers to the process whereby the dispersed and continuous phases of an emulsion are inverted or suddenly change form, from O/W emulsion to W/O emulsion or vice versa. Phase inversion in emulsion can be one of two types: *transitional inversion* and *catastrophic inversion.* The former is induced by changing factors, such as temperature or salinity, which affect the affinity of surfactant towards the two phases. Changing the *Hydrophile-Lipophile Balance* (HLB) of an emulsion, which depends on the

nature and concentration of emulsifying agents, can lead to inversion. Substantial amounts of literature reviews on this type of inversion can be found elsewhere [7, 8].

The *catastrophic inversion* is induced by increasing the volume fraction of the dispersed phase. This inversion usually occurs when the internal volume fraction exceeds some specific value, usually close to the limit of critical close-packing, 0.64 for random packing [9] and 0.74 for ordered packing [4] (the maximum possible packing of monodisperse spheres has volume fraction of $\pi/\sqrt{18} \approx 0.74$) for spheres with identical size. Above this limit, droplets are compressed against each other and the interfaces are deformed causing the emulsion to adopt a foam-like structure.

Emulsion viscosity tends to increase with volume fraction of dispersed phase. This increase is because of droplet crowding in an emulsion and causes non-Newtonian flow even before reaching the close-packing value (≈0.74), where starts to deform from their original shape as predicted by Becher [7]. The effect is greatly enhanced in more concentrated emulsions where the drops become polyhedral. Such highly concentrated emulsions also exhibit a yield stress. Arirachakaran et al [10] conducted an extensive study on oil-water flow in horizontal pipes for various viscosity values. They described the morphology of emulsion as function of water fraction as shown in Figure 2.2. It was shown that inversion can be achieved by increasing water cut where the system has no surfactant added to the emulsion and is maintained at constant temperature and shear.

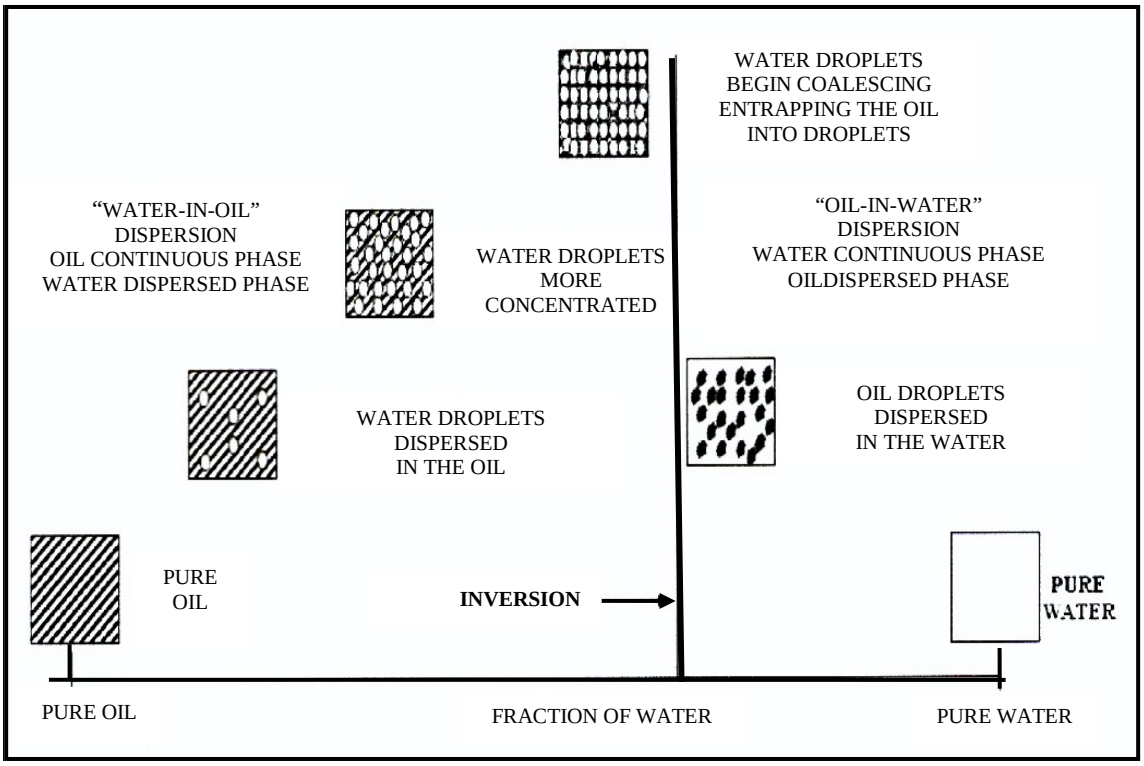

Figure 2.2: Schematic of Inversion Process for Water-Oil Flow [10].

There are other factors that have a bearing as well including the nature and concentration of the emulsifiers and physical influences such as temperature or the application of mechanical shear. The emulsification protocol characteristics which indicate the way the emulsion is made or modified or how the formulation or composition are changed as a function of time or space, can also be considered to be among the factors that phase inversion depends on [11, 12].

Estimation of emulsion inversion point is important to improve viscosity correlations. Therefore, many attempts to develop mathematical models for phase inversion in emulsions can be found in literature. Some of these models were based on experiments carried out in a stirred vessel, where phase inversion

was detected by a jump in emulsion conductivity [13], while others were based on experiments carried out in horizontal pipes to simulate two-phase flow of oil-water [14].

2.2.3 Drop size distribution

Characterizing an emulsion in term of a given droplet size is very common. The emulsion structure is usually characterized by its drop size statistical distribution. This is important in a number of respects: knowledge of size distribution provides information on the efficiency of emulsification process, and the monitoring of any changes in the size distribution as the emulsion ages gives information on the stability of the system. In practice, drops in emulsions always exhibit finite polydispersity in their sizes, which usually range between 0.1 μm and 1 mm. The corresponding drop size distribution is a statistical inventory of the dispersed phase. Valuable information can be obtained because the sizes of the droplets affect other properties of the emulsion such as its stability and rheology. The drop size distribution can be seen as the fingerprint of the emulsion characterization.

A number of studies have been performed with the aim of determining the drop sizes distribution in emulsions, including microscopy, photomicrography, video-microscopy (VM), light scattering, Coulter counting, turbidimetry, nuclear magnetic resonance (NMR) and others as will be discussed in the next *chapter*.

Whereas the collection of sizes in an emulsion is discrete, the number of drops is usually large enough to allow describing its size distribution with a continuous mathematical expression, most commonly a probability distribution function (p.d.f.) taken from statistics [3]. It is possible to determine the parameters of this distribution function as an analytical expression. A frequently used form is the log-normal function as defined in Eq.2.1.1below. This appears to be a reasonable description of the droplet size distribution of many emulsions [15, 16]. Moreover, it has only two parameters which make it convenient for modeling purposes [3, 17].

$$P(a) = \frac{1}{2a\sigma\sqrt{2\pi}} \exp\left(-\frac{(\ln 2a - \ln d_0)^2}{2\sigma^2}\right) \qquad (2.1)$$

Here *a* is the droplet radius, d_0 *represents* the diameter median and σ is the geometric standard deviation of the distribution or the measure of the width of the size distribution. There are some other cases where the lognormal distribution is not observed and an alternative distribution function must be adopted empirically. Figure 2.3 shows the drop size distributions that are commonly found in emulsions.

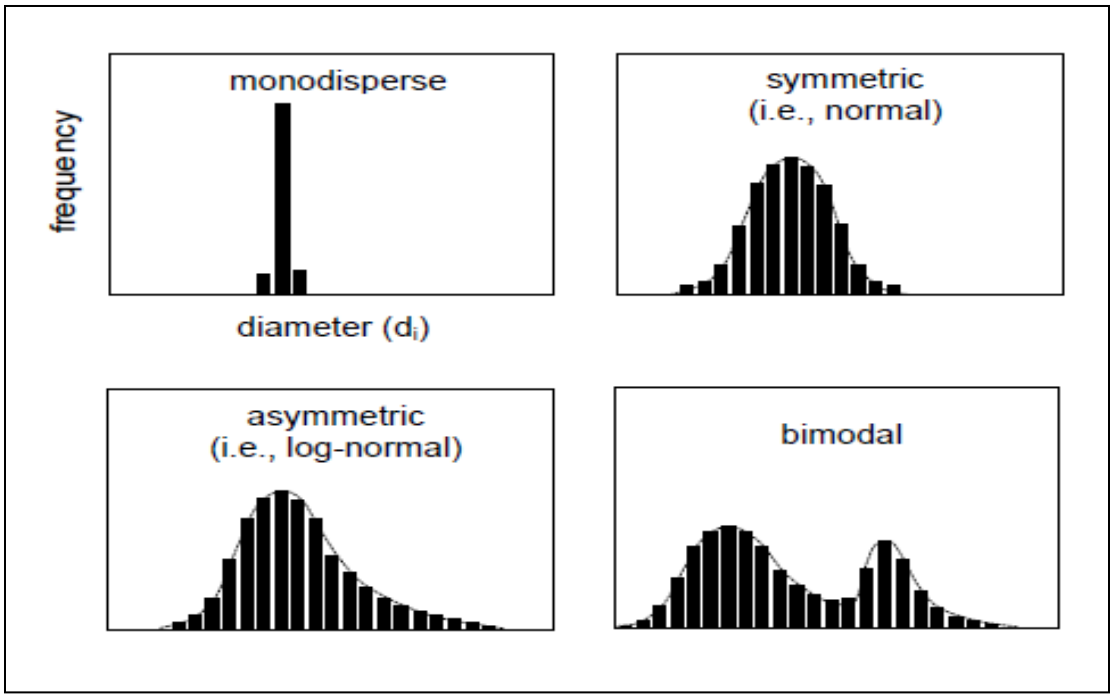

Figure 2.3: Drop size distributions commonly found in emulsions [3].

In these cases, an alternative distribution function must be adopted empirically. The most commonly reported characteristic of an emulsion is the mean drop size. Calculations of various types of average size are shown in Table 2.1. In addition, to decide which averages of those listed in Table 2.1 are more applicable, the property of the emulsion of primary interest should be considered [3].

Chapter 3 will demonstrate how the lognormal probability distribution function can be utilized to find the drop size distribution in emulsion sample.

Table 2.1: Mean drop sizes used to characterize emulsions [1, 18]. Here, d = 2a.

Descriptive name (alternative found in literature)	*Symbol (alternative)*	*Discrete distribution*	*Continuous distribution*[a]
Number-length mean (arithmetic mean)	d_{NL} (d_{av})	$\frac{\sum d\Delta N}{\sum \Delta N}$	$2\frac{\int ap(a)\mathrm{d}a}{\int p(a)\mathrm{d}a}$
Number-surface mean (surface mean)	d_{NA} (d_S)	$\left(\frac{\sum d^2\Delta N}{\sum \Delta N}\right)^{1/2}$	$2\left(\frac{\int a^2 p(a)\mathrm{d}a}{\int p(a)\mathrm{d}a}\right)^{1/2}$
Number-volume mean (volume mean)	d_{NV} (d_V)	$\left(\frac{\sum d^3\Delta N}{\sum \Delta N}\right)^{1/3}$	$2\left(\frac{\int a^3 p(a)\mathrm{d}a}{\int p(a)\mathrm{d}a}\right)^{1/3}$
Length-surface mean (linear mean, length diameter mean)	d_{LA} (d_{21})	$\frac{\sum d^2\Delta N}{\sum d\Delta N}$	$2\frac{\int a^2 p(a)\mathrm{d}a}{\int ap(a)\mathrm{d}a}$
Length-volume mean (volume-diameter mean)	d_{LV} (d_{31})	$\left(\frac{\sum d^3\Delta N}{\sum d\Delta N}\right)^{1/2}$	$2\left(\frac{\int a^3 p(a)\mathrm{d}a}{\int ap(a)\mathrm{d}a}\right)^{1/2}$
Surface-volume mean (Sauter mean diameter, surface mean)	d_{AV} (d_{32})	$\frac{\sum d^3\Delta N}{\sum d^2\Delta N}$	$2\frac{\int a^3 p(a)\mathrm{d}a}{\int a^2 p(a)\mathrm{d}a}$
Volume-(or weight-) moment mean [De Brouckere mean size, volume-(or weight-) mean]	d_{VM} or d_{WM} (d_{43})	$\frac{\sum d^4\Delta N}{\sum d^3\Delta N}$	$2\frac{\int a^4 p(a)\mathrm{d}a}{\int a^3 p(a)\mathrm{d}a}$

[a] Expressions for continuous distribution functions are obtained from their corresponding discrete definition in the limit of classes of drop sizes Δx infinitesimally small, with x = d, ln*d* or log*d* according to the selected size scale (see references [3] and [18] for details).

2.3. Emulsion Rheology and Shear Viscosity

Among the important properties of emulsions are their flow properties, in other words their rheology. Rheology in general is defined as the study of the deformation and flow of materials under influence of an applied shear stress. The rheological behavior of emulsions has been of great interest not only for fundamental scientific understanding but also for practical industrial applications [19, 20]. The rheological behavior of an emulsion can be either Newtonian or non-Newtonian depending upon its composition. At low to moderate values of dispersed phase concentration, emulsions generally exhibit Newtonian behavior. In the high concentration range, emulsions behave as shear-thinning fluids [21].

For the shear-thinning liquids, emulsions can be described by apparent shear viscosity η, which is similar to that of pure fluids. From Newton's law, η is the proportionality coefficient (or ratio) between shear stress (τ_{ij}) and rate of strain (or shear rate, γ_{ij}), $\eta = \tau_{ij} / \gamma_{ij}$.

Factors affecting the shear viscosity of an emulsion are the viscosity of the continuous phase (η_C), the dispersed phase content (φ), the viscosity of the dispersed phase, shear rate, temperature and the mean size and size distribution of droplets. The viscosity increases with the dispersed phase content due to interactions among droplets. If the pressure of a given emulsion sample is constant the main factors affecting the viscosity are the concentration of the dispersed phase and temperature. In the following sections some models that take into account these two factors are described.

2.3.1. Models at constant temperature

Since the emulsion viscosity is directly proportional to the continuous phase viscosity (η_C), most of the viscosity correlation equations proposed in literature are written in terms of relative viscosity (η_r) where:

$$\eta_r = \frac{\eta}{\eta_C} \qquad (2.2)$$

One of the earliest studies developed by Einstein [22, 23] from hydrodynamic considerations on suspensions of hard spheres:

$$\eta_r = (1 + 0.25\,\varphi) \qquad (2.3)$$

This equation is valid for dilute colloidal dispersions where (φ<0.02) and take into account the viscosity of continuous phase and assumes that the dispersed phase are solids or act like solids. Later correlation proposed by Taylor [24] considered the effect of both phases on the viscosity of emulsion with small concentration of dispersed spherical drops:

$$\eta_r = 1 + \left[0.25\left(\frac{k + 0.4}{k + 1}\right)\right]\ \varphi \qquad (2.4)$$

where k is the ratio of the viscosity of the dispersed phase to the continuous pahse:

$$k = \frac{\eta_D}{\eta_C} \qquad (2.5)$$

This equation reduces to Einstein's model (Eq.2.3) for the case when the dispersions are spherical solid particles where the ratio tends to infinity ($k \to \infty$).

As stated earlier, emulsions usually exhibit non-Newtonian behavior (shear-thinning fluids) at higher dispersed phase content. For this type of emulsion an empirical approach to correlate the viscosity data is needed. The corrected equation of Pal and Rhodes can be used [25]:

$$\eta_r = \frac{\eta}{\eta_C} = \left[1 + \frac{(\varphi/\varphi^*)}{1.187 - (\varphi/\varphi^*)}\right]^{2.49} \qquad (2.6)$$

here φ^* is the dispersed phase concentration at which the relative viscosity η_r = 100 and must be determined experimentally. The equation was based on an extensive amount of experimental data collected and can be used for both Newtonian and non-Newtonian emulsions.

2.3.2. Models with variation of temperature

All models stated above described the relation of viscosity with dispersed or continuous phase volume fractions only and ignored the significant effect of temperature. Ronningsen [26] has proposed a correlation for the viscosity of W/O emulsions as a function of the dispersed phase volume fraction and the temperature:

$$\ln \eta_r = a_1 + a_2 T + a_3 \varphi + a_4 T \varphi \qquad (2.7)$$

where a_1, a_2, a_3 and a_4 are the coefficients of the correlation. This correlation is based on the exponential relationship between the viscosity and the dispersed phase volume fraction originally suggested by Richardson [27] and was obtained

through an analysis of experimental data of viscosity at different temperatures and shear rates.

For crude oils and theirs fractions ASTM [28] recommends a modified form of Walther's model [29], for the variation of the kinematic viscosity (ν) with the temperature:

$$\ln(\ln z) = A - B\ln(T) \qquad (2.8)$$

$$z = \nu + 0.7 + f(v) \quad and \quad f(v) = e^{(-1.47-1.84\,v-0.51v^2)} \qquad (2.9)$$

If (ν), kinematic viscosity, is larger than 2x10^{-6} m^2/s, $f(v)$ is equal to zero where (z) is given by Eq.2.9, and (A) and (B) are parameters characteristic of each product, and (T) is absolute temperature (K). This is widely accepted mainly in the petroleum industry and recently verified by the work done by Farah et al [30]. They showed that this equation gives good correlation with the measured viscosity of water-in-oil emulsions as a function of both temperature and volume fraction of water. .

In addition, mean drop size in emulsion is another factor to consider when predicting the viscosity correlation. Friction between droplets is related to the interfacial area and therefore, an increase in viscosity should be expected when the surface-to-volume ratio of the dispersed phase increases [31]. Thus the apparent viscosity of an emulsion with smaller mean drop size should be higher than another with higher mean drop size. When the viscosity of the emulsion is high and emulsification is carried out by stirring, shearing is more efficient and the formation of smaller drops is favored [3]. Few correlations that account for the effect of droplet size on emulsion viscosity can be found in literature [7].

2.4. Emulsion Stability

Most emulsions are, by nature, thermodynamically unstable; that is, they tend to separate into two distinct phases or layers over time due to the high interfacial area and hence total surface energy of the system. Therefore, the emulsion characteristics (drop size distribution, mean drop size and other properties) will also change with the time. The stability of emulsion is characterized by the time-dependent behavior of its basic parameters.

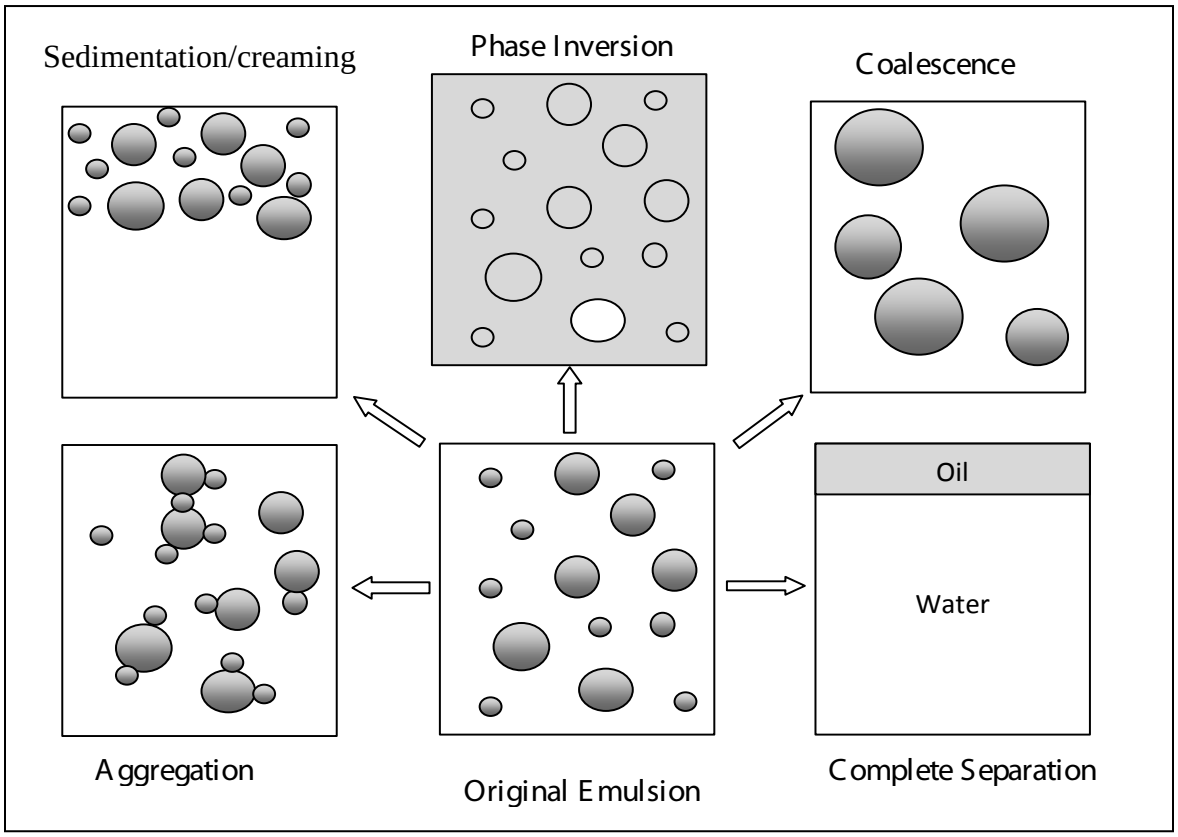

Figure 2.4: Destabilizing mechanisms in emulsions.

Various emulsion breakdown processes can be identified. Some of these instability mechanisms that lead to phase separation in emulsions are

represented schematically in Figure 2.4. These physical instability mechanisms are *Sedimentation* and *Creaming, Aggregation* and *Coalescence.* The theory of these physical breakdown processes will be briefly summarized below. In addition to these physical instability mechanisms, mass-transfer processes, such as Ostwald or Compositional ripening, can also take place in emulsions and their basic theory can be found elsewhere [32, 33].

2.4.1 Sedimentation and Creaming

Creaming is the opposite of sedimentation that results from density difference between the two liquid phases. The term sedimentation is used if the particles are displaced in the direction in which gravity acts (Δρ > 0). Otherwise (Δρ < 0), the process is referred to as creaming. The former applies to most W/O emulsions and solid dispersions, whereas the latter applies to most O/W emulsions and bubbles dispersed in liquids [3].

In both cases, the emulsion can be easily re-dispersed by shaking. If the density differences exist between the dispersed and continuous phases, dispersed droplets experience a vertical force in a gravitational field. This force is opposed by the fractional drag force. The resulting creaming (or sedimentation) rate v_S of a single droplet can be given be Stokes law:

$$v_S = \frac{2\, g r^2 (\rho_d - \rho_c)}{9\, \eta_C} \qquad (2.10)$$

in which r is the particle radius, ρ_d and ρ_c are densities of the dispersed and the continuous phases, respectively, η_C is the viscosity of continuous phase, *g* is the acceleration either due to gravity (*g* = 9.81 m/s2) or to centrifugation (*g* = $L\omega^2$, with *L* being the effective radius of the centrifuge and ω the angular velocity).

However, Stokes law (Eq.2.10) has several limitations and is strictly applicable only for non-interacting spherical droplets at low concentration with mono-disperse droplet size distribution (only satisfied for very dilute dispersions) and assumes that there is no internal flow within drops [34]. Thus an empirical relation is required taking the effect of the volume fraction of the dispersed phase into account.

If the volume fraction of the dispersed phase φ is significant (say $\varphi > 0.01$), so-called hindered sedimentation takes place. In general, the effect of increasing φ is to reduce the sedimentation rate due to hydrodynamic interactions among droplets. This is seen in expressions such that of Richardson and Zaki [35]:

$$\frac{\nu_{eff}}{\nu_S} = (1-\varphi)^n \qquad (2.11)$$

Here φ is the volume fraction of the dispersed phase, ν_{eff} is the effective terminal sedimentation velocity, *n* is an empirical constant, which ranges from 6.5 to 8.6.

2.4.2 Aggregation

Aggregation occurs when droplets stay very close to one another and form flocs. In other words, it is the process of forming a group of droplets that are held together. This process sometimes referred to as coagulation or flocculation. The approach that is most often referred to in emulsion literature to explain emulsion interaction is the so-called DLVO theory, developed by Derjaguin, Landau [36], and independently, Verwey and Overbeek [37], based on the long range London-van der Waals attractive forces and repulsive electrostatic forces between two close spheres.

For the case of two spherical particles, Hamaker [38] derived an expression for the London-van der Waals attraction by integrating the interaction energy dU_A over the total volumes of the two particles to obtain:

$$U_A = -\frac{A}{6}\left[\frac{2a^2}{h^2+4ah} + \frac{2a^2}{h^2+4ah+4a^2} + \ln\left(\frac{a^2+4ah}{h^2+4ah+4a^2}\right)\right]; \qquad (2.12)$$

$$where: \quad h = H - 2a$$

here ***a*** is particle radius, ***H*** is the center-center separation distance and ***h*** is the minimum distance between the two approaching surfaces. Eq. 2.12 can be simplified to:

$$U_A = -\frac{Aa}{12h} \qquad (2.13)$$

if h << a. In these expressions, A is the so-called Hamaker constant and depends on the dielectric properties of the two interacting particles and the intervening medium. When such properties are known, one can calculate Hamaker constant.

For two identical particles (subscript 1) interacting across a medium (subscript 2) [39]:

$$A = \frac{3kT}{4}\left(\frac{\varepsilon_1 - \varepsilon_2}{\varepsilon_1 + \varepsilon_2}\right)^2 + \frac{3h\nu}{16\sqrt{2}}\left(\frac{(n_1^2 - n_2^2)^2}{(n_1^2 + n_2^2)^2}\right) \qquad (2.14)$$

The hydrocarbon-water Hamaker constant usually has values in the range between 3 and 7 × 10^{-21} J [39].

On the other hand, the electrostatic interaction energy U_E for two approaching spheres exhibiting electrical double layers cannot be resolved analytically, and only approximate expressions have been provided, such as [40]

$$U_E = \frac{64\pi a c_0 N_A kT \varkappa_0^2}{\kappa^2} exp(-\kappa h) \qquad (2.15)$$

Here c_0 is the bulk concentration of the ionic specie, *NA* is the Avogadro's number (6.02 ×1023 mol-1), $\varkappa = tanh\,(ze_0\psi_0/4kt)$ with z being the magnitude of the ion valence, *e0* the electronic charge (1.60 × 10-19 C), κ^{-1} the so-called Debye length, which is a measure of the electrical double layer thickness, and ψ_0 the electrical potential at the interfaces. Eq. 2.15 is valid when the radius is much larger than the Debye length, i.e., $\kappa R >> 1$.

Now, the overall interaction energy *U* is given by:

$$U = U_A + U_E \qquad (2.16)$$

Here U_A and U_E are the attraction and repulsion energy respectively. Figure 2.5 shows a typical profile for *U* that can be calculated accordingly [3]. When two droplets are very close ($h \rightarrow 0$), attractive forces dominate and droplets are expected to aggregate irreversibly, which is referred to as coagulation. When *h*

reaches secondary energy minimum, droplets may form aggregates reversibly that can be re-dispersed which is usually termed flocculation. Generally aggregation is used to describe either coagulation or flocculation.

If $U_{max} \leq 0$, there is no energy barrier to prevent the two surfaces from approaching each other. In this case, so-called fast aggregation takes place. In contrast, if $U_{max} > 0$, an energy barrier must be overcome to achieve aggregation. This process is usually referred to as slow aggregation.

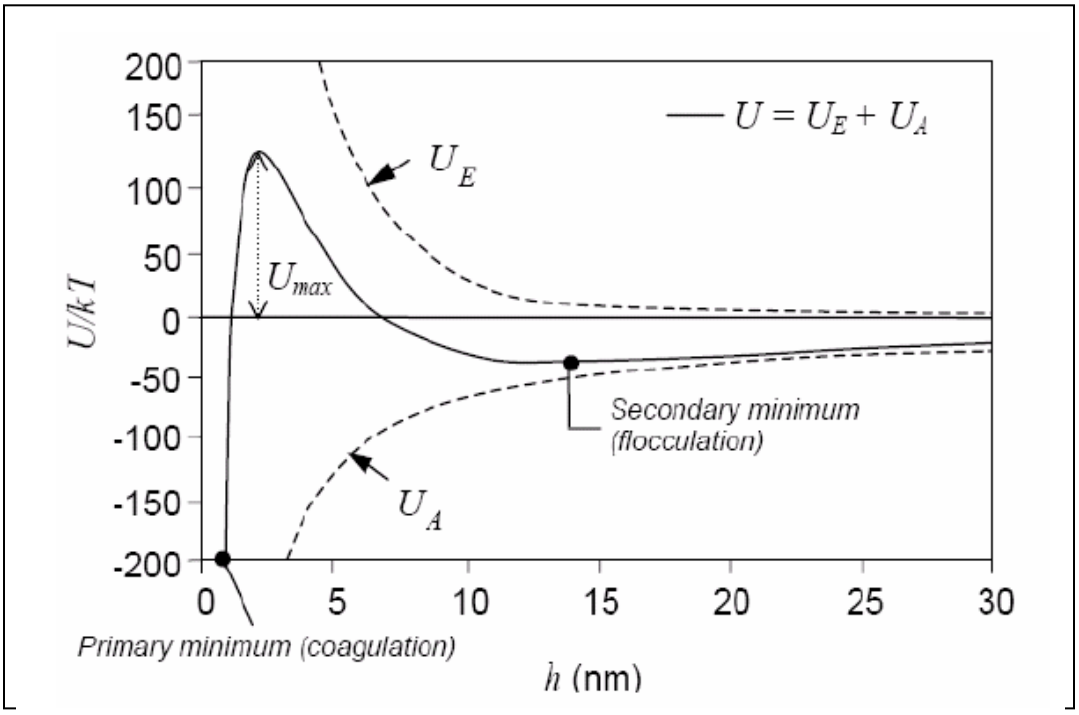

Figure 2.5: Energy of interaction between two spherical droplets [3]

The DLVO theory discussed above provides the basis to understand the role of inter-particle interactions on aggregation and emulsion stability. However, it is strictly valid in a reduced number of practical cases, particularly when emulsions are of the O/W type and are stabilized by small-molecule ionic

surfactants [34]. In the case of W/O emulsion, the theory can be extended to account for the steric repulsion mechanism, in which the molecules adsorbed at the interfaces are large and provide a physical barrier against flocculation and coalescence. In this case, an additional contribution to U due to steric repulsion, U_S, must be considered, i.e.,

$$U = U_A + U_E + U_S \qquad (2.17)$$

U_A and U_E are affected by the presence of the adsorbed molecules at the interfaces. U_S can be defined by two contributions, (a) a repulsive energy due to volume restrictions U_{VR}, and (b) an energy of mixing U_M, associated with the osmotic pressure that arises when the overlapping region of two approaching interfaces stabilized by macromolecules is depleted of solvent molecules [41]. Solvency is another important factor that has a significant effect on the overall interaction energy because it strongly affects the energy of mixing U_M. Another contribution to the overall energy of interaction arises in the presence of non-adsorbing macromolecules in the bulk phase, due to a phenomenon referred to as depletion interaction [3].

2.4.3 Coalescence

Coalescence is defined as the combination of two or several droplets to form a large drop. It takes place when the thin film of continuous phase between two drops breaks and they fuse rapidly to form a single droplet. The stability of an

emulsion system, therefore, depends on the rate of coalescence and it is obvious that the properties of this film will determine the stability of the emulsion.

Many authors have provided notable theoretical and experimental efforts to provide better understanding of the formation and thinning of a flat film between drops. Weber number is imported here, which refers the internal Laplace pressure P_L and external stress τ_{ext} exerted upon the doublet of drops]:

$$W_e = \frac{\tau_{ext}}{P_L} \qquad (2.18)$$

If W_e << 1, the stability criterion is suggested as [34]:

$$\frac{d^2U(h)}{dh^2} - \frac{dU(h)}{hdh} > -C\frac{\sigma}{R^2} \qquad (2.19)$$

Here *U (h)* is the interaction and repulsion energy in DLVO theory, $C > 0$ is a constant, σ is interfacial tension. From Eq. 2.19, coalescence would only take place if the drops get close enough as to reach the primary minimum (in Figure 2.5). When W_e >> 1, large flat films will form. Deformation is favored by large drop sizes and low interfacial tensions. In this case, coalescence is preceded by the drainage of the liquid present in the film. For the symmetrical drainage of a film of Newtonian liquid with viscosity η between two flat disks of radii *r* and separated by a distance *h* (*h/r* << 1) with the pressure difference ΔP, the rate of thinning of the film $-dh/dt$ is [42]:

$$-\frac{dh}{dt} = \frac{2r\Delta P}{3\eta}\left(\frac{h}{r}\right)^3 \qquad (2.20)$$

If the electrostatic repulsion is strong enough as to balance van der Waals attraction and the capillary pressure, the film is referred to as *common black film*

(*h* ~ 20-30 nm). If the electrostatic repulsion is weak and short range repulsive forces dominate instead, the film is very thin (*h* ~ 5-10 nm) and is referred to as *Newton black film* [3].

2.5. Demulsification

Chapter 1 briefly discussed the formation of the water-in-oil emulsions produced from deepwater oil fields and how the transportation problems may significantly affect the economics of petroleum industry. Crude oils are, in the vast majority of cases, produced together with formation water in the form of water-in-oil emulsions. These emulsions can be created either from the oil reservoir structure by flow through a porous medium, from well perforations or from processing after the well-head due to turbulence and pressure drop created by choke-valves and pipe flow constrictions [43–46]. In order to meet the oil specifications for production facilities, these emulsions need to be separated into their original phases. Two principal approaches of demulsification are chemical and physical methods. The chemical method is the addition of a proper demulsifier to the emulsion, and typical physical treatment techniques include heating, electrical, or a mechanical method such as centrifugation. Heating along with the addition of the demulsifier, which is called thermal chemical method, and electrical techniques, are the most popular methods in the industry [47].

As highlighted in the previous section (2.3), aggregation, sedimentation and coalescence are recognized as the principal mechanisms affecting water-in-

oil emulsion stability in many practical applications. Here, in this section, we are focusing on the destabilization of water-in-oil emulsions by chemical means.

2.5.1. Effect of surface-active materials

It is well known that the characteristics of a given crude oil play an important role not only in the formation of stable emulsions but also in deciding what method to use to destabilize these emulsions. Surface-active content of the oil, especially the amount of asphaltenes, naphthenates and resins, is crucially important.

The component of a crude oil that is soluble in light hydrocarbons such as n-pentane or n-heptane is referred to as the maltenes, and it contains three different classes of compounds: saturates, aromatics, and resins (SAR). Resins and asphaltenes exhibit similarities in chemical structure, and resins play a key role in the solubilization of asphaltene aggregates in crude oil. Asphaltenes are treated as molecules that are solubilized by oil where the molecular size and nonpolar van der Waals interactions dominate their phase behavior in reservoir fluids [48]. The chemical structure of the asphaltene affects its tendency to adsorb at the water/oil interfaces and therefore to stabilize emulsions [49].

In addition, naphthenic acids become surface-active when the corresponding salt (naphthenate) is formed after the ionization of the carboxylic group. Naphthenates could be considered as a sub-class of resins since the latter may exhibit other polar groups [3]. Goldszal et al. [50] concluded that naphthenates can play a key role in stabilizing water-in-oil emulsions. These

authors showed how emulsions of water dispersed in acidic crude oils from Angola and the North Sea exhibited a significant increase in stability, while the interfacial tension between the oil and the decanted water phase decreased, as the pH was raised. A plausible mechanism that was suggested to explain these findings is the ionization of naphthenic acid molecules initially present in the crude into naphthenates that migrate toward the water/oil interfaces and stabilize the dispersion via steric repulsion of the hydrophobic tails.

Demulsifiers are typically polymeric surface-active agents, as discussed in the next section. When added to emulsion, they migrate to the oil-water interface to displace the surface active material stabilizing the film and thus promote film rupture. This also allows the droplets of water phase to attract, collide and coalesce [51].

2.5.2. Chemical Demulsifier Efficiency

As stated before, chemical demulsification is in common use in oil fields. The demulsification ability of a demulsifier is mainly controlled by two factors: one is its hydrophilic-hydrophobic properties; the other is the ability to displace indigenous materials that are present at the water/oil interfaces, and to modify the mechanical and rheological properties of the films that prevent droplet coalescence [52, 53]. The structure of the demulsifier can influence both of above two factors. The demulsification mechanism of the demulsifiers is quite

complicated, and no demulsifier can be applied to break all kinds of crude oil emulsions [54, 55].

In formulation of demulsifiers, many components can play specific roles in their performance. A typical classification of demulsifiers can be according to their molecular weight as high molecular weight (HMW), low molecular weight (LMW) and pure solvents [56]. Amphiphilic molecules with moderate-to-high molecular weight (typically 3,000-10,000 Da), such as polyalkoxylated alkylphenolformaldehyde resins and complex block copolymers, are usually responsible for the separation of a large fraction of the dispersed aqueous phase. These molecules penetrate the stabilizing film at the water/oil interfaces and modify its compressibility and rheological properties by disrupting the tight conformation of adsorbed asphaltenes, which in turn favors coalescence [57].

Molecules with very high molecular weight (HMW) (>10,000 Da) such as ethoxylated/propoxylated amine polyols act as flocculants by adsorbing at the water/oil interfaces and interacting with like molecules also adsorbed at the interfaces of nearby drops. Different parts of a polyol molecule may adsorb on different drops, producing flocculation by a bridging mechanism. Such flocculation can enhance sedimentation rates. These molecules act more slowly due to their lower diffusivities, and are effective in removing remaining small water drops and tight, fine emulsions once most of the dispersed phase has been removed by the water droppers [58].

Low molecular weight (LMW) compounds (<3,000 Da), such as common surfactants, aid phase separation through several mechanisms [56]. Initially, they

exhibit high interfacial activity and diffuse faster than other components with higher molecular weight. Therefore, they can suppress more effectively the interfacial tension gradients.

Solvents are used to carry the active components. Since demulsifiers need to be surface active for their performance, solvents should be chosen which minimize aggregation. Aromatic hydrocarbons such as toluene and xylene and water-miscible hydroxycompounds are often used as solvents for demulsifiers [59].

The removal of water from emulsion is usually found to be affected by demulsifier composition, such as by an increase in the degree of ethoxylation (i.e., an increase in the hydrophilic-liphophilic balance (HLB); or by an increase in the number of polar groups or in aromaticity as found by Abdel-Azim et al. [60]. The authors showed in the same study that in all cases there is an optimum dosage for demulsification where addition of demulsifiers beyond this optimum resulted in an increase of the stability of the emulsion, probably due to the formation of a new stabilizing film in which the excess of demulsifier plays a significant role.

Also, oil phase aromaticity can play an important role in influencing demulsifier efficiency. Breen [58] shows that the efficiency of a given chemistry depends heavily on the H/C ratio of the oil phase. In this study, he found that demulsifiers are more effective when the oil phase exhibits high aromaticity.

A recent study by Peña et al [57] shows the effect of alkylphenol polyalkoxylated (EO + PO) resins and cross-linked polyurethanes of known

structure and composition on the stability and properties of brine-in-crude oil emulsions. The results were obtained experimentally via bottle tests, interfacial tension experiments, viscosity measurements, and nuclear magnetic resonance (NMR). The phenolic resins promoted coalescence of droplets. The fastest rate for water separation was obtained when the emulsions were treated with resins exhibiting intermediate EO + PO content. In contrast, cross-linked polyurethanes promoted flocculation and slow coalescence, and they were more effective with increase of molecular weight.

In the same work, they also added both types of molecules concurrently and found that water separation rates for some emulsions were significantly higher than those observed when they were used individually. In this case, it seems that at low concentrations polyurethanes contributed to increase the water separation rate, but they retarded coalescence when added at high concentrations. It was suggested that the cross-linked polyurethanes may act as “bridges” between droplets, both speeding sedimentation and increasing the probability for collisions among drops.

The most recent works by Al-Sabagh et al [61, 62] have highlighted the importance of surface-active properties on evaluating the demulsifiers’ performance in resolving asphaltenic crude oil emulsions. In this study, different factors affecting demulsification efficiency such as water-oil ratios, surfactant concentration, surfactant molecular weight, ethylene oxide content, alkyl chain length, and asphaltene content were investigated. The demulsifiers were

ethoxylated polyalkylphenol formaldehyde surfactants used to resolve asphaltenic crude oil emulsions.

They found that the demulsification efficiency increases by increasing the concentration, alkyl chain length and water content in the emulsion. Also it was found that the increase of asphaltene content in the crude oil impeded the demulsification efficiency. The optimal ethylene oxide content in the demulsifier molecule was found to be 40 units of ethylene oxide for maximum demulsification efficiency in their system. The maximum demulsification efficiency was obtained by TND5 (m.wt.=3800, EO=40 units). In addition, the surface, interfacial tension and hydrophilic lipophilic balance (HLB) of the investigated demulsifiers were studied.

The surface active properties can be used as a tool to evaluate the demulsifiers and the demulsification process. It has been found that if the surfactants are preferentially soluble in one phase, this phase tends to be the continuous phase of the emulsion. That is, if the surfactants are preferentially soluble in water, they are best for making oil-in-water emulsions and if they are preferentially soluble in oil, they are best for making water-in-oil emulsions [39]. The most unstable emulsions occur when surfactant is in “balanced” state in transition from being preferentially water soluble to preferentially oil soluble. Goldszal and Bourrel [63] suggested that a maximum in demulsification performance is achieved when the average interactions of the surface-active species are equal with oil and water and the interfaces have zero spontaneous curvature. The fact that the optimum demulsification performance occurs for

chemicals exhibiting intermediate hydrophilicity or balanced partitioning of the demulsifier between the liquid phases is widely accepted for many emulsions made with ordinary surfactants and oils [40]. It was the mechanism used by Peña et al [57] to explain their results and likely is consistent with the results of other studies where sufficient information was not obtained to indentify clearly the balanced state of zero spontaneous curvature.

CHAPTER 3

CHARACTERIZATION OF EMULSIONS BY NMR

3.1 Introduction

In order to characterize an emulsion, it is essential to determine the amount of phases present, the nature of dispersed and continuous phases, and the size distribution of the dispersed phase. The degree of polydispersity and average value of emulsion drop sizes also have a significant effect on some of the key properties such as emulsion stability [34,64] and the viscosity / rheological behavior [30,65-66] of emulsion. Therefore, many experimental techniques have been used to characterize emulsion properties based on either their electrical, scattering or physical properties. Examples of these techniques include Coulter counter, microscopy, X-ray and light scattering, acoustic spectroscopy and nuclear magnetic resonance (NMR). Several reviews on the emulsion characterization using different methods can be found in literature (Orr [67], Mikula [68]).

NMR spectroscopy offers the possibilities to measure relaxation time and diffusion data in an emulsion. This type of information might help in understanding the differences between emulsified water and continuous-phase water (or bulk water), especially in those emulsions that contain portions of both. Information on the restricted diffusion in the water phase helps in understanding

the effective size of the dispersed phase in an emulsion system and therefore, some of the factors affecting their stability.

This chapter focuses on how to estimate and characterize the emulsion properties using low-field nuclear magnetic resonance, NMR, techniques. A general fundamental description on the basics of NMR is introduced first. Then, different NMR techniques, namely CPMG and PGSTE, which usually used to measure the size of emulsion droplets, are discussed. Finally, the method of using T_1 weighted one dimensional (1-D) profile measurements to determine the transient behavior of emulsion is described.

3.2 Fundamentals

NMR is a spectroscopic technique and so it is very suitable for investigations of molecular arrangements and molecular dynamics. It is based on the fact that some nuclei are paramagnetic. Some nuclei, such as protons, have a permanent magnetic moment p. When a steady uniform magnetic field B_0 is applied on these nuclei, they take certain states which correspond to distinct energy levels. The magnetic moment p precesses around the direction of B_0 at the Larmor frequency $\omega_0 = \gamma B_0$, where γ is a constant. The nuclei exhibit net magnetization M in the direction of B_0. If a radio frequency (rf) pulse of a second magnetic field B_1 orthogonal to B_0 is applied, the net magnetization is rotated to an extent (typically 90º or 180º) that depends on the duration of the pulse. Transitions between neighboring energy levels take place due to the absorption

of electromagnetic radiation of characteristic wavelengths at Larmor frequency [69]. NMR is an extremely versatile spectrometer method because of the following reasons [70]:

1) It is not a destructive technique. This means that the system can be studied without any perturbation that will affect the outcomes of the measurement. The system can be characterized repeatedly with no time-consuming sample preparation in between runs.
2) A large number of spectroscopic parameters can be determined by NMR relating to both static and dynamic aspects of a wide variety of systems.
3) Low contribution to the system since RF has very low energy in comparison to other techniques.

Droplets in emulsions can be sized via NMR with at least two sequences of radio frequency and magnetic field gradient pulses [71]: the echo train (CPMG) and the pulsed magnetic field gradient spin-echo experiment (PGSE). The following sections describe these two NMR methods.

3.3 CPMG Pulsed Sequence

CPMG came from the initials of its original developers, Carr and Purcell [72], and of Meiboom and Gill [73], who later refined the technique. In the CPMG method, the spin echoes are produced by the a series of 180° rf pulses following the preparative 90° pulse, as shown in Figure 3.1. As time proceeds, relaxation

of the magnetization takes place and the amplitude of the spin-echo is generated after 180º re-phasing decay. In the experiment, decay of echo magnitude in the transverse plane is measured and the equation for the relaxation is [71]:

$$\frac{M_{xy}(2n\tau)}{M_{xy}(0)} = \sum_{i=1}^{m} f_i exp\left(-\frac{2n\tau}{T_{2,i}}\right);\ 0 \leq n \leq N;\ m < N;\ \sum_{i=1}^{m} f_i = 1 \qquad (3.1)$$

Here N is number of 180° rf pulses, M_{xy} (0) is the amplitude corresponding to the initial transverse magnetization, f_i is the fraction of protons with relaxation time $T_{2,i}$. T_2 distribution of the sample can be obtained using multi-exponential fitting to the raw data of spin echoes.

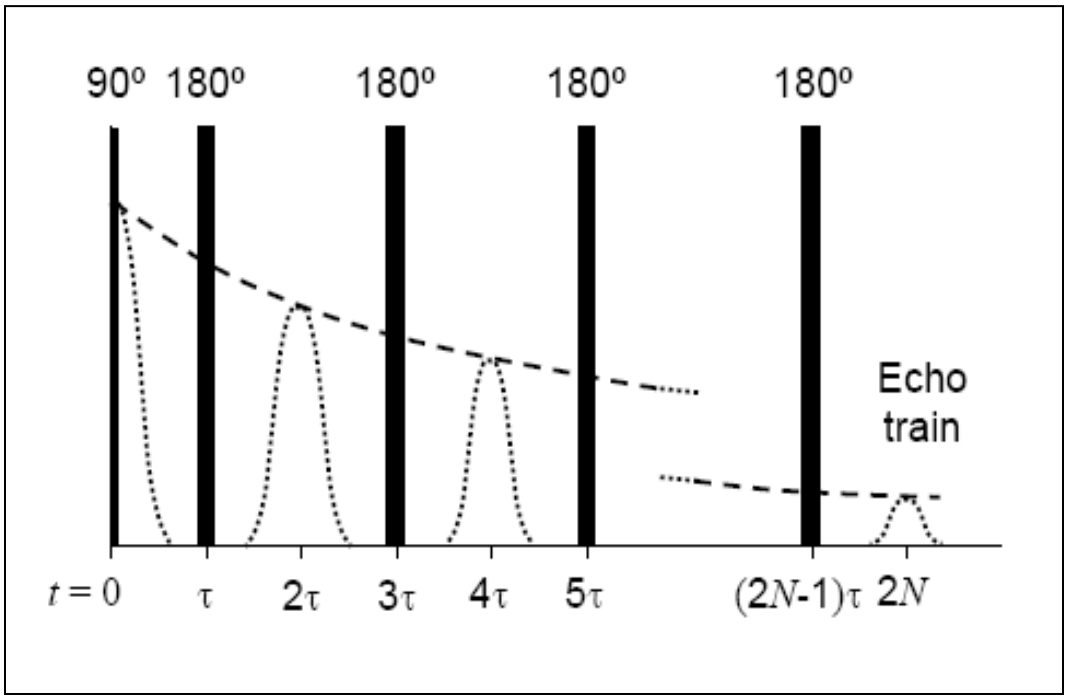

Figure 3.1: Sequence of events in a CPMG measurement [71].

The fact that in CPMG test the amplitude of the signal (for a given sample) is proportional to the number of spins in the sample allows relating the water/oil ratio to the T_2 distribution obtained by ^{1}H CPMG [74] provided that the phases can be distinguished:

$$\varphi_k \propto \frac{\sum(f_i)_k}{HI_k} \qquad (3.2)$$

φ_k is the volume fraction of phase *k* and *HI* is the hydrogen index, which is the ratio of proton density in the fluid and that in water [74]. In general, *HI* is about 1 for aqueous solutions, and 0.9~1.0 for most crude oils, except aromatic oils, which have value of 0.6~0.8 [71].

If Eq.3.2 holds, we have:

$$\varphi_{DP} = \frac{\left[\sum \frac{(f_i)_{DP}}{HI_{DP}}\right]}{\left[\sum \frac{(f_i)_{CP}}{HI_{CP}}\right] + \left[\sum \frac{(f_i)_{DP}}{HI_{DP}}\right]} \quad ; \quad \varphi_{CP} = 1 - \varphi_{DP} \qquad (3.3)$$

Here the suffix DP identifies the drop phase and CP identifies the continuous phase.

Among all available techniques, low-field NMR-CPMG has been considered to be the best for the determination of water content in heavy oil, bitumen and oilfield emulsions and it is quickly becoming a standard procedure in the oil industry for such tasks [75].

CPMG is also used to determine the droplet size in emulsions. If the relaxation of magnetization is modeled for an isotropic fluid confined in a planar, cylindrical or spherical cavity then it can be written as follows [76]:

$$\frac{1}{T_{2,i}} = \frac{1}{T_{2,bulk}} + \rho\left(\frac{S}{V}\right)_i \qquad (3.4)$$

Here ρ is surface relaxivity, $(S/V)_i$ is the surface to volume ratio of cavity i. For a sphere of radius a_i, $(S/V)_i = 3/a_i$. So, Eq.3.4 will be:

$$\frac{1}{T_{2,i}} = \frac{1}{T_{2,bulk}} + \rho\frac{3}{a_i} \qquad (3.5)$$

or

$$a_i = 3\rho\left(\frac{1}{T_{2,i}} - \frac{1}{T_{2,bulk}}\right)^{-1} \qquad (3.6)$$

In a given volume of sample, the number of protons present determines the signal amplitude. For this reason, the fraction f_i that is associated to each $T_{2,i}$ value renders a direct measurement of the fraction of droplets with the radius a_i. Hence, the drop size distribution of emulsions can be obtained from T_2 distribution. The following factors are required for Eq.3.6 to be used to calculate the volume-weighted drop size distribution of emulsions containing spherical droplets [71]:

(a) Measurements are performed in the “fast diffusion” mode, that the characteristic time scale t_D for molecule diffusion should be much smaller than that of surface relaxation t_ρ.

$$\frac{t_D}{t_\rho} = \frac{a_i/D}{a_i^2/D} \ll 1, \qquad whence, \quad \frac{\rho a_i}{D} \ll 1$$

(b) The surface relaxivity (ρ) and the bulk relaxivity (1/ $T_{2,\,bulk}$) of the drop phase are known. $T_{2,\,bulk}$ can be easily measured from a CPMG experiment.

(c) $T_{2,bulk}$ for the dispersed phase is indeed single-valued and not a distribution of characteristic bulk relaxation times

(d) Two independent sets of $T_{2,i}$ - f_i values can be resolved from the T_2 distribution of the emulsion for the oil and water phases, respectively.

But in some cases, T_2 distribution of dispersed phase is very close to that of continuous phase. As a result, CPMG method is not the most appropriate method because the T_2 distribution is not very distinguishable. The alternative methods for estimating the water fraction and drop size distribution will be discussed in the following sections.

3.4 PGSE and PGSTE Pulsed Sequences

The stimulated spin-echo pulsed magnetic field gradient experiment (PGSTE) was developed by Tanner [77]. It is useful for system exhibiting different values of its longitudinal (T_1) and transverse (T_2) relaxation times. The

stimulated pulsed field gradient spin-echo experiments consists of a rf 90º pulse, followed by a second rf 90º pulse at time τ. Then, a third rf 90º pulse reposition M_{xy} in the transverse plan. As a result of this sequence, a "stimulated" spin-echo is collected after the third pulse at time equal to that between the first two pulses. As shown in Figure 3.2 there are two magnetic field gradient pulses of absolute strength g and duration δ that are separated by a time span Δ. This sequence allows increasing diffusion time Δ with reducing the effect of extended relaxation upon the signal-to-noise ratio [78].

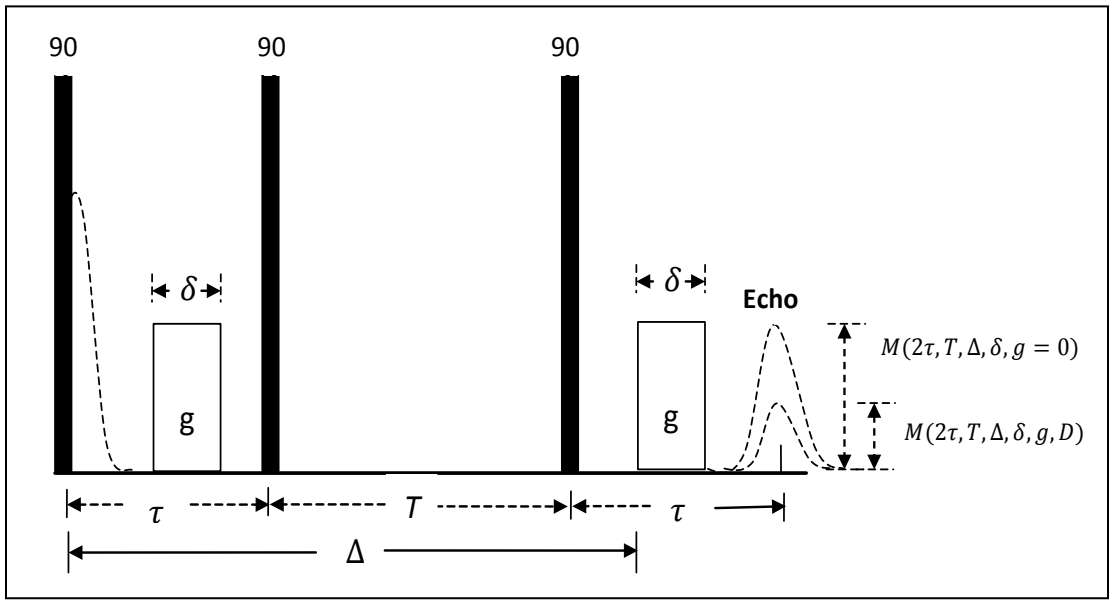

Figure 3.2: Sequence of events in a PGSTE measurement [78].

In the PGSE experiment, the amplitude ratio R of spin-echoes in the presence and absence of gradient pulses ($g > 0$ and $g = 0$) is measured.

$$R = \frac{M_{xy}(2\tau, g, \Delta, \delta, D)}{M_{xy}(2\tau, g = 0, \Delta, \delta)} \; ; 0 \leq R \leq 1 \qquad (3.7)$$

R is called the spin-echo attenuation ratio. In the PGSTE experiment, the same equation (3.7) for R can be used with replacing 2τ by $2\tau + T$ ($\approx \Delta + \tau$) . All expressions that will be derived below are also true for both method, PGSE and PGSTE [78].

For isotropic bulk fluids in which molecules can diffuse freely (Fickian diffusion), the expression for *R* is [79]:

$$R_{bulk} = exp\left[-\gamma^2 g^2 D\delta^2\left(\Delta - \frac{\delta}{3}\right)\right] \qquad (3.8)$$

The constant γ is the gyromagnetic ratio of the nuclei (γ = 2.67 × 108 rad.T^{-1}·s^{-1} for ^{1}H). This method can be used to measure self-diffusion coefficients.

The PGSE method is used to determine the drop size in emulsions. Eq.3.8 is limited to bulk fluids. But in many cases, the fluids are confined in small geometrics such as pores or droplets, which cannot diffuse freely. In these cases, for the restricted diffusion within a sphere of radius *a*, the attenuation ratio R_{sp} can be found from the following equations developed by Murday and Cotts [80]:

$$R_{SP} = \exp\left\{-2\gamma^2 g^2 \sum_{m=1}^{\infty} \frac{1}{\alpha_m^2(\alpha_m^2 a^2 - 2)}\left[\frac{2\delta}{\alpha_m^2 D} - \frac{\Psi}{(\alpha_m^2 D)}\right]\right\} \qquad (3.9)$$

$$\Psi = 2 + e^{-\alpha_m^2 D(\Delta-\delta)} - 2e^{-\alpha_m^2 D\Delta} - 2e^{-\alpha_m^2 D\delta} + e^{\alpha_m^2 D(\Delta+\delta)} \qquad (3.10)$$

Where α_m is the mth positive root of the equation:

$$\alpha\, a\, J_{5/2}(\alpha a) - J_{3/2}(\alpha a) = 0 \qquad (3.11)$$

and J_k is the Bessel function of the first kind, order *k*.

If $\Delta >> \alpha^2/2D$, $\Delta >> \delta$, Eq. 3.9 can be simplified as:

$$R_{SP} = exp\left[-\frac{\gamma^2 g^2 \delta^2 a^2}{5}\right] \qquad (3.12)$$

For emulsion with a finite distribution of (spherical) droplet sizes, the attenuation ratio of the dispersed phase (R_{DP}) can be calculated as the sum of the attenuation ratios $R_{SP}\,(a)$, weighted by the probability of finding drops with such sizes in the dispersion as first proposed be Packer and Rees [81]:

$$R_{DP} = \frac{\int_0^\infty P_v R_{SP}(a)\,da}{\int_0^\infty P_v\, da} \qquad (3.13)$$

Here $P_v(a)$ is the volume-weighted distribution of sizes. $R_{SP}\,(a)$ is determined from Eq. 3.9.

As discussed previously in section 2.2.3, the lognormal probability distribution function can be assumed to find the drop size distribution. Hence Eq.2.1 is used to find $P_v\,(a)$.

$$P(a) = \frac{1}{2a\sigma\sqrt{2\pi}} \exp\left(-\frac{(\ln 2a - \ln d_0)^2}{2\sigma^2}\right) \qquad (2.1)$$

Eq. 3.13 is useful to determine the drop size distribution when the following assumptions are valid [78, 81]:

(a) The spin-echo is originated solely from only one component of the emulsion, i.e. the drop phase. Thus,

$$R_{emul} = R_{DP} \qquad (3.14)$$

By this assumption, the method is limited to emulsions for which the signal from the continuous phase is concealed. Eq.3.13 also valid if the transverse magnetization of the continuous phase has relaxed completely and the natural (bulk) relaxation of the drop phase is small at the time the "stimulated" spin-echo is acquired. That is:

$$\left(T_{2,bulk}\right)_{CP}\Delta + \tau \ll \left(T_{2,bulk}\right)_{DP}$$

where $\left(T_{2,bulk}\right)_{CP}$ and $\left(T_{2,bulk}\right)_{DP}$ are the characteristic bulk relaxation times of the continuous and drop phases, respectively.

(b) The distribution of drop sizes is indeed lognormal, which is a real deficiency of the method. This is because the shape of the distribution is not resolved independently, but assumed a priori.

(c) The effect of surface relaxation on the amplitude of the spin-echo is negligible.

For continuous phase, Eq.3.8 is also valid. For a continuous phase with the effective diffusivity distribution $p\,(D_{CP})$, the equation for the attenuation is [78]:

$$R_{DP} = \frac{\int_0^\infty P_D(D_{CP})R_{bulk,CP}(D_{CP})dD_{CP}}{\int_0^\infty P_D(D_{CP})(D_{CP})dD_{CP}} \qquad (3.15)$$

The total attenuation for the emulsion can be written as:

$$R_{emul} = (1 - \kappa)R_{DP} + \kappa R_{CP}; \quad 0 \leq k \leq 1 \qquad (3.16)$$

κ is a parameter associated with the bulk relaxation of the transverse component of the magnetization of both phases and can be found from T_2 distribution as follows:

$$\kappa = \left[1 + \frac{\sum(f_i)_{DP}\, exp\left[-2\tau/\left(T_{2,i}\right)_{Dp}\right]}{\sum(f_i)_{CP}\, exp\left[-2\tau/\left(T_{2,i}\right)_{Cp}\right]}\right]^{-1}$$

$$\kappa \approx \left[1 + \frac{\varphi_{DP} HI_{DP} \sum(x_i)_{DP}\, exp\left[-2\tau/\left(T_{2,i}\right)_{Dp}\right]}{\varphi_{CP} HI_{CP} \sum(x_i)_{CP}\, exp\left[-2\tau/\left(T_{2,i}\right)_{Cp}\right]}\right]^{-1} \quad ; \; x_i = \frac{f_i}{\sum f_i} \qquad (3.17)$$

The determination of the drop size distribution consists of performing least-squares fit of the experimental data for R_{emul} with Eqs. 3.9 – 3.16, using $d_{gV,}$ $\sigma_{,}$ and κ as fitting parameters. If the T_2 distribution of the dispersed phase and the continuous phase are known, it is possible also to calculate the water fraction in the emulsion [78].

When the signal of the continuous phase is suppressed, or it has relaxed completely at the time the spin-echo is acquired, $\kappa \to 0$ according to Eq. 3.17. Hence, Eq. 3.16 reduces to Eq. 3.14.

3.5 T_1 weighted 1-D Profile Measurement

Magnetic resonance imaging (MRI) is sensitive to any NMR-active nuclei, such as protons. This allows one to distinguish different chemical environments in which these nuclei find themselves, including oil versus water. It was shown by Jiang et al [82] that NMR one-dimensional (1-D) T_1 weighted profile measurements can be utilized to distinguish the composition variation of the sample with position and time and hence determine the transient behavior of emulsion. The work in this thesis utilized the same experimental and calculation procedure developed by Jiang et al [82] to characterize the emulsion in term of its time dependant behavior.

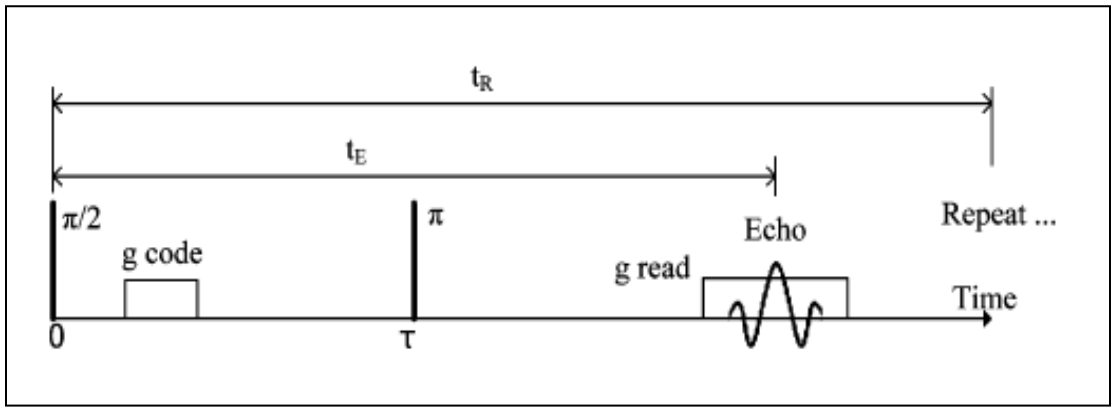

Figure 3.3: Sequence of 1-D profile measurement repeated at time t_W [82]

The sequence of events in the MRI 1-D profile measurement consists of a 90º radio-frequency (rf) pulse, followed by a rf 180º pulse at time τ. This rf 180º pulse is between two magnetic field gradient pulses with strength *g.* A spin-echo is collected at time t_E, as shown in Figure 3.3. The magnetic gradient is along the

vertical direction *z*. A Fourier transform of the spin-echo yields the signal amplitude for each position.

The amplitude of the spin-echo signal is [83]:

$$A = A_0 \left[1 - \exp\left(\frac{-t_R}{T_1}\right)\right] exp\left(\frac{-t_E}{T_2}\right) \qquad (3.18)$$

In some cases, one needs to perform a T_1 weighted spin density profile measurement in order to get contrast between oil and water based on their relaxation time differences. This is because the contrast in the hydrogen index is not large enough to give useful information about the oil and water concentration variation along the z-direction.

In this case, $t_E << T_2$, $exp\left(\frac{-t_E}{T_2}\right) \approx 1$, and the amplitude $A(z)$ at a given position z is given by:

$$A(z) = A_\infty \left[1 - \sum \varphi_i(z)\, exp\left(\frac{-t_W}{T_{1,i}}\right)\right] \qquad (3.19)$$

Here, φ_i is the volume fraction for component *i*. A_∞ is the amplitude when t_W is sufficiently long. The parameter t_W represents the waiting time ($t_W = t_R - t_E \approx t_R$); it is chosen to be intermediate between the relaxation times of the oil and the emulsified water, so that different phases can be distinguished.

For W/O emulsions, Eq.3.19 can be written as:

$$A(z) = A_\infty \left[1 - \varphi_{oil} exp\left(\frac{-t_w}{T_{1,oil}}\right) - \varphi_{water} exp\left(\frac{-t_w}{T_{1,water}}\right) - \varphi_{drop} exp\left(\frac{-t_w}{T_{1,drop}}\right)\right] \qquad (3.20)$$

Here suffixes oil, water and drop correspond to continuous oil, bulk water and water droplets, respectively.

The T_1 value of water is greater than for oil, so the attenuation of water is smaller than for oil based on the Eq.3.18. Thus in the profile results, the signal amplitude of water is smaller than that of oil. Based on the T_1 difference, the signal amplitudes of different phases in the emulsion become distinguishable.

If profile measurements are performed over time, the evolution of the emulsion (such as sedimentation and coalescence) can be obtained from the results. The detailed description on how to calculate the water fraction profile will be discussed in chapter 5.

CHAPTER 4

EXPERIMENTAL PROCEDURES

This chapter presents the experimental setup and resources used in this work. In the beginning, the materials used in this study including their properties and the tools used for measurements are discussed. Then, the procedures of executing the NMR experiment and emulsion preparation are described. The following section explains in detail some experimental protocols that were applied in order to find the optimal demulsifier. Then, the procedure of measuring the emulsion viscosity is described. Finally, the accuracy and reproducibility of the results obtained in this work are discussed.

4.1 Materials

The oil used in this study was heavy black crude oil (API gravity, about 26.5) obtained from a Gulf of Mexico deepwater field. To identify the presence of any additives in the crude oil sample, the interfacial tension (IFT) of this oil with synthetic seawater was measured using the pendant drop method. This method involves the determination of the profile of oil drop suspended in brine at mechanical equilibrium where the profile is determined by the balance between gravity and surface forces.

Water-in-crude oil emulsions were prepared by dispersing brine (3.5 wt.% NaCl) in crude oil. No additives were used to stabilize the emulsions. Related bulk fluid properties are listed in Table 4.1. Here the densities were measured by

using a Pycnometer and the viscosities were measured with a Brookfield DV-III + rheometer. For bulk fluid viscosity measurements, a spindle (type SC4-18, viscosity range = 1.3 - 30,000 mPa.s) is immersed in a cylindrical cell containing approximately 7 mL of sample, and it is further set to rotate at a given angular velocity. More detail on the operation mechanism of this viscometer will be presented in section 4.4. T_2 and diffusivity were measured using MARAN II NMR Spectrometer (2.2 MHz, Resonance Inc.).

Table 4.1 Bulk fluid properties at 30°C

Bulk fluids	**Density** (g/mL)	**Viscosity** (cP)	T_2 **peak** (s)	**Diffusivity** (10^{-9} m^2 /s)
Brine (3.5% NaCl)	1.02	1.34	2.6	2.4
Crude Oil	0.894	36.5	0.035	0.15

4.2 NMR Measurements

For NMR measurements, the emulsions were prepared at different water cuts. For each sample, a 60-mL batch of emulsion was prepared by mixing brine and crude oil in a flat-bottom NMR glass tube (outer diameter 48 mm, inner diameter 44 mm and length 230 mm) with a six-blade turbine as shown in Figure 4.1. Stirring was performed at about 1800 to 2100 rpm measured by using a Photo Tachometer; and the mixing time was 10 minutes. Prior to the emulsification process, the aqueous and oil phases were left in contact in an oven (30 ± 0.1 ºC) for 24 hours.

As described in Chapter 3, the T_2 distribution was obtained by using Carr-Purcell-Meiboom-Gill (CPMG) measurement, and the drop-size distribution of the emulsion was measured by restricted diffusion measurement (PGSTE). Also, to get the volume fraction profiles for different phases, a magnetic resonance imaging (MRI) one-dimensional (1-D) profile measurement was used.

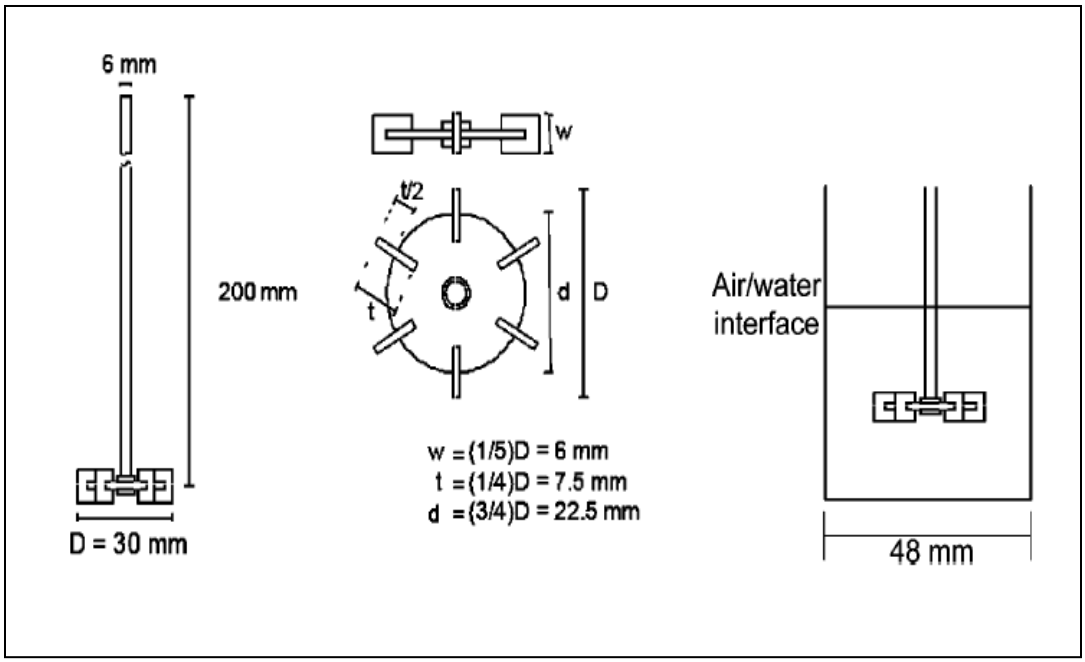

Figure 4.1 Sketch of the mixer and emulsion preparation [82].

4.3 Demulsifier Selection

In these experiments, the coalescers (or demulsifiers) are polyoxyethylene (EO)/ polyoxypropylene (PO) alkylphenolformaldehyde resins (referred to as PR_X) provided by Nalco Energy Services, L.P., with molecular weights around 3,500 Da and varying amounts of EO/PO groups in their structure with a constant

EO/ PO ratio of 3:1 as shown in Table 4.2. A plausible chemical structure for these compounds is shown in Figure 4.2.

Table 4.2 EO/PO content of the phenolic resins PR_X used in this experiment [57].

Phenolic resin	PR_1	PR_2	PR_3	PR_4	PR_5	PR_6
EO + PO in molecule (wt.%)	25 %	33 %	41 %	46 %	54 %	66 %

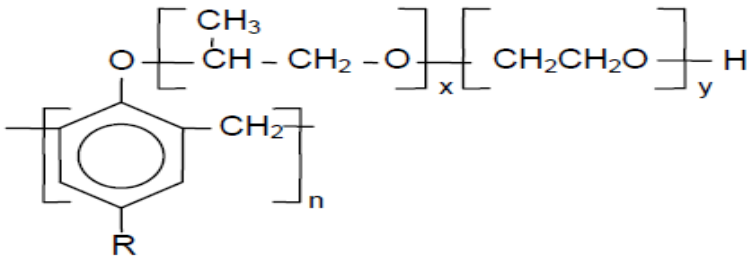

Figure 4.2 Plausible structures of EO/PO alkylphenolformaldehyde resins (PR_X) used in demulsification experiments [57].

A well known procedure called bottle testing was used in which different chemicals were added to bottle samples of an emulsion to determine which chemical, or coalescer, is the most effective at breaking, or separating, the emulsion into oil and water. In the experiment, series of six PR_X coalescers were added to labeled bottles containing same amounts of water-in-oil emulsion (50% water cut). First, batches of 20 mL fresh emulsion were added to the bottles

(outer diameter 25 mm), then 250 ppm of PR_X coalescer solution (50 µL 10 % PR_X xylene solution) was added to each emulsion sample. After that, all the samples were shaken by hand at the same time for one minute and then put into the required temperature medium (e.g. oven, oil or water baths). The bottle test was done for three different temperatures: 7 ^oC, 30 ^oC and 80 ^oC.

In addition to the bottle testing, viscosity measurements of emulsions with different coalescers, PR_X, were also used to further identify the optimal coalescer at different temperatures namely 15 ^oC, 25 ^oC, 50 ^oC, and 80 ^oC. In this experiment, the coalescer is added to a 20 ml sample of emulsion prepared at the desired temperature, and then it is shaken by hand for 1 minute. The emulsion then put into the viscometer that was programmed previously to read the change of viscosity with time at specific shear rate and temperature. The performance of coalescers, PR_X can be identified by how fast can each one lowers viscosity to a nearly constant value.

4.4 Viscosity Measurements

The apparent viscosities of emulsions undergoing phase separation were measured with the same Brookfield DV-III + Rheometer described above. A smaller diameter spindle (type SC4-31, viscosity range = 12 – 600,000 mPa.s) was used to measure the emulsions' viscosities with a cell containing approximately 10 mL of sample. This type of measurement is usually referred to as Couette method, and it measures the fluid parameters of shear stress and

viscosity at given shear rates. The principle of operation of this unit is to drive a spindle which is immersed in the test fluid. The viscous force of the fluid against the spindle is measured by the spring deflection. This spring deflection is measured with a rotary transducer. The measuring range of the unit (in centipoises) is determined by the rotational speed of the spindle, the size and shape of the spindle, the container the spindle is rotating in, and the full scale torque of the calibrated spring.

Before any measurement was made, the rheometer was checked with a calibration fluid (Brookfield Standard Fluid, 516 cp at 25 ^{o}C). Furthermore, each sample was pre-equilibrated for at least 12 hours to allow reaching the required temperature. The rheometer was thoroughly cleaned between measurements of different emulsion samples. The same turbine described in Figure 4.1 was used for emulsion preparation. Here, shorter bottles were used with almost the same diameter as the one used for NMR experiment to facilitate the ease of sampling and avoid wasting oil. A schematic diagram for the spindle and sample holder that were used to measure the emulsions' viscosities in this experiment is shown in Figure 4.3.

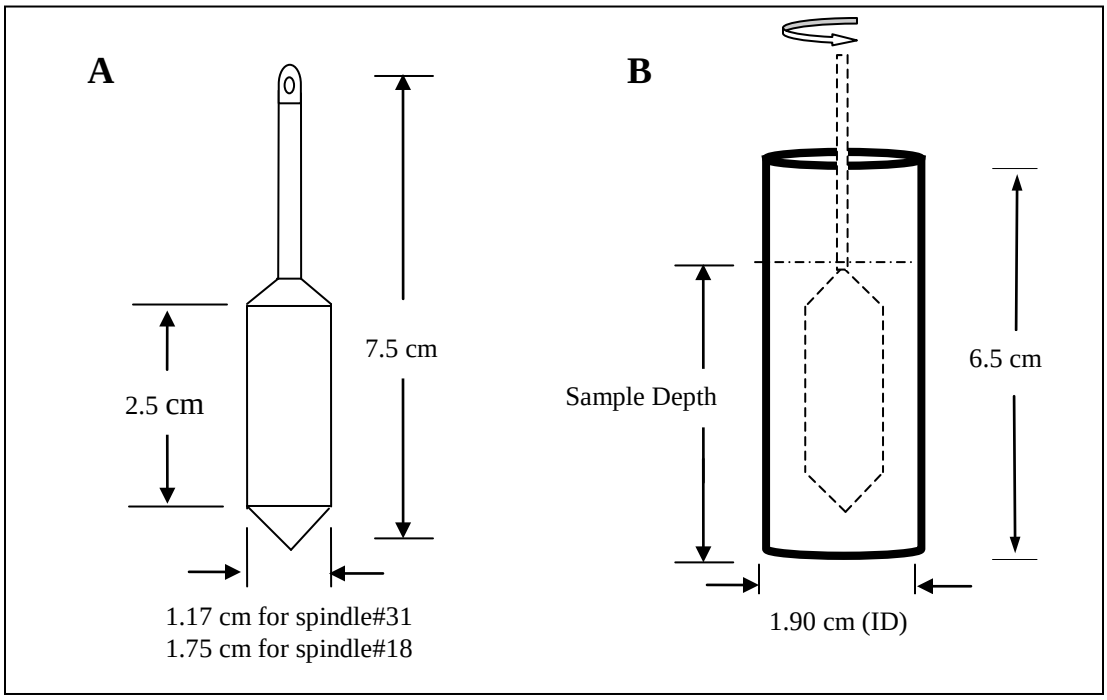

Figure 4.3 Schematic diagrams for the SC4 spindle (A) and sample holder (B) used for emulsion viscosity measurements.

Once the emulsion was made, the demulsifier to be tested was dosed in the required amount. As explained for the bottle tests, the sample was shaken by hand for 1 minute and an aliquot was placed in the cylindrical container of the rheometer. Viscosity measurements were performed for a range of temperatures. To maintain the required temperature, the container was placed within a jacket where fluid was circulated from the constant-temperature circulating bath. This bath is provided with auxiliary cooling devices for operation at or below ambient temperature. The spindle was set to rotate at different rpm. The rheometer device could be programmed to measure and automatically store in memory a previously defined set of user-specified parameters.

4.5 Accuracy and Reproducibility

A lot of variables, such as viscometer and spindle type, sample container size, sample temperature, bulk fluids used and the emulsion sample preparation technique, all contribute to affect the accuracy of viscosity measurements. To prevent errors, those variables were kept constant during each set of measurement. Brookfield Viscometers are designed to be accurate to within ± 1% of the full-scale range of the spindle/speed combination in use.

In this experiment, the effect of losing some of the light hydrocarbons components (by evaporation) especially in the high temperature range was estimated. The sample was weighed before it was put into the oven at 80 ^{o}C for about 12 hrs, and then the weight was measured again after opening the sample for about 20 min at ambient temperature, the estimated time required for emulsion preparation. The maximum weight lost was found to be less than 2 % of the original mass.

It is also worth mentioning that during emulsion preparation, the glass tubes' cleanliness and the mixer position were found to have significant effects on the reproducibility of the results. For these reasons, a special cleaning protocol was applied. After the normal cleaning with toluene and acetone, the glass tubes were further cleaned using Nochromix dissolved in sulfuric acid and then neutralized by sodium bicarbonate (NaHCO3) in order to get water wetted glass surface. Also, previously in the initial experiments, the mixer was placed in the center of the sample and operated directly at the desired speed of 1800 to 2100 rpm for 10 minutes. When using this preparation method along with the

normal glass tubes cleaning procedure, the results were not always reproducible especially near the emulsion inversion point (70% water cut). To avoid this, in the later experiments in addition to applying the new cleaning protocols, the mixer was initially placed in the center of the sample just below the interface and operated at about 1300 rpm for 1 minute, then further moved to the bottom of the container and operated at the required speed of 1800-2100 rpm for the remaining 9 minutes. This later method helped in minimizing vortex formation and intake of air bubbles and , therefore, getting a reproducible results

CHAPTER 5

RESULTS AND DISCUSSION

This chapter mainly discusses the results obtained in this study. The chapter starts with section related to crude oil property by measuring the interfacial tension of the oil sample. Section 5.2 discusses the characterization of 50% water-in-oil (W/O) emulsion using various NMR techniques with and without presence of demulsifier. The rheology of W/O emulsions made at different water volume fractions and at different temperatures is then presented in section 5.3. Finally, the selection of optimum demulsifier by using bottle testing assisted with viscosity measurements at different range of temperatures is discussed in section 5.4.

5.1 Interfacial Tension Measurements

Surface tension is a measure of the force acting at a boundary between two phases. If these attractive forces are between two immiscible liquids, like oil and water, they are referred to as interfacial tension. The surface and interfacial tensions of petroleum are important because they are indicative of the ease of formation and stability of emulsions and foams, that is, they indicate the relative interfacial properties of a crude oil sample. Interfacial tension (IFT) provides information pertaining to the presence and concentration of surface-active

agents. These compounds play an important role in the performance of emulsion systems [84].

Therefore, before starting any further experiments and once the crude oil sample was received, the interfacial tension (IFT) of this oil with synthetic sea water (3.5% NaCl) was measured using the pendant drop method. It was found to be approximately 30 mN/m at ambient temperature as shown in Figure 5.1. This relatively high tension confirms that the sample of crude oil supplied was not contaminated with additives such as corrosion or scale inhibitors.

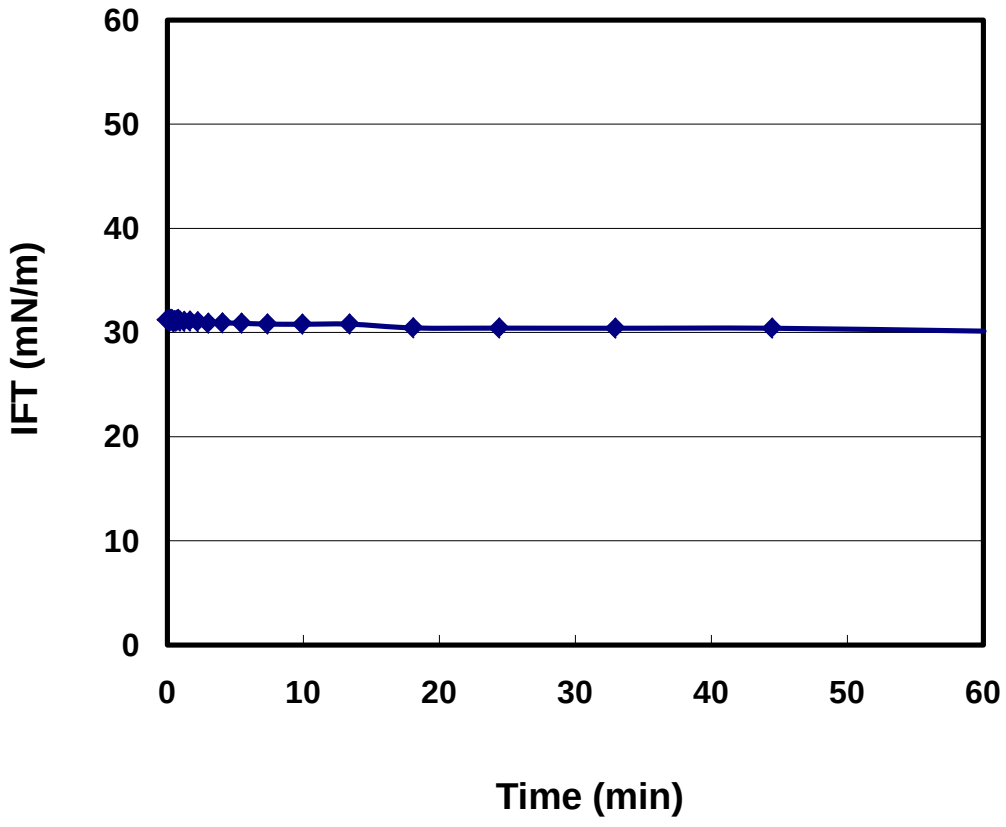

Figure 5.1 Interfacial tension (IFT) of sample crude oil with synthetic sea water (3.5% NaCl) at ambient temperature.

5.2 Emulsion Characterization by NMR

In this study, the emulsion properties were characterized by NMR measurement. The effects of a demulsifier that acts as a coalescer were investigated. Beside the bulk fluids, two 50 % (v/v) emulsion samples are studied here:

- Sample 1: emulsion without demulsifier and
- Sample 2: emulsion with PR_3 as a demulsifier

The reason for choosing PR_3 in particular will be discussed in section 5.4. The emulsification procedures for emulsion samples were described Chapter 4.

5.2.1 T_2 Distribution from CPMG Measurements

The CPMG result for the T_2 distribution of the oil used in these experiments, along with the corresponding logarithmic mean, were calculated and shown in Figure 5.2. Broad distribution of relaxation time was observed for this oil. A CPMG test was also performed on a sample of pure bulk water. In this case, the decay of magnetization could be described with a single relaxation time of 2.6 s. This is indeed agrees with our assumption that the $T_{2,\ bulk}$ for the dispersed phase is single-valued and not a distribution of characteristic bulk relaxation time (see section 3.3).

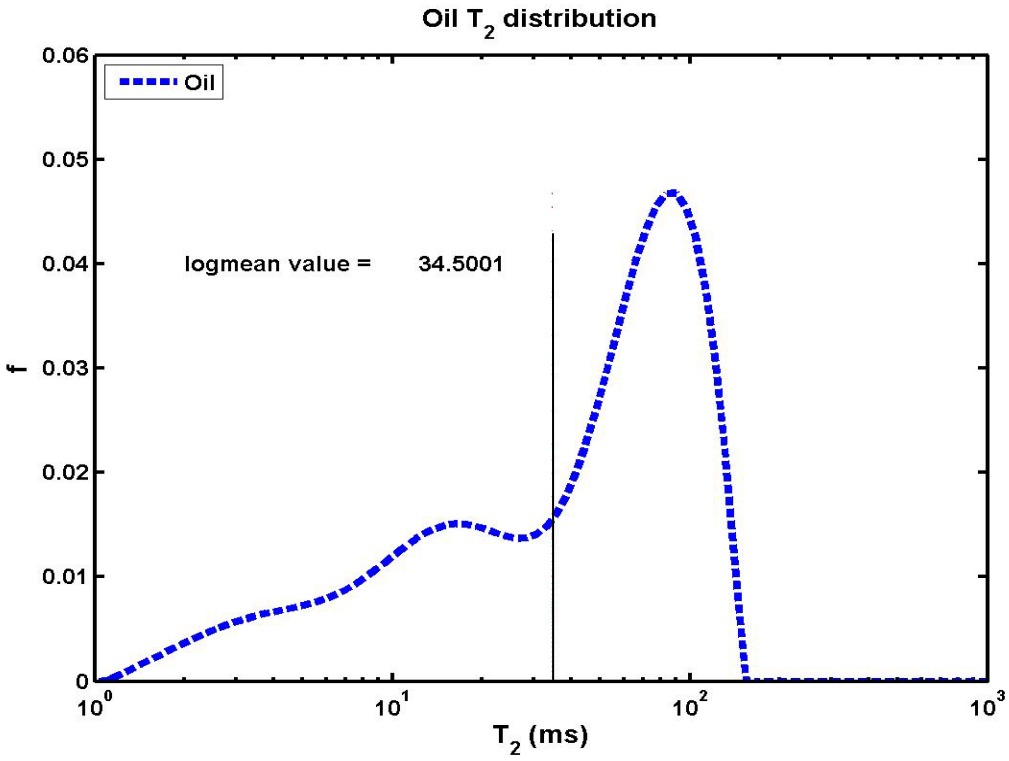

Figure 5.2. T_2 distributions of the oil used in this study.

The hydrogen index (*HI*) was determined from the same CPMG transverse magnetization data for the oil reported above, and also from relaxation data for an equal-volume sample of water. The hydrogen index (*HI*) of a fluid is defined as the proton density of the fluid at any given temperature and pressure divided by the proton density of pure water in standard conditions. It can be expressed as [85]:

$$HI = \frac{Amount\ of\ hydrogen\ in\ sample}{Amount\ of\ hydrogen\ in\ an\ equal\ volume\ of\ pure\ water} \quad (5.1)$$

The hydrogen index should be a quantity independent of measurement methods. In this work, the hydrogen index can be expressed as:

$$HI_k = \frac{\sum(f_i)_k}{\sum(f_i)_{water}} \qquad (5.2)$$

From this equation, *HI* for this oil was found to be equal to about ~ 0.9.

Evolution of T_2 distribution of the two emulsion samples from CPMG measurement are shown in Figures 5.3 and 5.4. In the figures, T_2 distribution of layered mixture and picture of emulsion after completing the experiment are also shown for reference.

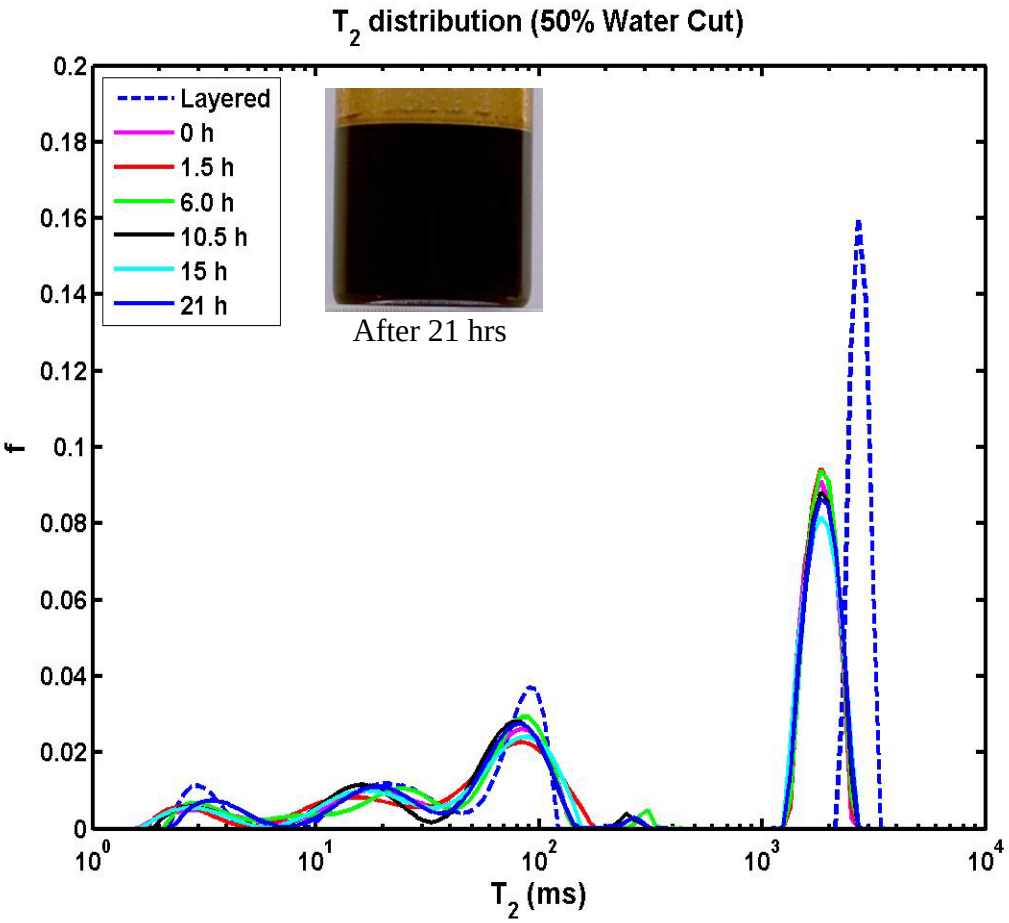

Figure 5.3 T_2 distribution of 50% emulsion (Sample-1)

In sample 1 (Figure 5.3), the T_2 distribution for emulsion sample has two peaks, one for oil and the other one for emulsified water. As can be seen from the photo, the emulsion is very dark and homogenous after 21 hrs. The peaks of the emulsified water at different times are layered on top of each other, which confirm that this emulsion is very stable during the 21 hrs. Also, the water peak is smaller than that of bulk water. This shows the effect of surface relaxivity on the T_2 distribution. Another important observation is that the emulsified water peak is very close to that for bulk water which will make it difficult to distinguish between them in the case where separation may exist. This will be shown next in sample 2 where separation is observed and the sample has both emulsified and bulk water.

In sample 2, 250 ppm of PR_3 coalescer solution (120 µL 10 % PR_3 xylene solutions for the 60 mL emulsion sample) was added immediately after emulsion preparation. Afterwards, the sample was shaken by hand for 1 minute.

In this sample (Figure 5.4), T_2 distribution of oil peaks is very close to that of bulk oil, and water peaks are moving toward bulk water with time. This suggests the separation of the oil and water. This is consistent with the experimental observation shown by the photo taken after experiment. T_2 distribution of water peak is smaller than that of bulk water but getting wider during the time. Ideally, there should be two peaks for water; one for emulsified water and one for bulk water. However, since the emulsified water peak is very close to and partially overlaps with bulk water peak as shown before in Figure 5.2, the observed peaks is wider. That is, the wider peak contains both emulsified

and bulk water. This overlapping makes it difficult to calculate the water content using CPMG as suggested by Eq 3.17 (see section 3.4). From the picture of the emulsion, the water layer is clear, but not completely separated (50%) which means that some emulsified water still exists in the system. This will be much clearer after the profile measurements are shown.

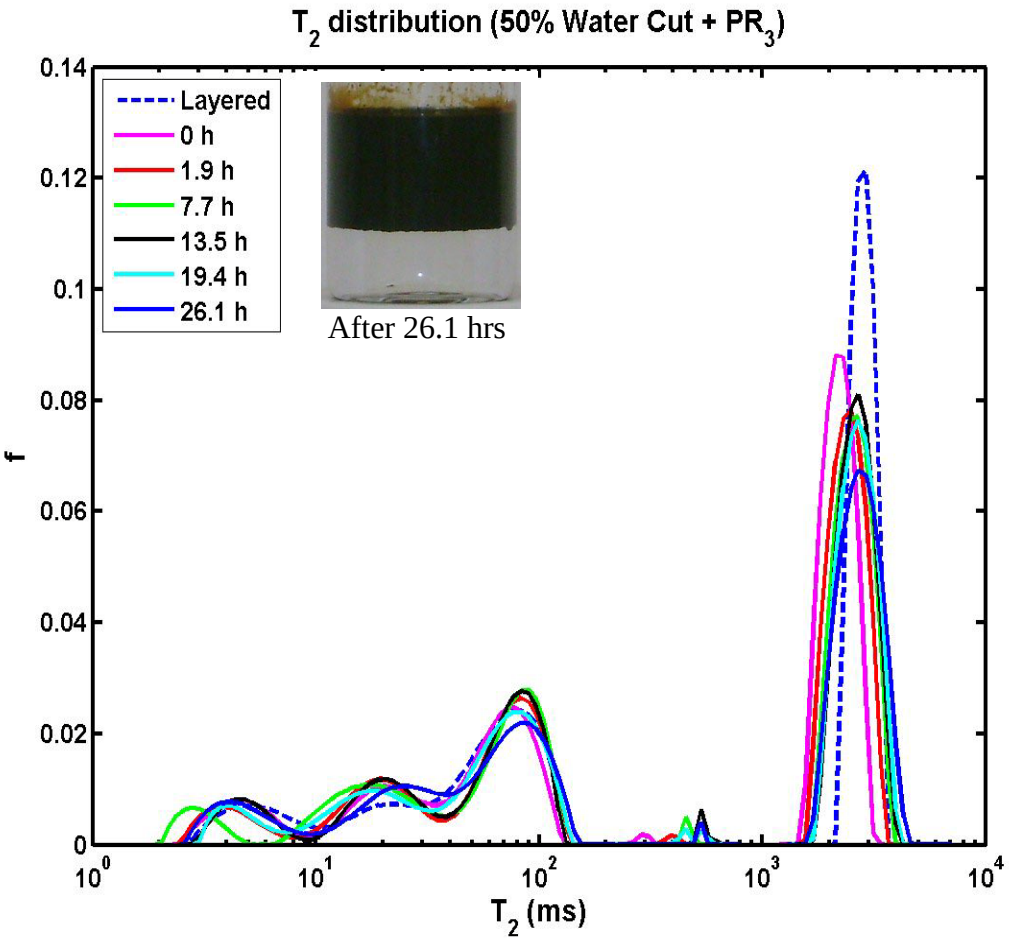

Figure 5.4. T_2 distribution of 50 % emulsion with 250 ppm of PR_3 (Sample-2)

5.2.2 Drop size distribution from restricted diffusion measurement

In chapter 3, how to obtain drop size distribution of emulsions via restricted diffusion measurement has been discussed. Here the diffusion time Δ is 1000 ms, the gradient pulse duration δ is 5 ms and the range of magnetic gradient is 0.3 ~ 36 G/cm.

Using this method, the self-diffusivity of bulk water can be obtained by Eq. (3.8):

$$R_{bulk} = exp\left[-\gamma^2 g^2 D\delta^2\left(\Delta - \frac{\delta}{3}\right)\right] \qquad (3.8)$$

Where (γ = 2.67 × 10^8 rad.T^{-1}·s^{-1} for ^{1}H).

When the above equation holds, a plot of the log R vs. $-\gamma^2 g^2 \delta^2\left(\Delta - \frac{\delta}{3}\right)$ renders a straight line, and D can be calculated from the slope. The value was found to be 2.36 x 10^{-9} m^2/s as shown in Figure 5.5, in good agreement with the literature [86]. Crude oils usually exhibit a distribution of diffusivities, assuming a multi-exponential fitting for the diffusivity distributions; one can get the log mean value of oil diffusivity to be 1.55 x 10^{-10} m^2/s, as shown in Figure 5.6.

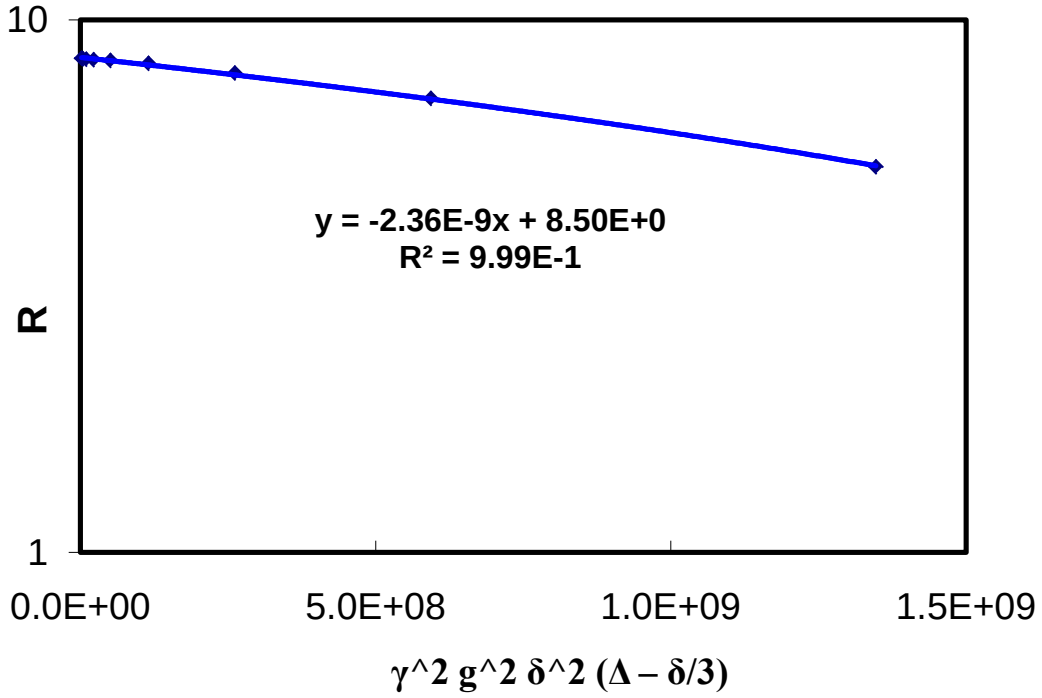

Figure 5.5 Self-diffusivity of bulk water from restricted diffusion measurements

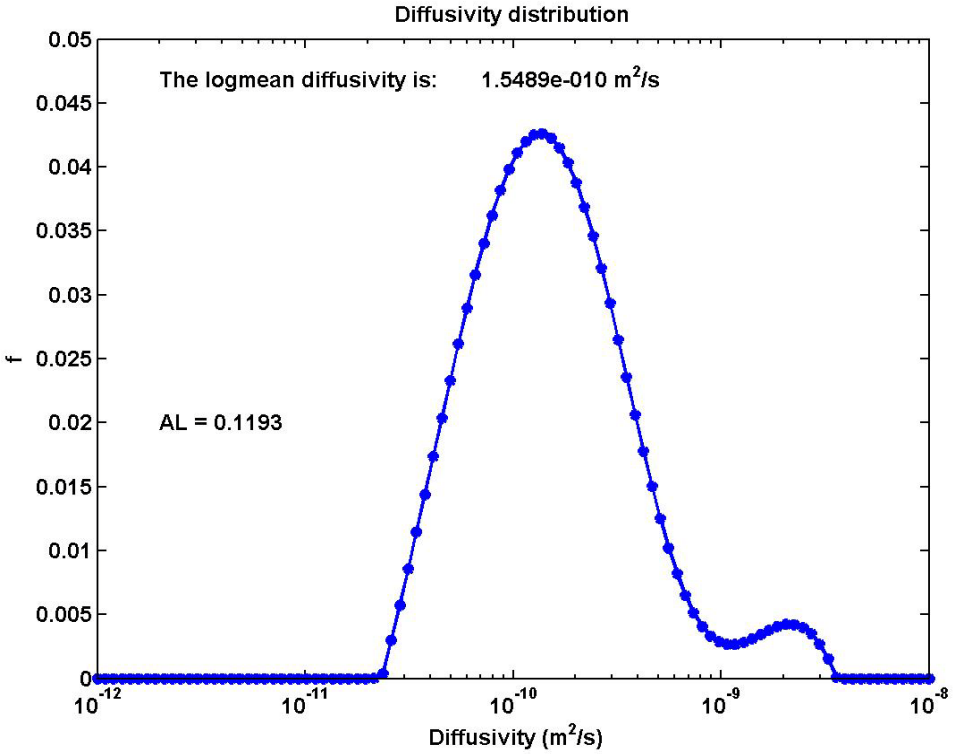

Figure 5.6. Distribution of diffusivities of crude oil.

According to Eq. 3.16, the NMR signal attenuation of the emulsion is the combination of continuous oil phase and dispersed water phase. However, in this case, the signal of the continuous phase is suppressed since the oil has relaxed completely at the time the "stimulated" spin-echo is collected, $\kappa \rightarrow 0$ according to Eq. 3.17. Hence, Eq. 3.16 reduces to Eq. 3.14.

$$(R_{emul} = R_{DP}) \qquad (3.14)$$

Since the diffusion time Δ used in this experiment (1 sec) is much greater than T_2 of oil phase, i.e., $\Delta \gg T_{2,oil}$, the oil phase will have no effect on the total attenuation obtained from the sample. In order to distinguish between the bulk water and emulsified water signals, Eq.(3.15) can be written as:

$$R_{emul} = (1 - \kappa)R_{DP} + \kappa\, R_{water} \qquad (5.4)$$

The determination of the drop size distribution consists of performing a least-square fit of the experimental data for R_{emul} with Eqs. 3.9 - 3.15, and replacing Eq.3.16 with Eq.5.4, then using d_{gV}, σ and κ as fitting parameters. The fitting results for both samples, 1 and 2, can be seen in Figures 5.7 and 5.8, respectively. Here κ is the contribution ratio of each component to the total attenuation. The lognormal distribution (with mean drop diameter and standard deviation as the parameters) is assumed for the emulsion drop size.

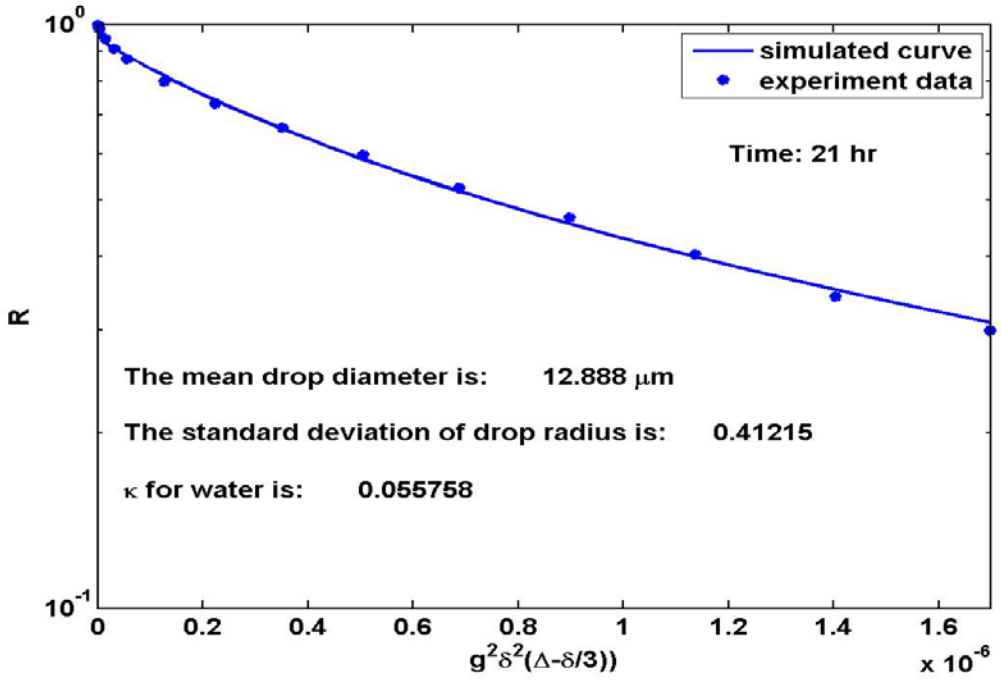

Figure 5.7 Fitting results of diffusion measurement at 21hr for 50% emulsion (Sample 1)

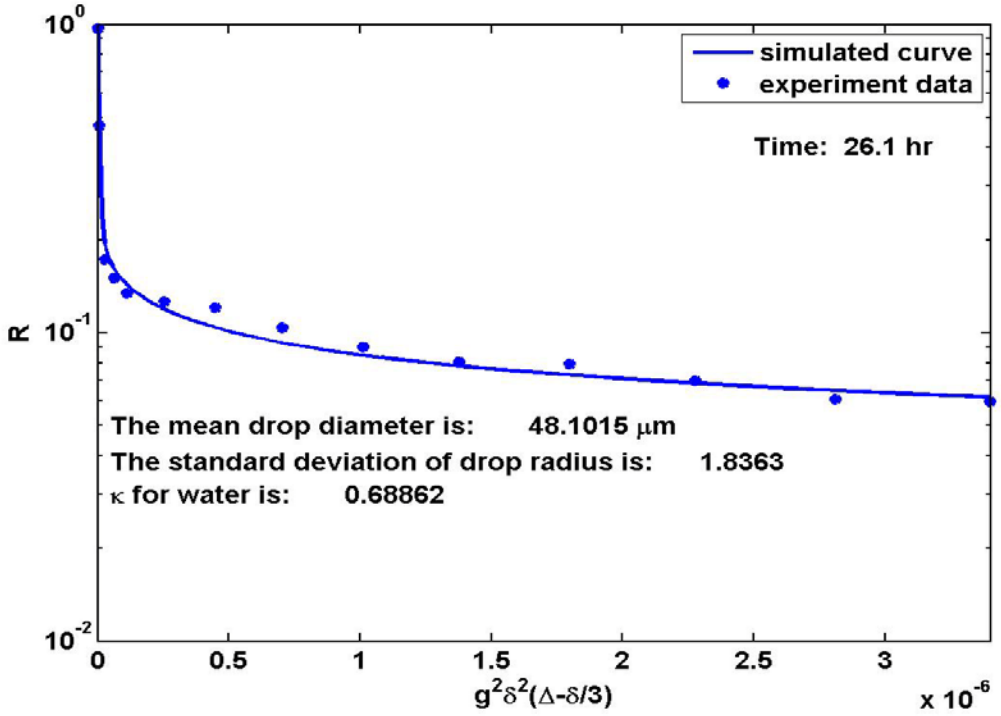

Figure 5.8 Fitting results of diffusion measurement at 26.1 hr for 50% emulsion with 250 ppm of PR_3 (Sample-2)

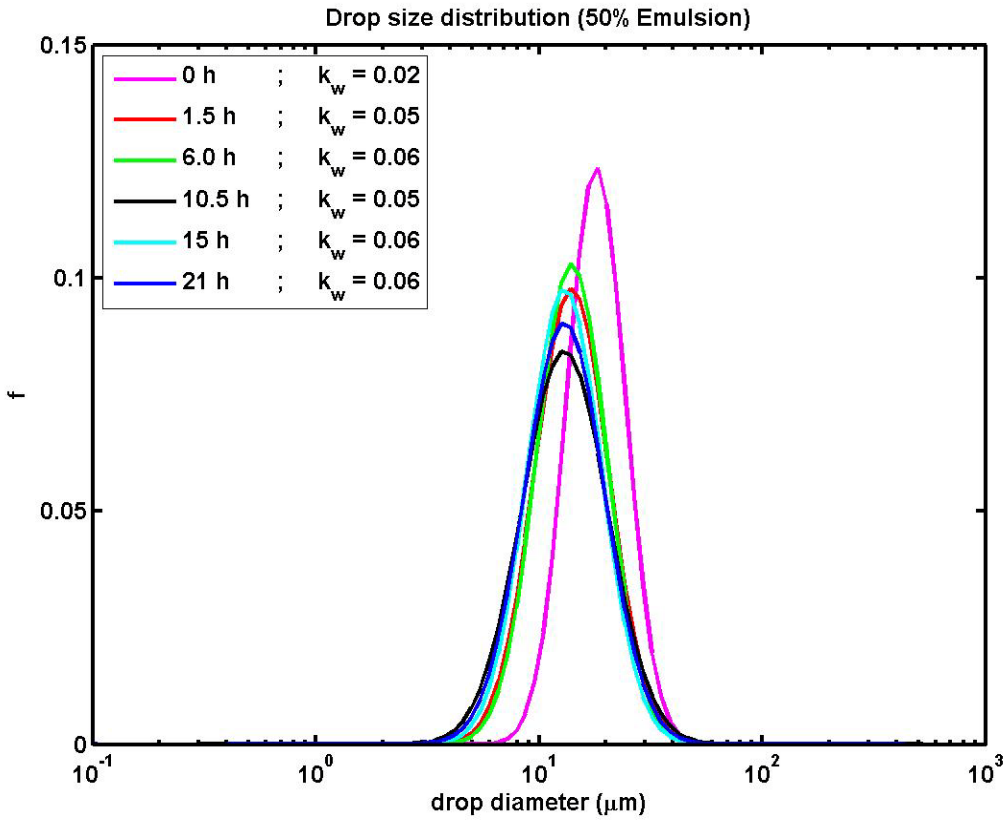

Figure 5.9 Drop size distributions for 50% emulsion (Sample 1)

Figure 5.9 demonstrates the drop size distribution for the emulsion with no addition of PR_3 (sample 1) where a very stable emulsion with a mean drop size of about 13 μm is present after 1.5 hr. In the same figure, the κ_w values for bulk water are also shown to be very small for all measurements compared to that for emulsified water. Hence, it can be concluded that most of the water present in the sample is emulsified water.

In addition, Figure 5.9 shows also a discrepancy between the first measurements compared to the others. The time-dependent diffusion results of sample 1 also confirm this difference as shown in Figure 5.10. A possible reason is that for 50 % emulsions the droplets didn't reach the limit of the critical close-packing, (~0.64 for random packing [9] and 0.74 for ordered packing [4]). Hence, droplets have some freedom for movement, especially immediately after the emulsification process. At later times, they tend to stick to each other and the movement is restricted. Physical microscopic observations confirm this justification.

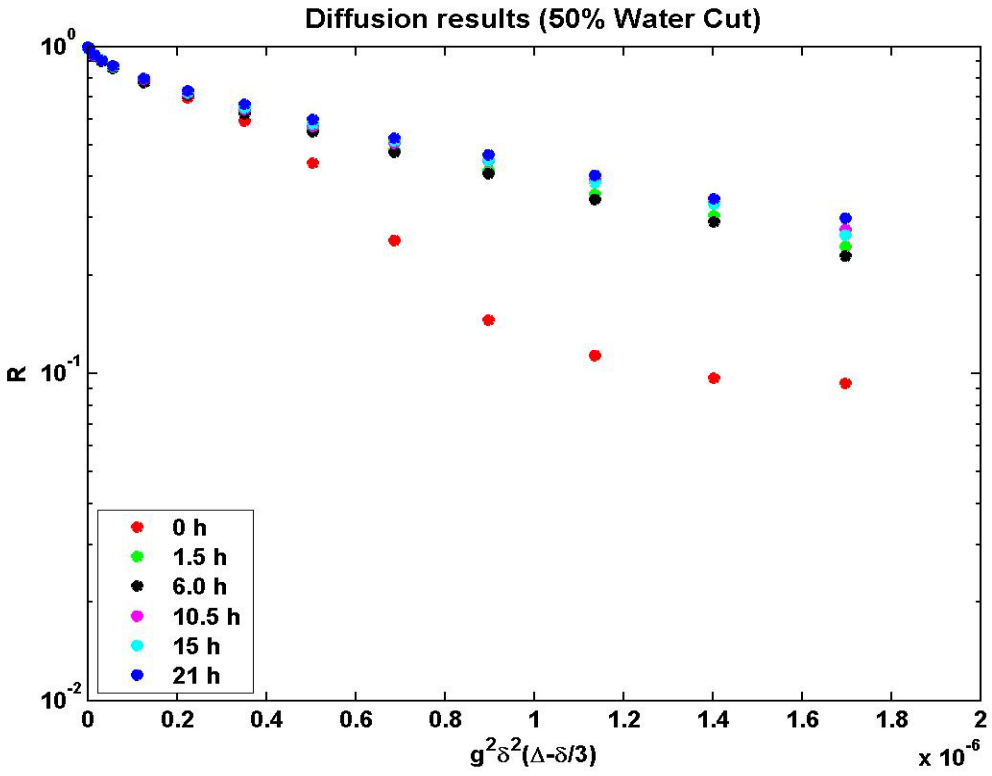

Figure 5.10 Diffusion results for 50% emulsion (Sample 1)

Table 5.1 Summary of calculation results for 50% emulsion (Sample 1)

Time (hr)	Mean Diameter (μm)	δ	κ_{water}	κ_{emul}
0.0	18.1	0.30	0.02	0.98
1.5	13.8	0.38	0.05	0.95
6.0	14.0	0.36	0.06	0.94
10.5	13.4	0.44	0.05	0.95
15.0	13.3	0.38	0.06	0.94
21.0	12.9	0.41	0.06	0.94

A summary of all calculation results for 50% emulsion (sample 1) are shown in Table 5.1. As stated earlier, the emulsion is very stable and κ_{water} values are very low, which shows that the coalescence is very slow, or even negligible, in the absence of demulsifier.

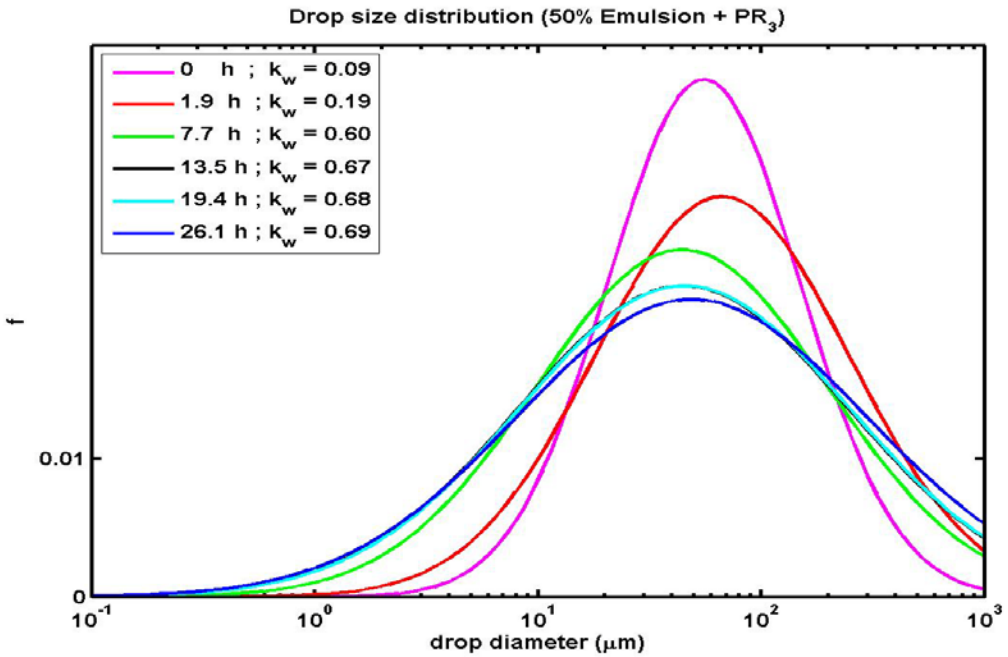

Figure 5.11 Drop size distributions for 50% emulsion with 250 ppm of PR_3 (Sample 2);

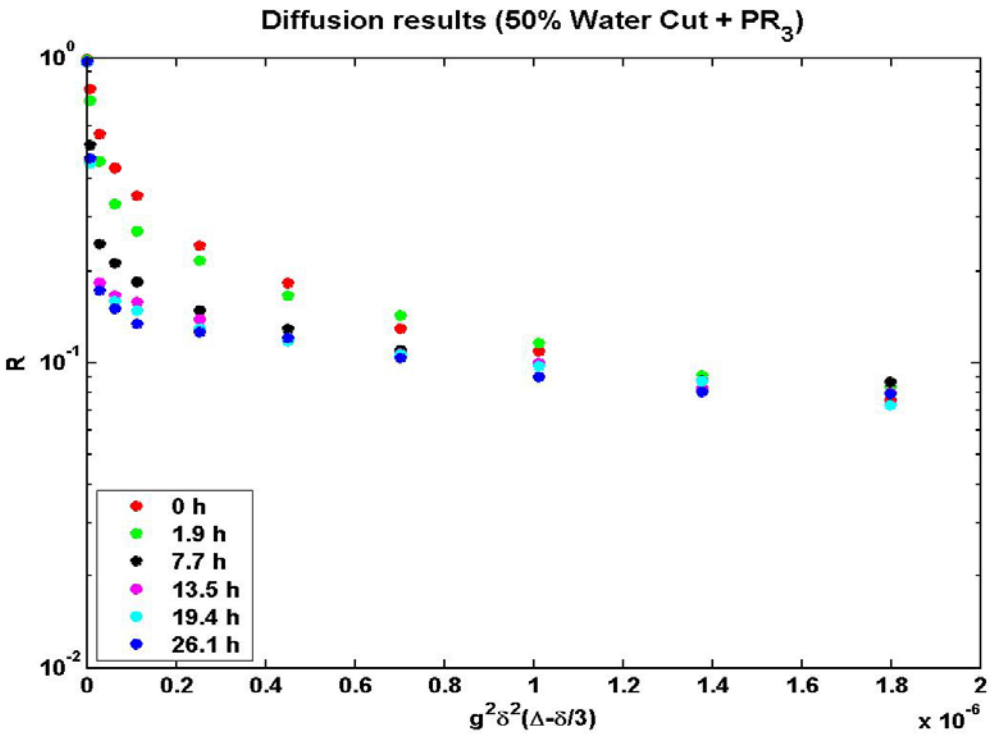

Figure 5.12 Diffusion results for 50% emulsion with 250 ppm of PR_3 (Sample 2)

For the emulsion with adding 250 ppm of PR_3 as a demulsifier (sample 2), the drop size distribution exhibits a wider range with increasing time. This may be indicative of a separation process in which droplets coalesce against a layer of bulk fluid. Excluding the first two readings, the mean drop size seems to be increasing with time evolution. Since the shape of the distribution is not resolved independently, but priori assumed to be lognormal, the calculation may not be sensitive to the larger droplets that may form due to coalescence in the later time. The sedimentation rate can also play a significant rule since it is proportional to the droplet radius, r^2 (Eq. 2.10). The coalescence of large droplets is favored, since they travel faster throughout the bulk and therefore

collide with a larger number of droplets per unit time. The time-dependent diffusion results of sample 2 are shown in Figure 5.12.

Table 5.2 Summary of calculation results for 50% emulsion with 250 ppm of PR_3 (Sample 2)

Time (hr)	Mean Diameter (μm)	δ	κ_{water}	κ_{emul}
0.0	55.3	0.99	0.09	0.91
1.9	66.7	1.27	0.19	0.81
7.7	44.2	1.48	0.60	0.40
13.5	44.7	1.75	0.67	0.33
19.4	45.3	1.66	0.68	0.32
26.1	48.1	1.84	0.69	0.31

From Table 5.2, it can be noticed that κ_{water} increases over time, which demonstrates the effects of adding PR_3. As expected the demulsifier accelerates the coalescence rate between the droplets in the emulsion. However, we also observe the κ_{emul} values, which contribute to emulsified water, are still present in the sample after the 26 hrs. This is consistent with CPMG results and implies that the emulsion was not completely separated during the experiment and some emulsified water still exists in the system.

5.2.3 1-D T_1 weighted profile measurement

As previously described in section 3.5, NMR 1-D T_1 weighted profile measurement is based on the T_1 difference of different components. Figure 5.13 shows the profile measurement results of brine and crude oil layered mixture. The waiting time, t_w, and the imaging pulse field gradient used in this experiment are 1.0 s and 0.82 G/cm, respectively. The sample consists of a total of 4 cm height with equal amounts of oil (2 cm) and water (2 cm). In the figure, *x*-axis (*A)* represents the signal amplitude of the sample and *y*-axis (*position)* is the position measured from the bottom to the top of the sample.

The T_1 value of water is greater than oil, so the attenuation and, therefore, the signal amplitude of water is smaller than oil based on the Eq. 3.18. This technique is useful to characterize emulsion since the signal amplitudes of different phases in the emulsion become distinguishable.

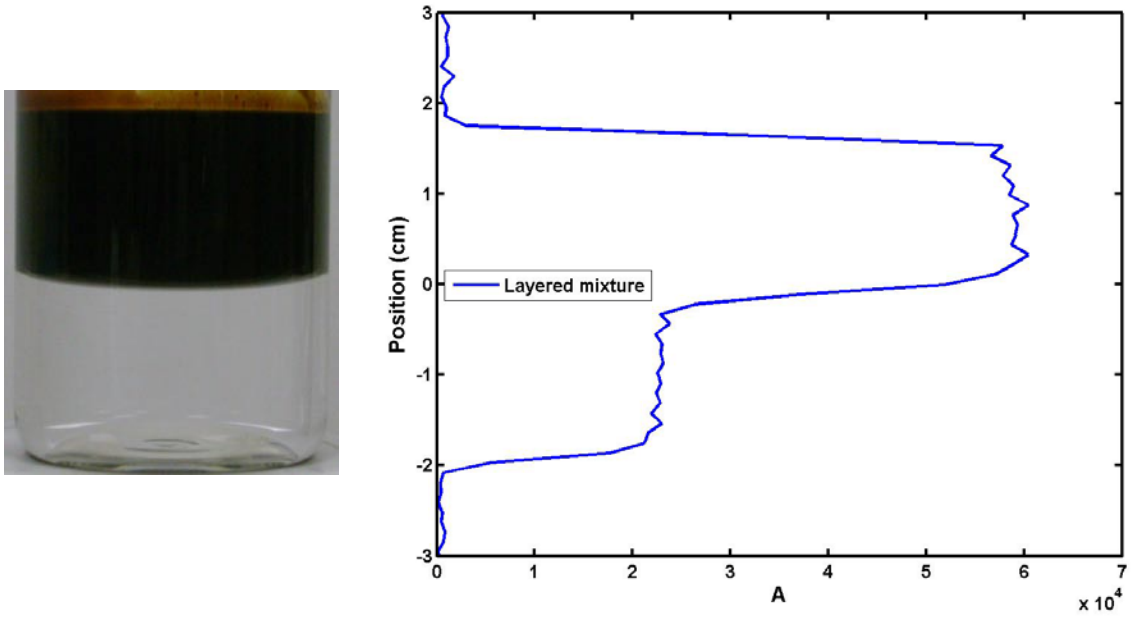

Figure 5.13 Profile measurement results of brine/ oil layered mixture

The technique was developed by Jiang et al. [82] and found to be useful to find the time-dependent behavior and water fraction profile in emulsions. The authors though pointed out that this procedure can be applied if some simple assumptions are valid [82]:

- T_1 for the oil, water droplet, and bulk water can be considered as distinct single values, rather than a distribution.
- The changes in T_1 during the experimental time can be ignored. So, the fresh homogeneous emulsion can be utilized to calibrate for later times.
- In samples with demulsifier present, emulsified water coexists with either clean oil or free water, but not both.

The detailed calculation procedure was also shown in the same reference [82] and will be briefly discussed here. These calculations are based on Eq. 3.20 and can be summarized in Figure 5.13 for emulsion sample 1.

First, knowing the value of T_{1w}, the water amplitude data A_w can be used in the following equation to calculate A_∞,

$$A_W = A_\infty \left[1 - exp\left(\frac{-t_W}{T_{1W}}\right)\right] \rightarrow A_\infty \qquad (5.5)$$

After that, the value of A_∞ along with the oil amplitude data A_o are used to calculate T_{1o} for oil according to:

$$A_0 = A_\infty \left[1 - exp\left(\frac{-t_W}{T_{1o}}\right)\right] \rightarrow T_{1o} \qquad (5.6)$$

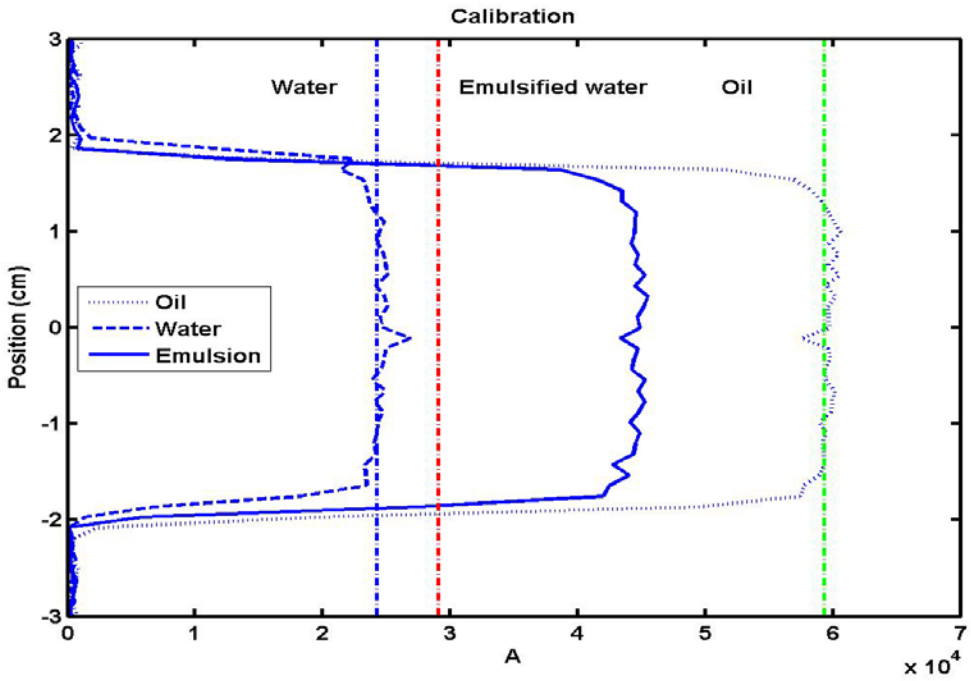

Figure 5.14 Calibration for calculation of water fraction for 50% emulsion (Sample 1)

The amplitude of the fresh homogenous emulsion A_{emul} and Eq. 5.7 are used to calculate T_{1emul} for emulsified water:

$$A_{emul} = A_{\infty}\left[1 - \varphi_{emul} exp\left(\frac{-t_W}{T_{1emul}}\right) - (1 - \varphi_{emul}) exp\left(\frac{-t_W}{T_{1o}}\right)\right] \rightarrow T_{1emul} \quad (5.7)$$

Finally, the water fraction in emulsion can be calculated using Eq. 3.20. Since emulsion sample without PR_3 (sample 1) contains only oil and emulsified water, Eq. 3.20 can be written as:

$$A_{emul}(z) = A_{\infty}\left[1 - \varphi_{oil} exp\left(\frac{-t_w}{T_{1,oil}}\right) - \varphi_{drop} exp\left(\frac{-t_w}{T_{1,drop}}\right)\right] \quad (5.8)$$

where: $\varphi_{oil} + \varphi_{drop} = 1$

In the top part of sample 2 with PR_3, emulsified water coexists with clean oil; hence Eq.5.8 can also be used to calculate the emulsified water fraction in the top region. On the bottom of the sample, W/O/W multiple emulsions exist and the following equation can be used to calculate free water fraction:

$$A_{emul}(z) = A_{\infty}\left[1 - \varphi_{water} exp\left(\frac{-t_w}{T_{1,water}}\right) - \varphi_{drop} exp\left(\frac{-t_w}{T_{1,drop}}\right)\right] \qquad (5.9)$$

where: $\varphi_{water} + \varphi_{drop} = 1$

Figure 5.14, shows the calculated value emulsified water from calibration as red dash line. This is the lower bound of the amplitude for the system. Also, the green dash line for pure oil is considered to be the upper bound. Values below or above these bounds can be considered as a mixture of emulsified water and free water or clean oil, respectively.

For consistency, the total water content (0.50) is used for calibration in the initial time. From other water-fraction profile figures at later times, the total water content (φ) was obtained by integration over the vertical position.

Using this method for the emulsion with no demulsifier (sample 1), it was demonstrated that the emulsion is very stable during the 21 hr period and exhibits no sign of coalescence or sedimentation. For this emulsion sample, T_1 for bulk water, oil and emulsified water are 2.60 s, 0.50 s and 2.08 s, respectively. Figure 5.15 shows the profile of emulsion signal amplitude, and it clearly confirms that the emulsion is homogeneous, and thus very stable. Figure 5.17 also shows that at all vertical positions the sample consists approximately 50% of oil and 50% “emulsion” (~0.5 water-fraction).

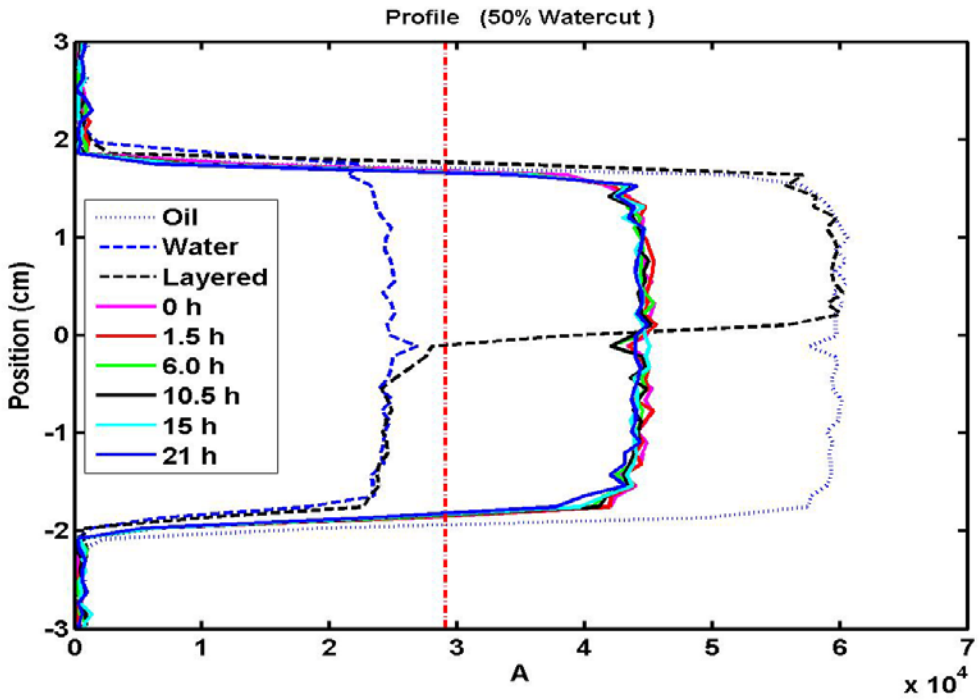

Figure 5.15 Profile results of 50% emulsion without adding PR_3 (Sample 1) as a function of signal amplitude.

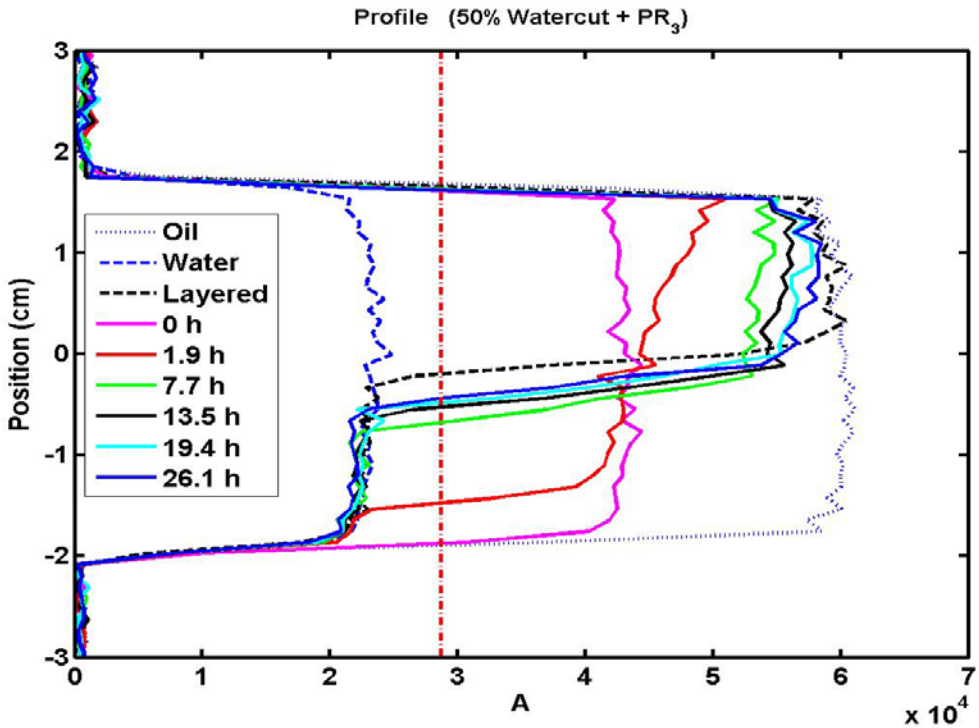

Figure 5.16 Profile results of 50% emulsion with adding 250 ppm of PR_3 (Sample 2) as a function of signal amplitude

In the calculation of emulsion with PR_3, T_1 for bulk water, oil, emulsified water and separated free water are again 2.60 s, 0.50 s 2.08 s, respectively. Here T_1 for emulsified water is obtained from the calibration of sample 1, because at initial time sample 2 is not homogeneous.

For sample 2, Figures 5.16 & 5.18, show the water fraction profiles of emulsion with adding PR_3 as a coalescer. The separation of oil and water is clearly shown as time proceeds, which demonstrates the effect of enhancing the coalescence rate by adding PR_3. On the top, water fraction is close to zero, which corresponds to a nearly clean oil layer. At the bottom, water fraction is 1.0, which corresponds to free water. However, as observed earlier from CPMG and restricted diffusion measurements, the emulsion is not completely separated during the 26 hrs and some emulsified water still exists in the system.

It is clear from these results that this method can distinguish the composition variation of the sample with position and time and hence determine the transient behavior of emulsion with and without adding demulsifier.

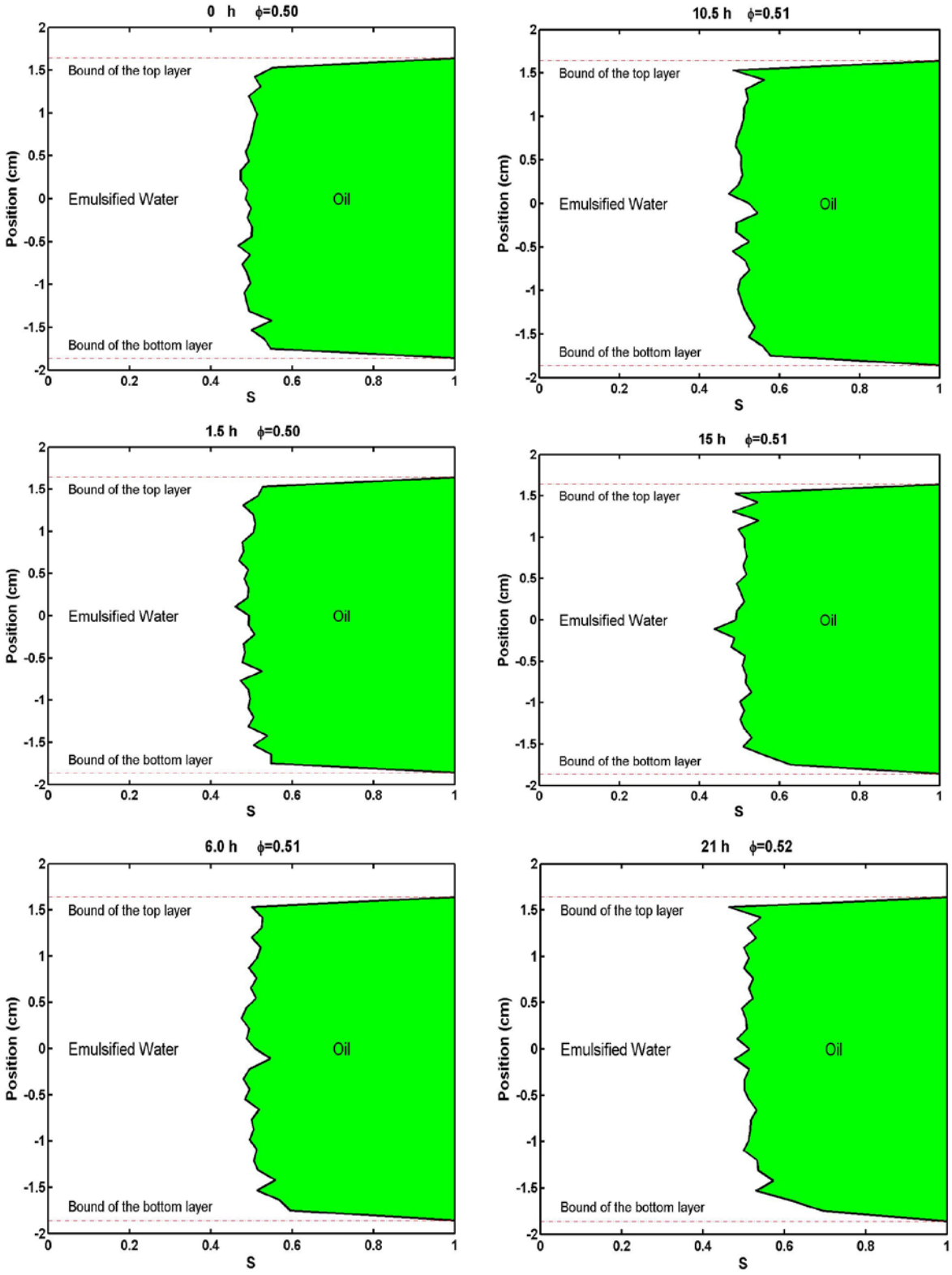

Figure 5.17 Profile results of 50% emulsion without adding PR_3 (Sample 1) as a function of vertical position

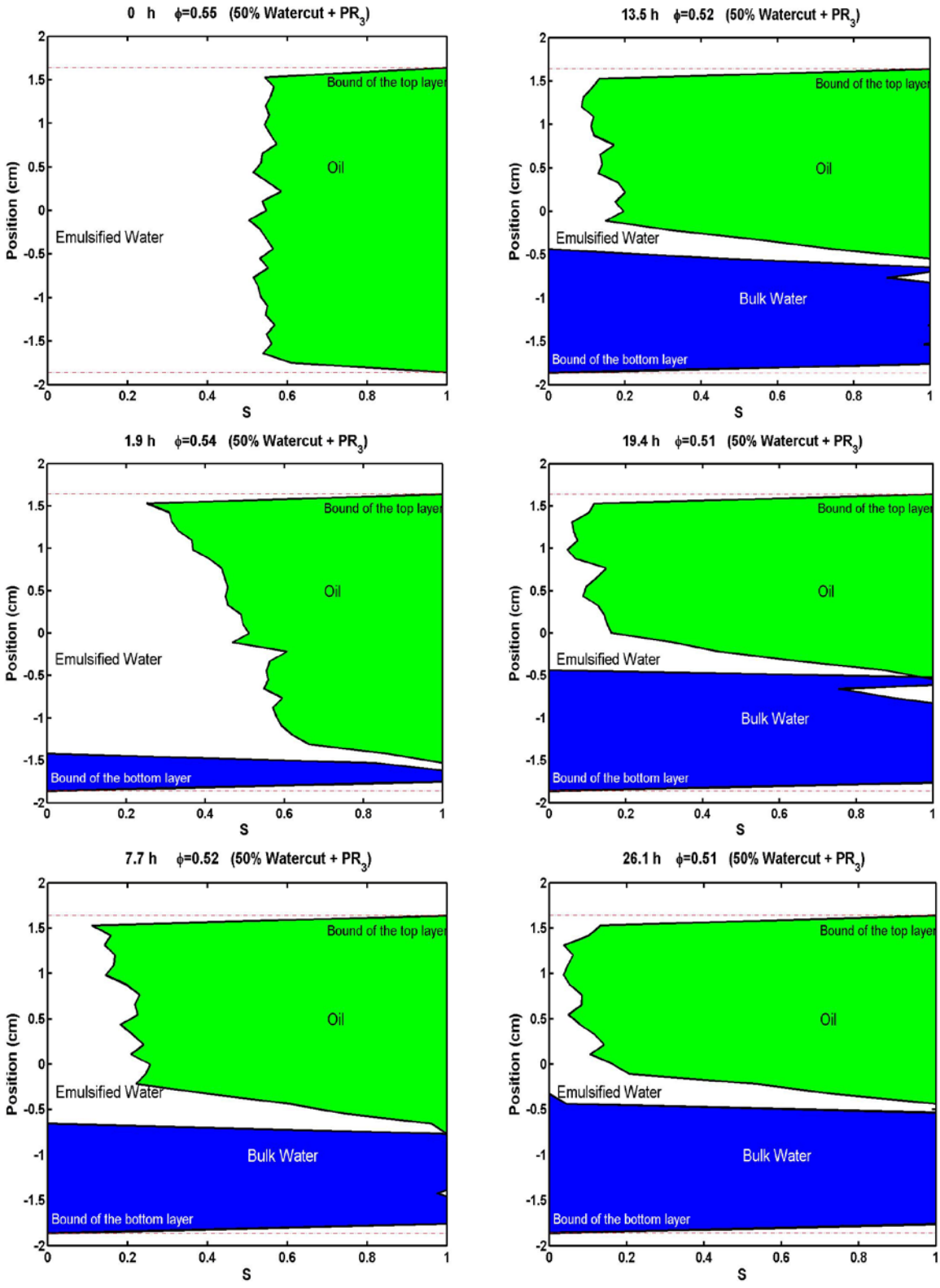

Figure 5.18 Profile results of 50% emulsion with adding 250 ppm of PR_3 (Sample 2) as a function of vertical position

mulsion prepared with

me fractions and

ere made with a

l procedure was

ows the crude oil

e. The crude oil

ence on shear rate

lewtonian fluid with

strong intermolecular

refore, the viscosity will

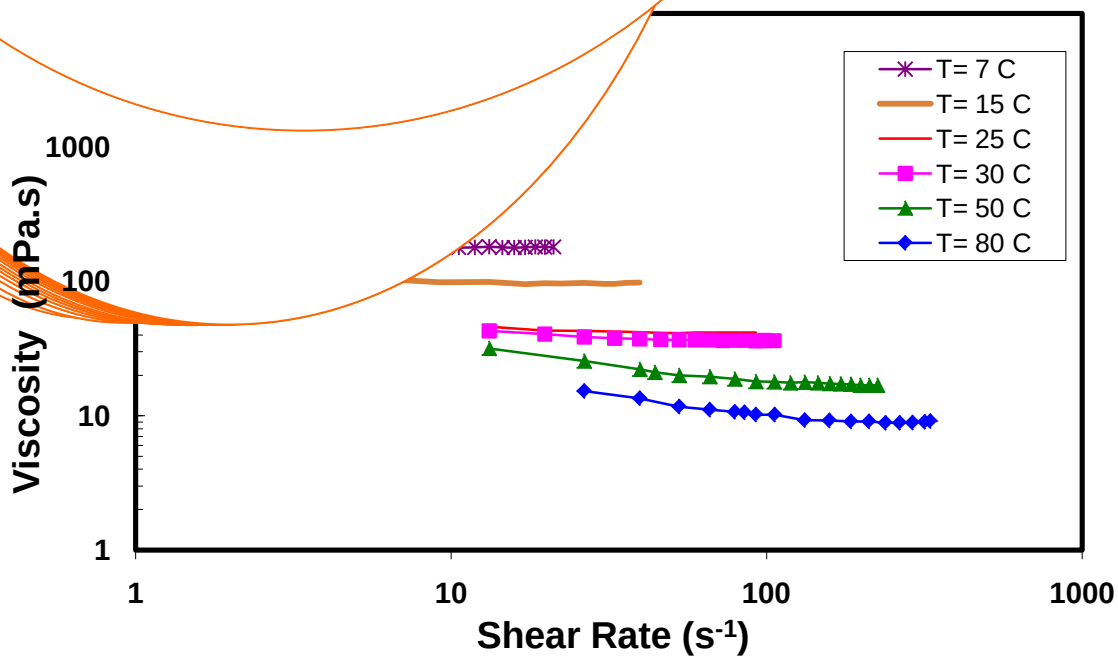

Figure 5.19 Oil viscosities at different temperatures as function of shear rate

As discussed in section 2.3, emulsion viscosity is usually affected by many factors such as the viscosity of the continuous phase (η_C), the dispersed phase content (φ) and temperature. The following sections discuss, individually, the effect of some of these important factors on emulsion viscosity.

5.3.1 Effect of temperature and shear rate

Figure 5.20 shows the viscosity of 50% emulsion as a function of temperature. The crude oil data is included where a similar trend is observed. One can notice the difference between the viscosities when changing the temperature. There is a difference of one order of magnitude, nearly 1400 cP, between emulsion with the highest and lowest viscosity. This difference could be significant to the deepwater fields' production where the temperature varies widely along the flow path from the reservoir to production platform.

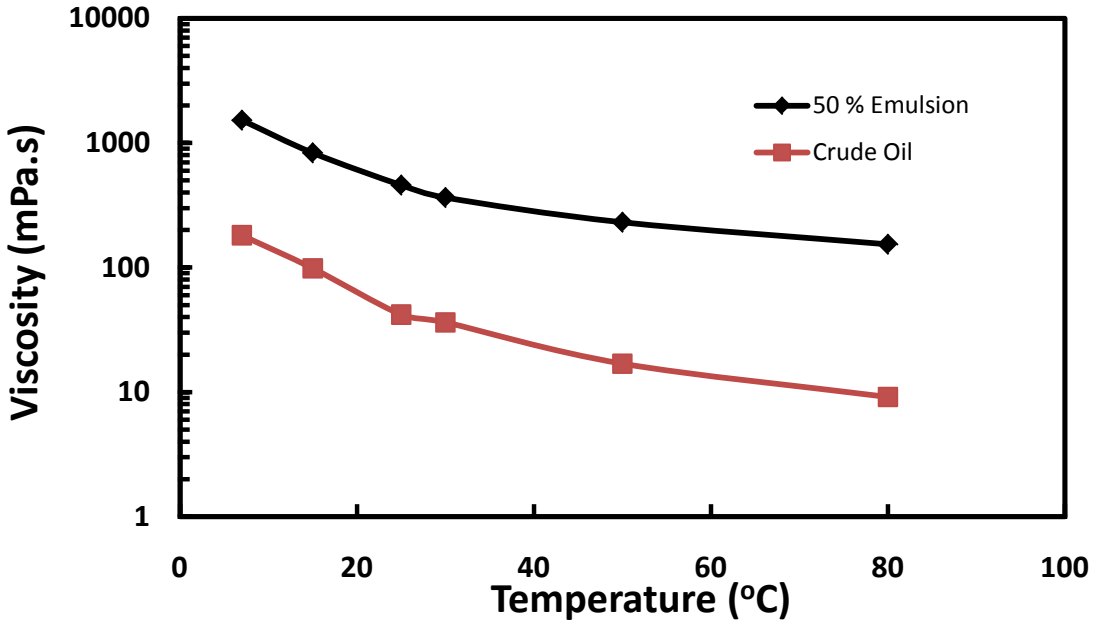

Figure 5.20 Apparent viscosities vs. temperature for 50% emulsion and crude oil

It should be mentioned that these data reported in Figure 5.20 were not taken at same shear rates due to the limitation of viscometer used and the wide range of shear rate as can be seen in Figure 5.21. Instead, the viscosity at highest shear rate at each temperature is taken because the Brookfield Viscometers are designed to be more accurate at highest torque.

Figure 5.21 shows the variation of the viscosity with shear rate at several temperatures and fixed volume fraction (50%) of dispersed phase. For low temperatures, the viscosity varies with shear rate, indicating that the emulsions behave as non-Newtonian fluids. At lower temperatures, the presence of paraffinic crystals formed may provoke the non-Newtonian behavior.

Also, Wax Appearance Temperature (WAT) of oil could play a significant role in the behavior of oil emulsions. Many experimental works have identified different emulsion behavior below and above WAT for petroleum emulsion. Examples of such work were that done by Farah et al [30] and Oliveira et al [87]. Both works reported an increase in the degree of the non-Newtonian behavior of emulsion below the WAT. Figure 5.22 shows the relation between shear stress and shear rate for all temperatures that illustrates the increase of shear-thinning behavior of emulsion as the temperature decreases. In Figure 5.22, the linear regression of all data has a coefficient of correlation (R^2) greater than 0.999, which suggests a Bingham fluids behavior. The degree of non-Newtonian behavior is considered by the deviation of intercept values of regressed lines from origin. Table 5.3 shows the summary of all linear regression results where the slope represents the viscosity and intercept is the value of yield stress.

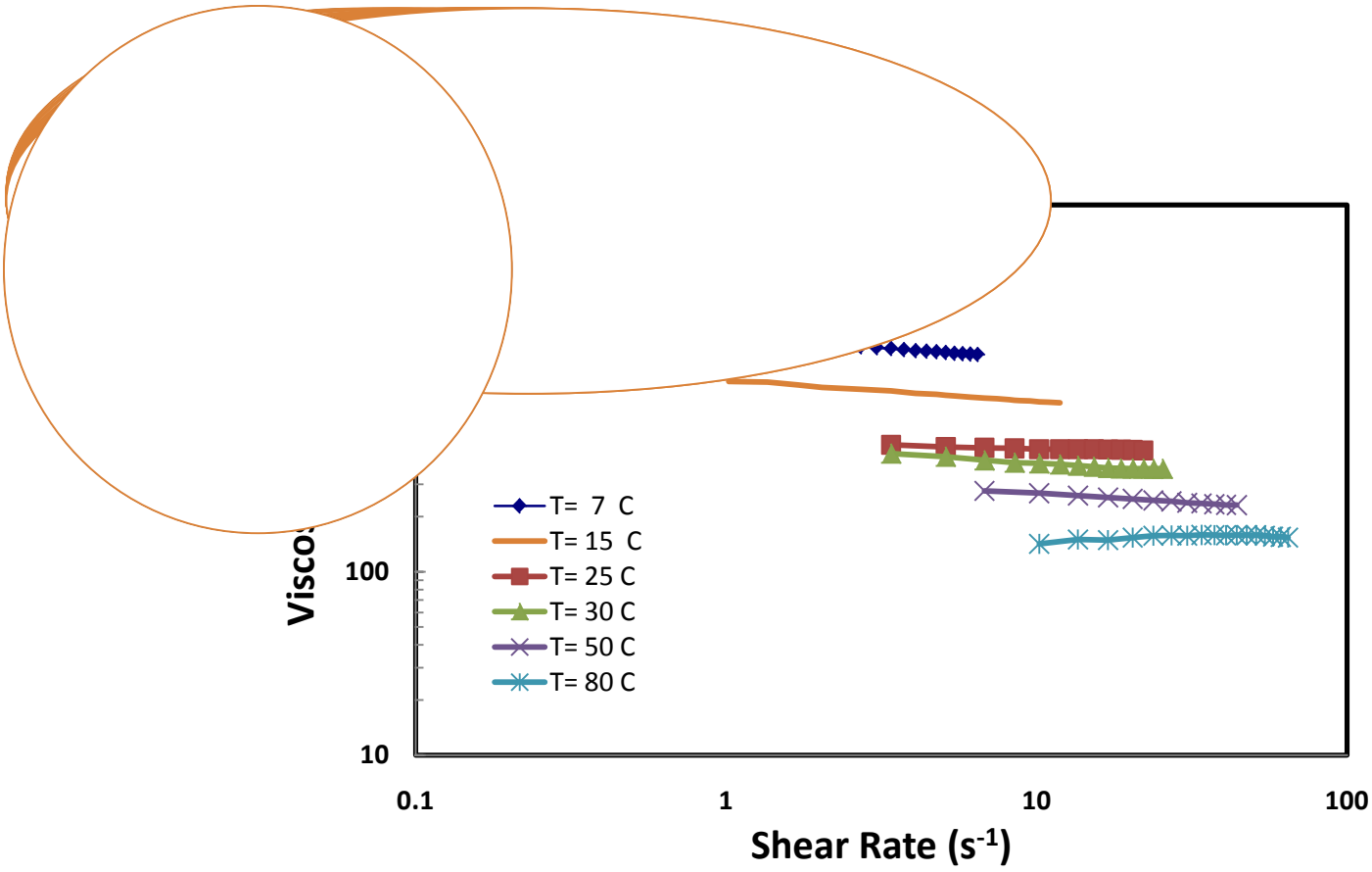

Figure 5.21 Viscosity of 50% emulsion at different temperatures as function of shear rate

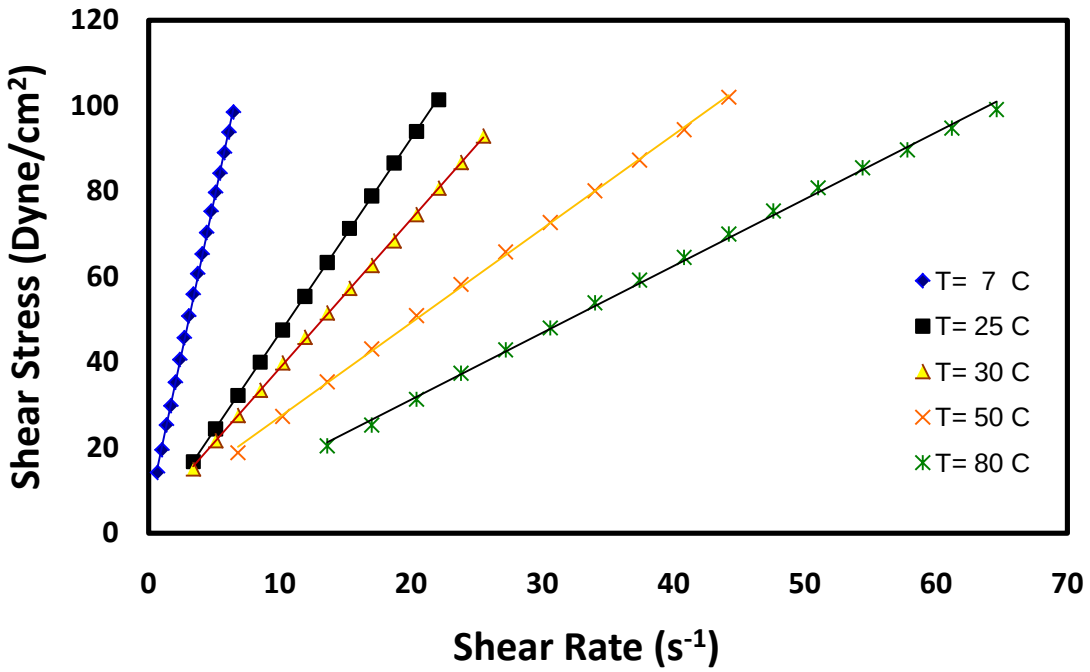

Figure 5.22 Shear stress vs. Shear rate for 50% emulsion at different temperatures

Table 5.3 Summary of linear regression results reported in Figure 5.22

Temperature (^oC)	Slope (mPa.s x 10^2)	Intercept (Dyne/cm^2)	R^2
7	14.48	3.63	1.00
15	7.98	5.22	1.00
25	4.55	1.28	1.00
30	3.48	3.78	1.00
50	2.2	5.2	1.00
80	1.56	0.0	1.00

5.3.2 Effect of water cut

The viscosity of water-in-oil emulsion increases with increasing the water cut before reaching what is called inversion point, beyond which the continuous phase changes to water. The viscosity of water-in-oil emulsions increases as much as two orders of magnitude over the viscosity of dry crude as can be easily seen in Figure 5.23 below. During the experimental work, the highest stable emulsion that can be observed (without seeing any separation) was about 60% water cut. This suggests that the inversion point of this emulsion at 25 ^oC is about 70% ($\pm$ 5). The high viscosity measurement at this water cut confirms this prediction. Reducing such a high viscosity that can be reached either by higher water cut or lower temperature requires a separation mean such as chemical demulsification, which will be described in the next section.

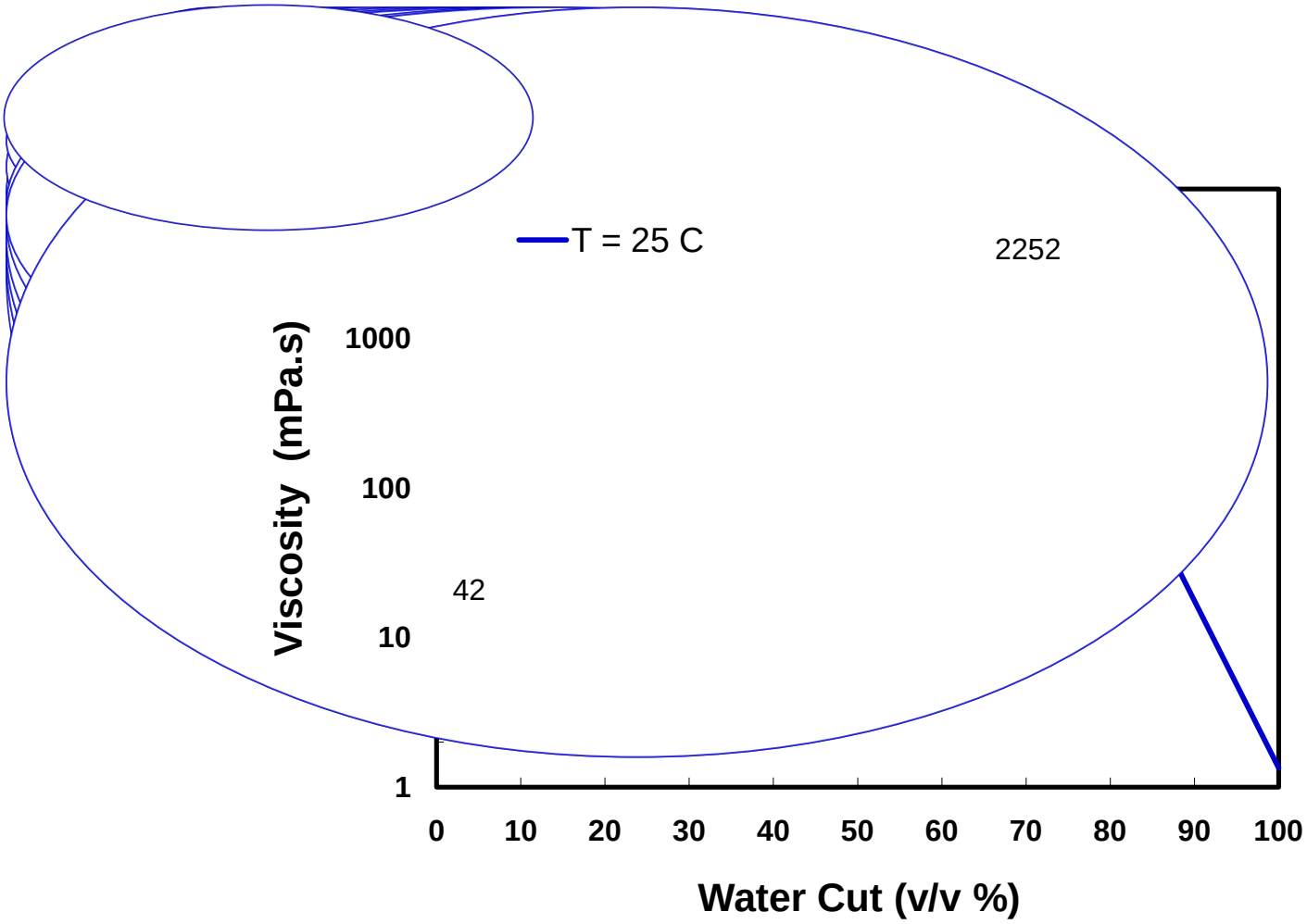

Figure 5.23 Apparent viscosities vs. water cut at 25 ^{o}C

5.4 Demulsifier Performance and Selection

Chemical demulsification is the most applied method of treating water-in-oil emulsions and involves the use of chemical additive to accelerate the emulsion breaking process. More than one experimental method are utilized in this study to evaluate the performance of our phenolic resins demulsifier series (PR_1-PR_6). These include the well known bottle testing and viscosity measurements.

5.4.1 Bottle testing

Bottle tests were performed on emulsions treated with all the phenolic resins listed in Table 4.2. This method was used for physical observations. The intent was not to measure the amount of the separated water as this was done by NMR technique.

Figures 5.24-5.26 show the results of adding the series of six PR_X coalescers to bottles containing same amounts of water-in-oil emulsion (50% water cut) at three different temperatures: 7 ^oC, 30 ^oC and 80 ^oC, respectively. At temperature of 7 ^oC, the dosage was almost doubled compared to the other two since no separation was observed using the same dosage (250 ppm) as at 30 or 80 ^oC. This is due to the highly stable emulsion at 7 ^oC that has the highest viscosity as seen before. The results show that PR_3 can work at all temperature. However, it seems there is a shift of the best separation toward the more hydrophilic resins as the temperature increases. For this reason, viscosity measurements for emulsion including these demulsifier were needed.

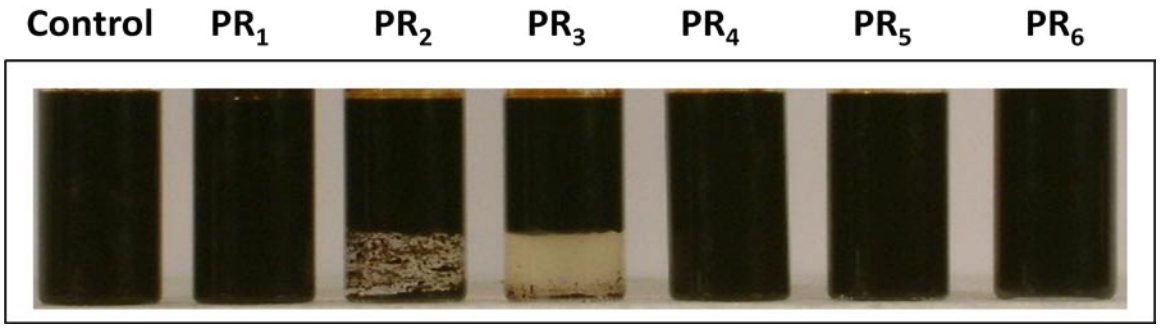

Figure 5.24 Bottle test for 50% emulsion samples adding different demulsifiers (500 ppm of PR_1-PR_6) @ 7 ^oC, 24 hours after preparation.

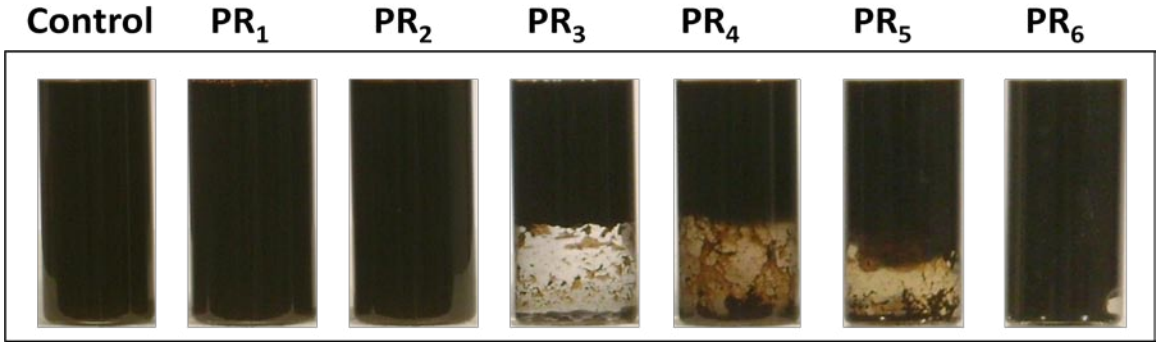

Figure 5.25 Bottle test for 50% emulsion samples adding different demulsifiers (250 ppm of PR_1-PR_6) @ 30 ^oC, 24 hours after preparation.

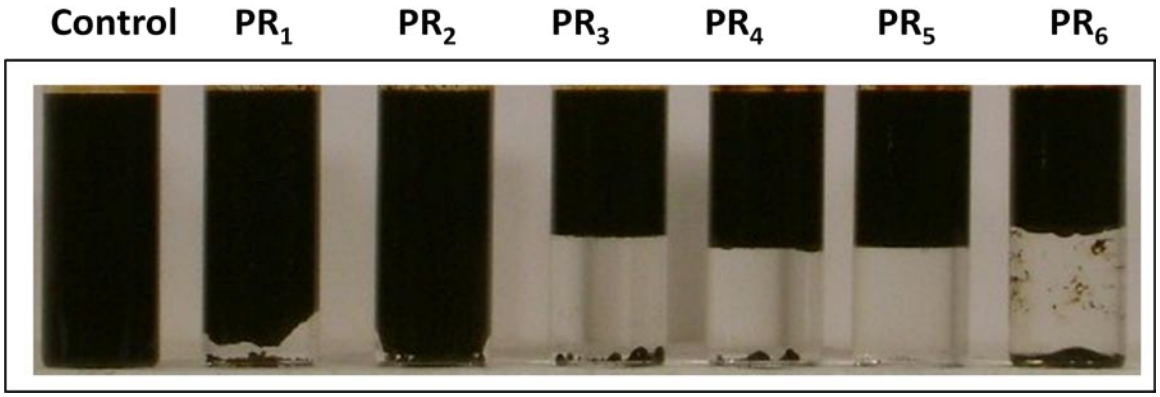

Figure 5.26 Bottle test for 50% emulsion samples adding different demulsifiers (250 ppm of PR_1-PR_6) @ 80 ^oC, 24 hours after preparation.

5.4.2 Viscosity reduction and optimum dosage

Viscosity measurements of emulsions with different coalescers, PR_X, were also used to further identify the optimal coalescer at different temperatures. Figure 5.27 shows the results of 50% emulsion viscosity treated with 250 ppm of the six PR_x at 25 ^oC. The viscosity values reported in the figure are taken after 30 min inside the viscometer at constant shear rate. The crude oil viscosity at the same temperature is also shown for comparison. At this temperature (25 ^oC), PR_3 is the optimal demulsifier in term of viscosity reduction. This result is consistent with the bottle tests, and also with the fact that emulsion stability exhibits a minimum at the optimum formulation for demulsification.

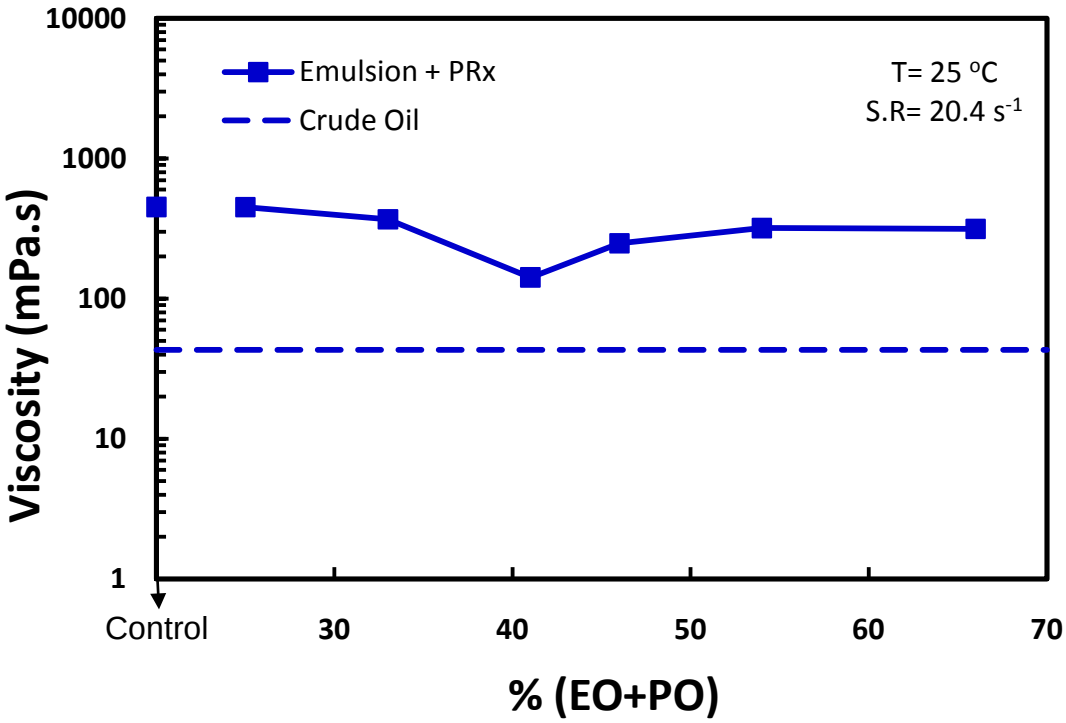

Figure 5.27 Viscosity of 50% emulsion samples adding different demulsifiers (250 ppm of PR_1-PR_6) @ 25 ^oC and shear rate of 20.4 s^{-1}, after 30 min inside viscometer. Points in y-axis are for emulsion with no addition.

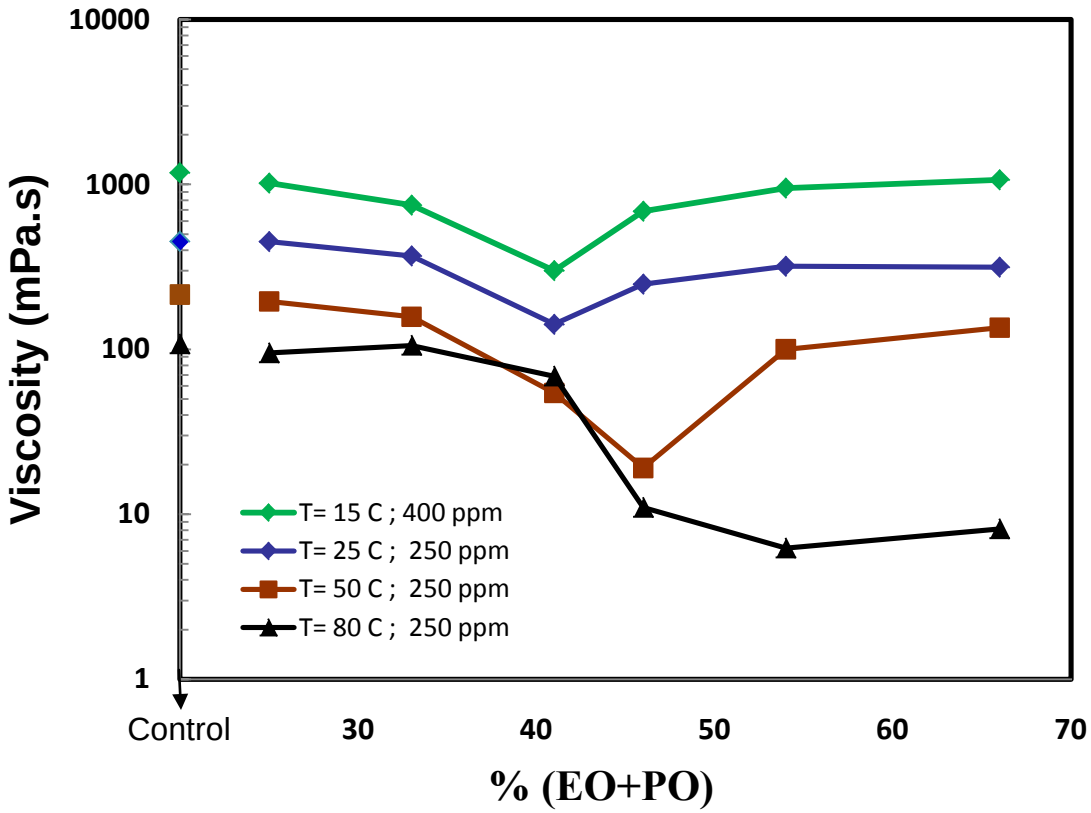

Figure 5.28 Viscosity of 50% emulsion samples adding different demulsifiers (PR1-PR_6) @ different temperatures, after 30 min inside viscometer. Points in y-axis are for emulsion with no addition.

The same experiment was repeated at different temperatures. Figure 5.28 summarizes the viscosity measurements for emulsions treated with these phenolic resins (PR1-PR6) as a function of their EO/PO content at all temperatures. It can also be seen that the decrease in shear viscosity was dependent on temperature. Increasing the temperature shifts the optimum demulsifier toward more hydrophilic resins since affinity of the resin shifts from lipophilic to hydrophilic as the EO + PO content is increased [57]. Table 5.4 summarizes the results obtained in these experiments. It can be seen that at higher temperatures the viscosity of emulsion is very close to oil viscosity itself.

The reasons for PR_3 being the optimal at lower temperatures may be that it provides a balance state where the oil/water interfaces have no tendency toward either O/W or W/O configuration, which is known to be the condition for least stable emulsions in many system (see *section 2.5.2*). Similar conclusions have been reported for other crude oil systems by Abdel-Azim [60] and Goldzsal and Bourrel [63]. The interactions between the nonionic demulsifier and the water phase decrease if the temperature increases. Hence, an increase in temperature requires an increase in the fraction of EO/PO groups present in the phenolic resin to maintain the balance state and observe maximum water separation. This explains why the optimal demulsifiers in Figure 5.28 at 50 and 80 ^{o}C are shifted to be PR_4 and $PR_{5,}$ respectively. Working with the same phenolic resins and another crude oil, similar observation was made by Pena et al [57].

Figure 5.28 also shows that at higher temperatures the viscosity of emulsion is much lower than that at lower ones. This is because the increase of temperatures causes a reduction in the viscosity of the oil phase as shown in Figure 5.20, and therefore leads to an increase in the sedimentation rate of droplets and to faster drainage of thin film between water drops, which facilitates coalescence.

e 5.4 Summary of viscosity measurements reported in Figure 5.28

Dosage	**Viscosity** (mPa.s) after 30 min inside viscometer							
ppm	Oil	No PR_x	PR_1	PR_2	PR_2	PR_4	PR_5	PR_6
400	98	1178	1019	748	300	688	950	1067
250	43	451	451	369	142	249	319	315
250	21	215	195.2	158	54	19	100	135
250	11	108	95	106	69	11	6	8

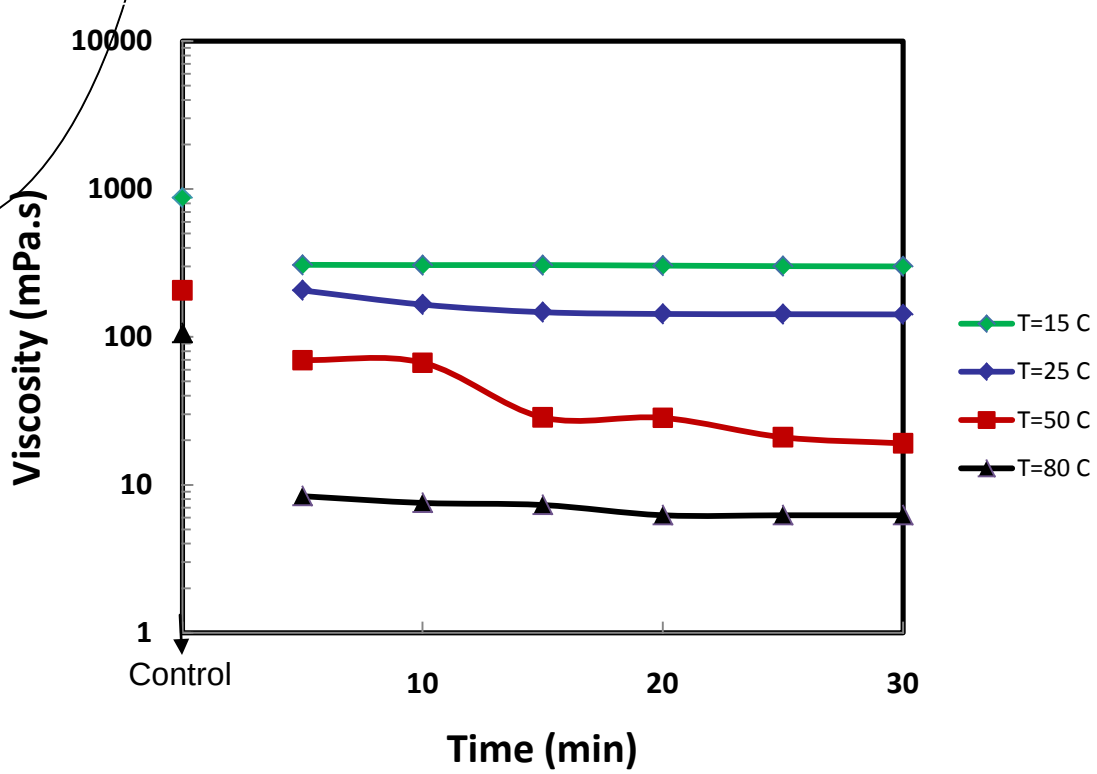

Figure 5.29 Viscosity vs. time for the optimum demulsifiers shown in Figure 5.28 for the 50% emulsion samples at different temperatures. Points in y-axis are for emulsion with no addition.

In Figure 5.29, the viscosities as function of time for the measurements reported at Figure 5.28 are shown for the optimum demulsifiers at each temperature. It is seen that much of the decrease in the viscosity occurs during the first 5 minutes. The change of viscosity was not so large between 5 and 30 minutes.

Figure 5.30 demonstrates the effect of demulsifier dosage on viscosity reduction. Increasing dosage up to 150 ppm causes a substantial decrease in viscosity. After that no significant benefit of increasing dosage can be observed during the 30 minutes experimental time.

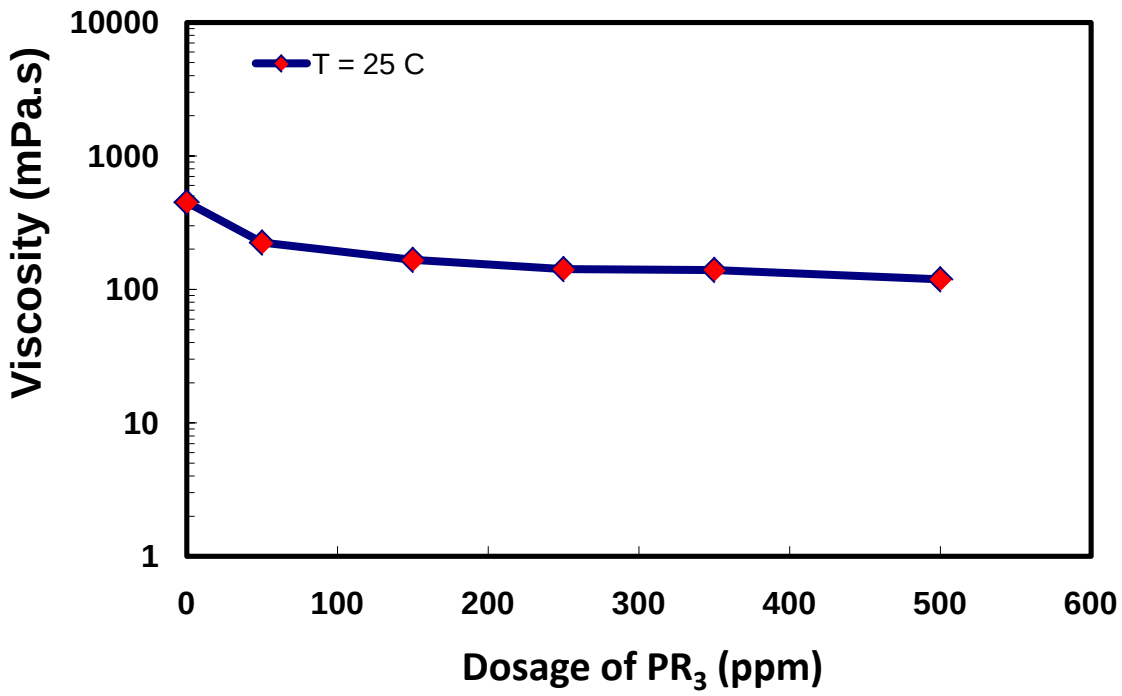

Figure 5.30 Viscosity of 50% emulsion samples adding different dosage of PR_3 @ 25 ^{o}C, after 30 min inside viscometer.

5.4.3 Effect of mixing order

Emulsions can be created either from the oil reservoir structure or from processing after the well-head due to turbulence and pressure drop created by choke-valves. Therefore, it is important to identify where the best possible location to inject these demulsifiers is. Here, the performance of demulsifier was also studied via transient viscosity measurements.

Figure 5.31 shows the results obtained from evaluating different mixing order of PR_3 demulsifier. The untreated emulsion viscosity measurements along with oil viscosity for a period of 3 hrs are also shown for comparison.

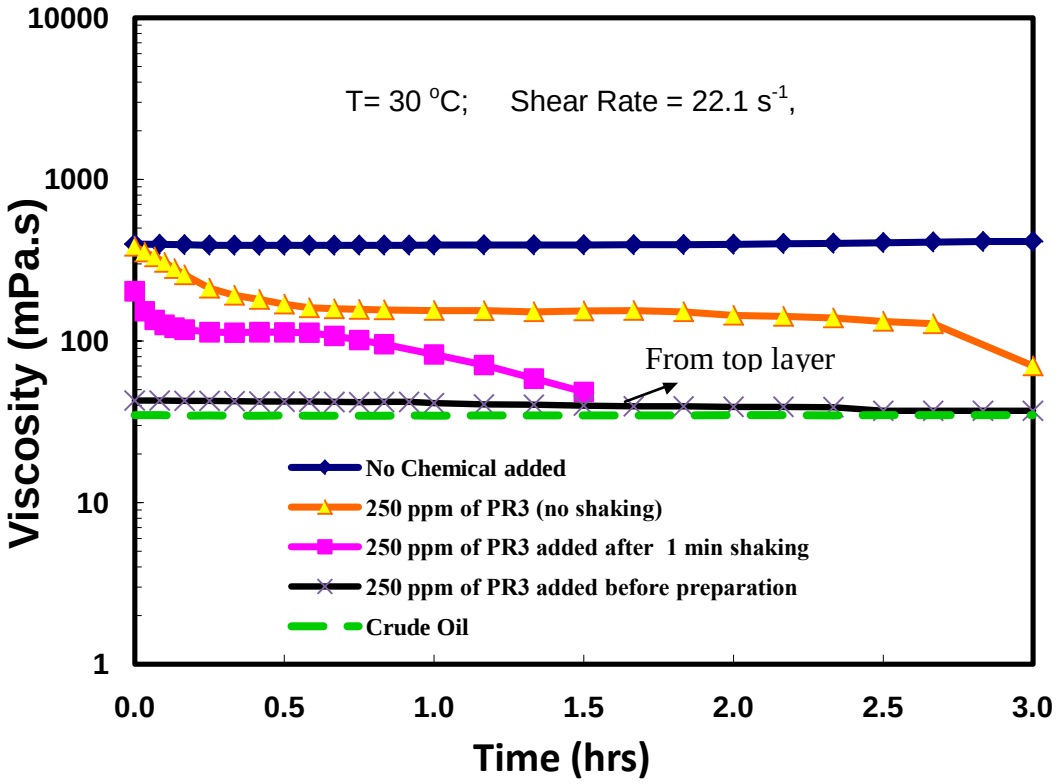

Figure 5.31 Viscosity vs. time for 50% emulsion using different order of mixing with adding 250 ppm of PR_3. The viscosity of the crude oil is also shown for comparison.

Figure 5.31 indicates stability of the untreated emulsion during the experimental time. Clearly, the addition of the phenolic resin significantly enhanced the water separation rate. The viscosity of the emulsion with demulsifier present can be reduced to almost crude oil viscosity. However, the effect of shaking (strong mixing) can be illustrated by the difference between the plot with no shaking compared to the one with 1 min shaking. The viscosity plot for 1 min shaking shows a strong reduction in almost half the time required with no shaking.

In addition, the experiment was done with PR_3 added before emulsification process (on the layered mixture). In this case the emulsion separated into bulk phases directly after the 10 min emulsification time and the viscosity measurement was taken from the top layer (oil phase).

By doing this experiment it is clear that in order to obtain the best separation or viscosity reduction the demulsifier is preferably injected before strong mixing can happen and as early as possible such as before the choke valve in a pipeline.

CHAPTER 6

CONCLUSIONS AND FUTURE WORK

6.1 Conclusions

In this study, the emulsion properties were characterized by NMR measurement techniques. The effects of a series of demulsifiers that act as coalescers were also investigated. Untreated 50% W/O emulsion was found to be very stable during the 21 hr measurement time. The separation of oil and water with adding PR_3 was clearly shown via NMR, which demonstrates the effect of enhancing the coalescence rate by adding PR_3.

From an analysis of the experimental data obtained for the rheology of the crude oil studied and its emulsions at different temperatures and dispersed phase volume fractions, the following can be concluded:

- At 50% water cut, emulsion viscosity decreases from about 1500 cp at 7 ^{o}C to about 150 cp at 80 ^{o}C, a tenfold decrease.
- Viscosity of emulsions increases by almost two orders of magnitude with higher water cut. The highest stable emulsion viscosity was observed at 60% water cut. The inversion point was also predicted to be about 70% ($\pm$5) where the highest viscosity was also observed. This reveals that in order to maintain low pumping pressure in pipelines, crude oil emulsions should be pumped either at low water cut or extremely high water cut in

the absence of demulsifiers where low viscosity is observed for these conditions.

- The choice of optimal coalescer depends on temperature where the best separation result shifts toward the more hydrophilic resins as the temperature increases. This behavior is consistent with the balance between hydrophilic and lipophilic properties of the optimal demulsifier being maintained because all the nonionic demulsifiers used become less hydrophilic with increasing temperature.
- Addition of demulsifier reduces the apparent viscosity of emulsions with intermediate water cut by order of magnitude.
- Mixing order and time affect emulsion rheology. In order to obtain the best separation or viscosity reduction the demulsifier is preferably injected before strong mixing can happen and as early as possible such as before the choke valve in a pipeline.

6.2 Suggested Future Work

Possible further study will need to focus on the following areas summarized below:

- Effect of addition of demulsifiers on crude oil-brine emulsion flow in horizontal tubes to simulate seafloor pipeline transport.
- Using different types of demulsifers and evaluting their performance compared to the phenolic resins used here in this study.

- Investigating the morphology of flow with and without demulsifiers.
- Investigatiing the effect of pH of and salinity on the rheological behavior of emulsion.
- In the flow study, study of effect of demulsifiers on viscosity reduction at temperatures and water cuts over the range of expected conditions in the field .
- Microscopic observation of rapid transient behavior with presence of demulsifier can help undestanding the rapid change of viscosity in the presence of demulsifer.

REFERENCES

[1] “Deep Water Where the Energy Is”. U.S. Dept. of the Interior, *Minerals Management Service (MMS)*: Securing Ocean Energy and Economic Value for America, 2004, Internet Web site: <http://www.mms.gov/Assets/PressConference11152004/MSGlossySingle_110404.pdf >

[2] L. D. Nixon, N. K. Shepard, C. M. Bohannon, T. M. Montgomery, E. G. Kazanis and M. P. Gravois; “Deepwater Gulf of Mexico 2009: Interim Report of 2008 Highlights”, U.S. Dept. of the Interior, *Minerals Management Service*, Gulf of Mexico OCS Region, New Orleans, LA. OCS Report MMS 2009-016.

[3] Peña, A.A., *Dynamic aspects of emulsion stability*, Ph.D thesis. Houston: Rice University, 2004.

[4] Schramm, L.L., “Petroleum Emulsion: Basic Principles”, in *Emulsions Fundamentals and Applications in the Petroleum Industry*, Schramm, L. L., Editor, Advances in Chemistry Series-231: Washington DC, 1992, Chapter-1.

[5] Miller, C.A., “Spontaneous emulsification produced by diffusion - a review”, *Colloids and Surfaces*, 29 (1988) 89-102.

[6] Nishimi, T. and Miller, C.A., “Spontaneous emulsification produced by chemical reactions”, *J. Colloid Interface Sci*., 237 (2001) 259-266.

[7] Becher, P., *Emulsions: theory and practice*, 3rd Ed.; Washington, D.C.: American Chemical Society; Oxford; New York: Oxford University Press, 2001.

[8] Brooks, B.W., Richmond, H.N. and Zerfa, M., “Phase inversion and drop formation in Agitated liquid-liquid dispersions in the presence of nonionic surfactant”, in *Modern Aspect of Emulsion Science*, Binks, B.P. Editor, Chapter-6, The Royal Society of Chemistry, UK.

[9] Berryman, J.G., “Random close packing of hard spheres and disks”, *Phys. Rev. A*, 27 (1983) 1053-1061.

[10] Arirachakaran, S., Oglesby, K.D., Malinowsky, M. S., Shoham, O. and Brill, J.P., “An Analysis Of Oil-Water Flow Phenomena In Horizontal Pipes [A]”. *Society of Petroleum Engineers* (*SPE-1883).* Oklahoma City, 1989.

[11] Becher, P., *Principles of Emulsion Technology*, Reinhold Pilot Book -5, Chapman & Hall, 1955.

[12] Salager, J.L., "Emulsion Phase Inversion Phenomena", in *Emulsions and emulsion stability*, Sjöblom J., Editor, Surfactant science series, *Vol*.132. CRC Press, Taylor & Francis Group, 2006.

[13] Vaessen, G.E.J., Visschers M., and H.N. Stein, "Predicting Catastrophic Phase Inversion on the Basis of Droplet Coalescence Kinetics", American Chemical Society, *Langmuir*, Vol. 12, No. 4, 1996.

[14] Jing, G., Qing-ping, L., Hai-yuan, Y. and Da, Y., "A Model For Predicting Phase Inversion In Oil-Water Two Phase Pipe Flow", *J. Hydrodynamics*, *Ser.B,* 18(3) (2006) 310-314.

[15] Epstein, B., "Logarithmico-normal distribution in breakage of solids", *Ind. Eng. Chem*., 40 (1948) 2289-2290.

[16] Lachaise, J., Mendiboure, B., Dicharry, C., Marion, G., Bourrel M., Cheneviere, P., and Salager, J.L., "A simulation of emulsification by turbulent stirring", *Colloids Surf. A: Phys. Chem. Eng. Aspects*, 94 (1995) 189-195.

[17] Söderman, O., Balinov, B., "NMR Self-Diffusion Studies of Emulsions", in *Emulsion and Emulsion Stability*, Sjöblom J., Editor, Surfactant science series, *Vol*.61., Marcel Dekker, Inc., 1996, pp. 369-392.

[18] Orr, C., "Emulsion droplet size data", in *Encyclopedia of Emulsion Technology*, Becher, P., Editor. Vol.1, Marcel Dekker, New York, 1983, Chapter-6.

[19] Barnes, H. A Barnes, "Rheology of emulsions - a review", *Colloids Surf. A*, 91 (1994) 89-95.

[20] Tadros, T.F., Fundamental principles of emulsion rheology and their applications, *Colloids Surf. A,* 91, (1994) 39-55.

[21] Pal, R., Yan, Y. and Masliyah, J., "Rheology of Emulsion", in *Emulsions Fundamentals and Applications in Petroleum Industry*, Schramm L.L., Editor, Advances in Chemistry Series-231: Washington DC, 1992, Chapter-4.

[22] Einstein, A., Eine neue bestimmung der moleküldimensionen, *Ann. Physik,* 19 (1906) 289-306.

[23] Einstein, A., Berichtigung zu meiner arbeit: "Eine neue bestimmung der moleküldimensionen", *Ann. Physik*, 34 (1911) 591-592.

[24] Taylor, G.I., “The viscosity of a fluid containing small drops of another liquid”. *Prec. R. Soc. A,* 138 (1932) 41-48.

[25] Pal, R. and Rhodes, E., “Viscosity-concentration relationships for emulsions”, *J. Rheol.,* 33 (1989) 1021-1045.

[26] Ronningsen, H.P., “Correlations for predicting viscosity of w/o emulsions based on North Sea crude oils”. *Proc. SPE Int. Symp*., *Oil Field Chem*., SPE- 28968, Houston, 1995.

[27] Richardson, E. G., “The formation and flow of emulsion”, *J. Colloid Sci.,* 5 (1950) 404-413.

[28] ASTM Standard D341, Standard Test Method for Viscosity-Temperature Charts for Liquid Petroleum Products1, ASTM International, West Conshohocken, PA, 2003, <DOI:10.1520/D0341-03, www.astm.org>.

[29] Walther, C. Walther, “The evaluation of viscosity data”, *Erdol und Teer*, 7 (1931) 382– 384.

[30] Farah, M.A., Oliveira, R.C., Caldas, J.N., Rajagopal, K., “Viscosity of water-in-oil emulsions: Variation with temperature and water volume fraction”, *J. Petro Sci. Eng.,* 48 (2005) 169–84.

[31] Pal, R., “Effect of droplet size on the rheology of emulsions”, *AIChE J.*, 42 (1996) 3181-3190.

[32] Peña, A.A., Hirasaki, G.J. and Miller, C.A., “Solubilization rates of oils in surfactant solutions and their relationship to mass transport in emulsions”, *Adv. Colloid Interface Sci*., 123–126 (2006) 241–257.

[33] Weiss, J., Canceliere, C. and McClements D.J., “Mass Transport Phenomena in Oil-in-Water Emulsions Containing Surfactant Micelles: Ostwald Ripening”, *Langmuir,* Vol. 16, No. 17, 2000.

[34] Walstra, P., “Emulsion stability”, in *Encyclopedia of Emulsion Technology*, Becher, P., Editor. Vol.4. Marcel Dekker, Inc.: New York, 1990, pp. 1-62.

[35] Richardson, J.F. and Zaki, W.N., “Sedimentation and fluidisation: Part I”, *Trans. Inst. Chem. Eng.*, 32 (1954) 35-53.

[36] Derjaguin B.V. and Landau, L., “Theory of the stability of strongly charged lyophobic sols and of the adhesion of strongly charged particles in solution of electrolytes”, *Acta Physicochem. URSS*, 14 (1941) 633.

[37] Verwey, E.J.W. and Overbeek, J.T.G., *Theory of the Stability of Lyophobic Colloids*, Elsevier: Amsterdam, 1948.

[38] Hamaker, H.C., “The London-van der Waals attraction between spherical particles”, *Physic*a, 4 (1937) 1058-1072.

[39] Israelachvili, J., Intermolecular & Surface Forces, 2nd Ed., Academic Press: London, 1992.

[40] Miller, C.A. and Neogi, P., *Interfacial Phenomena: Equilibrium and Dynamic Effects*, 2nd Ed., CRC Press: Houston, 2008.

[41] Tadros, T.F. and Vincent, B., Emulsion stability, in “Encyclopedia of Emulsion Technology”, P. Becher, Editor. Chapter 1. Marcel Dekker, Inc., New York, 1983, pp. 129-284.

[42] Reynolds, O., “On the theory of lubrication and its application to Mr. Beauchamp Tower's experiments, including an experimental determination of the viscosity of olive oil”, *Philos. Trans. R. Soc. London*, 177 (1886) 157-234.

[43] Pal R., “Techniques for measuring the composition (oil and water content) of emulsions — a state of the art review”, *Colloids Surfaces A.,* 84 (1994) 141–193.

[44] Sjöblom, J., Aske, N., Auflem, I.H., Brandal, Ø., Havre T.E., Sæther Ø., Westvik A., Johnsen E.E., and Kellevik, H., *Adv. Colloid Interface Sci*., 100–102 (2003) 399–473.

[45] Galinat, S., Masbernat, O., Guiraud, P., Dalmazzone, C. and Noıök C., “Drop break-up in turbulent pipe flow downstream of a restriction”, *Chem. Eng. Sci.* 60 (2005) 6511–6528.

[46] Noıök, C. and Dalmazzone, C., “Formation of dispersions or emulsions under controlled flow conditions”, *In Proceedings 3rd North American Conference on Multiphase Technology*, June 6–7, Banff (Canada), 2002.

[47] Lissant, K.J., *Demulsification: Industrial Application*; Surfactant science series vol.13, Marcel Dekker: New York, 1983.

[48] Ting, P., Gonzalez, D., Hirasaki G. and Chapman, W., “Application of the PC-SAFT Equation of State to Asphaltene Phase Behavior”, in *Asphaltenes, Heavy Oils, and Petroleomics*, Mullins O., Sheu E., Hammai A. and Marshall A., Editors, Springer: New York, 2007.

[49] Masliyah, J., Xu, Z., Nandakumar, K., Yeung, A., and Czarnecki, J., “Emulsion studies associated with bitumen recovery from Canadian oil sands: Part I”, *Proceedings of the 3rd International Conference on Petroleum Phase Behavior and Fouling*, New Orleans, 2002, pp. 316-322.

[50] Goldszal, A., Bourrel, M., Hurtevent, C. and Volle, J-L., “Stability of water in acidic crude oil emulsions”, Proceedings of the 3rd International Conference on Petroleum Phase Behavior and Fouling”: New Orleans, 2002; pp. 386-400.

[51] Leopold, G., “Breaking produced-fluid and process-stream emulsions”, in *Emulsions Fundamentals and Applications in the Petroleum Industry*, Schramm L.L., Editor, Advances in Chemistry Series-231: Washington DC, 1992, Chaptre-10.

[52] Wang, Y., Zhang, L., Sun, T. Sun, Zhao, S. and Yu, J., “A study of interfacial dilational properties of two different structure demulsifiers at oil–water interfaces”, *J. Colloid Interface Sci.,* 270 (2004) 163-170.

[53] Kim, Y.H. and Wasan, D.T., “Effect of Demulsifier Partitioning on the Destabilization of Water-in-Oil Emulsions”, *Ind. Eng. Chem. Res.,* 35(4) (1996) 1141-1149.

[54] Kang, W., Jing, G., Zhang, H., Li, M. and Z. Wu, “Influence of demulsifier on interfacial film between oil and water”, *Colloids Surf. A*, 272 (2006) 27-31.

[55] Sjöblom, J., Sounderlund, H., Lindblad, S., Johansen, E.J. and Skjarvo, I M., “Water-in-crude oil emulsions from the Norwegian continental shelf Part II. Chemical destabilization and interfacial tensions”, *Colloid Polym. Sci*., 268 (1990) 389-398.

[56] Sjöblom, J., Johnsen, E.E., Westvik, A., Ese, M.-H., Djuve, J., Auflem, I.H. and Kallevik H., “Demulsifiers in the oil industry”, in *Encyclopedia handbook of emulsion technology*, Sjöblom J., Editor, Marcel Dekker: New York, 2001, pp. 595-619.

[57] Peña, A.A., Hirasaki G.J. and Miller C.A., “Chemically Induced Destabilization of Water-in-Crude Oil Emulsions”, *Ind. Eng. Chem. Res.*, 44 (2005) 1139-1149.

[58] Breen P.J., Yen, A. and Tapp, J., “Demulsification of asphaltene-stabilized emulsions-correlation of demulsifier performance with crude oil composition”, *Proceedings of the 3rd International Conference on Petroleum Phase Behavior and Fouling*, New Orleans, 2002, pp. 359-366.

[59] Angle, C. W., “Chemical demulsification of stable crude oil and bitumen emulsions in petroleum recovery -A review”, In *Encyclopedic handbook of emulsion technology*; Sjoblom, J., Ed.; Marcel Dekker: New York, 2001, p.541.

[60] Abdel-Azim, A.A., Zaki, N.N. and Maysour, N.E.S., “Polyalkoxylated amines for breaking water-in-oil emulsions: effect of structural variations on the demulsification efficiency”, *Polym. Adv. Technol*., 9 (1998) 159-166.

[61] Al-Sabagh, A.M., Maysour, N.E. and Noor El-Din, M.R., “Investigate the Demulsification Efficiency of Some Novel Demulsifiers in Relation to Their Surface Active Properties”, *J. Disp. Sci. Tech.,* 28 (2007) 547-555.

[62] Al-Sabagh, A.M., Noor El-Din, M.R., Abo-El Fotouh, S. and Nasser N.M., “Investigation of the Demulsification Efficiency of Some Ethoxylated Polyalkylphenol Formaldehydes Based on Locally Obtained Materials to Resolve Water-in-Oil Emulsions”, *J. Disp. Sci. Tech.,*30 (2009) 267- 276.

[63] Goldszal, A. and Bourrel M., “Demulsification of crude oil emulsions: correlation to microemulsion phase behavior”, *Ind. Eng. Chem. Res*., 39 (2000) 2746-2751.

[64] Peña, A.A. and Miller C.A., “Transient behavior of polydisperse emulsions undergoing mass transfer”, *Ind. Eng. Chem. Res*., 41 (2002) 6284-6296.

[65] Otsubo, Y. and Prud'homme, R.K., Effect of drop size distribution on the flow behavior of oil-in-water emulsions, *Rheologica Acta,* 33 (1994) 303-306.

[66] Ramírez, M., Bullón, J., Andérez, J., Mira, I. and Salager J.L., “Drop size distribution and its effect on O/W emulsion viscosity”, *J. Disp. Sci. Technol.*, 23 (2002) 309-321.

[67] Orr, C., “Determination of particle size”, in *Encyclopedia of Emulsion Technology*, P. Becher, Editor, Vol. 3. Marcel Dekker: New York, 1988, Chapter-3.

[68] Mikula, R. J., “Emulsion Characterization”, in *Emulsions Fundamentals and Applications in Petroleum Industry*, Schramm, L.L., Editor, Advances in Chemistry Series-231: Washington DC, 1992, Chapter-3.

[69] Callaghan, P., *Principles of Nuclear Magnetic Resonance Microscopy*, Oxford University Press: New York, 1991.

[70] Balinov, B. and Söderman O., "Emulsions-the NMR perspective", in *Encyclopedic handbook of emulsion technology*, Sjöblom, J., Editor. Marcel Dekker, Inc.: New York, 2001.

[71] Peña, A.A. and Hirasaki, G.J., "Enhanced characterization of oilfield emulsions via NMR diffusion and transvers relaxation experiments", *Adv. Colloid Interface Sci.,* 105 (2003) 103-150.

[72] Carr, H.Y. and Purcell, E.M., "Effects of diffusion on free precession in nuclear magnetic resonance experiments", *Phys. Rev*., 94 (1954) 630–638.

[73] S. Meiboom, D. Gill, Modified spin-echo method for measuring nuclear relaxation times, *Rev. Sci. Instrum*. 29 (1959) 688–691.

[74] LaTorraca, G.A., Dunn, K.J., Webber, P.R. and Carlson, R.M., "Low-field NMR determinations of the properties of heavy oils and water-in-oil emulsions", *Magn. Reson. Imaging*, 16 (1998) 659-662.

[75] Allsopp K., Wright I., Lastockin D., Mirotchnik K. and Kantzas A., "Determination of oil and water compositions of oil/water emulsions using low field NMR relaxometry", *J. Can. Pet. Technol.*, 40 (2001) 58-61.

[76] Brownstein, K.R. and Tarr, C.E., "Importance of classical diffusion in NMR studies of water in biological cells", *Phys. Rev. A*, 19 (1979) 2446-2453.

[77] Tanner, J.E., "Use of the stimulated echo in NMR diffusion studies", *J. Chem. Phys.,* 52(5) (1970) 2523-2526.

[78] Peña, A.A. and Hirasaki, G.J., "NMR Characterization of Emulsions", in *Emulsions and Emulsion Stability*, Sjöblom, J., Editor, Surfactant science series, *Vol*.132. CRC Press, Taylor & Francis Group, 2006. p. 283.

[79] Stejskal, E.O. and Tanner, J.E., "Spin diffusion measurements: spin echoes in the presence of a time-dependent field gradient", *J. Chem. Phys*., 42 (1965) 288-292.

[80] Murday, J.S. and Cotts R.M., "Self-diffusion coefficient of liquid lithium"*, J. Chem. Phys*., 48 (1968) 4938-4945.

[81] Packer, K.J. and Rees, C., "Pulsed NMR studies of restricted diffusion. I. droplet size distribution in emulsions", *J. Colloid Interface Sci.*, 40 (1972) 206-218.

[82] Jiang, T., Hirasaki, G.J., Miller, C.A., Moran, K. and Fleury, M., “Diluted Bitumen Water-in-Oil Emulsion Stability and Characterization by Nuclear Magnetic Resonance (NMR) Measurements”, *Energy & Fuels*, 21 (2007) 1325-1336.

[83] Liang, Z.-P. and Lauterbur, P.C., *Principles of Magnetic Resonance.* Akay, M., Ed.; IEEE: New York, 2005, Chapter-7.

[84] Speight, J.G., Handbook of Petroleum Analysis. Johan Wiley & Sons: New York, 2001, pp. 118-125.

[85] Dunn, K.J., Bergman, D.J. and Latorraca C.A., *Nuclear Magnetic Resonance Petrophysical and Logging Applications*, Pergamon: Amsterdam; New York, 2002.

[86] Mills, R., “Self-Diffusion in Normal and Heavy Water in the Range 1-45º”, *J. Phys. Chem*., **77** (1973) 685-688.

[87] Oliveira, R.C.G. and Goncalves, M.A.L., “Emulsion Rheology- Theory vs. Field Observation”, Paper presented at *Offshore Technology Conference, OCT-17386*, Houston TX (May 2005).